EUROPEAN COMMISSION

nuclear science and technology

Integrated *in situ* corrosion test on α-active high-level waste (HLW) glass – Phase 2

(CORALUS-2)

Contract N^{o} FIKW-CT-2000-00011

Final report

Work performed as part of the European Atomic Energy Community's
R&T specific programme Nuclear Energy 1998-2002, key action Nuclear Fission Safety
(Fifth Framework Programme)
Area: Safety of the fuel cycle

2007

Directorate-General for Research
Euratom

Project coordinator (responsible for this final report)

E. Valcke, SCK•CEN, Mol, BE

Project partners

E. Valcke, S. Smets, S. Labat, K. Lemmens, P. Van Iseghem, M. Gysemans, P. Thomas, P. Van Bree, B. Vos, and S. Van den Berghe (SCK•CEN), BE

N. Godon, P. Jollivet, J.P. Mestre, G. Parisot, M. Bojat, J.M. Boubals, and X. Deschanels (CEA-Valrhô), FR

N. Jockwer and K. Wieczoreck (GRS), DE

C. Pozo, J.C. Petronin, and J. Raynal (CEA-Cadarache), FR

Preface

The CORALUS-2 project was performed as part of the European Atomic Energy Community (Euratom) Fifth Framework Programme. The project was a continuation of the CORALUS-1 project under the Fourth Euratom Framework Programme.

The purpose of this final scientific and technical report is twofold: firstly to present a comprehensive overview of the scientific work and results obtained and secondly to compile all relevant and detailed technical information gathered throughout the project.

Acknowledgements

This project has been co-funded by the European Commission. We highly appreciate the critical follow-up by Dr. T. McMenamin (EC, DG Research, Fission Unit).

NIRAS/ONDRAF (Belgian Agency for Radioactive Waste and Enriched Fissile Materials) is gratefully acknowledged for the co-funding of SCK•CEN's contribution to the CORALUS-2 project (contracts CCHO 98/332, CCHO 2000/0773, and CCHO-2004-2470/00/00). The critical follow-up by and fruitful discussions with Dr. Robert Gens, Dr. Ann Dierckx, and Mr. H. Van Humbeeck are very much appreciated.

The collaboration with JAEA (formerly JNC; Tokai, Japan) on the modellisation of the radionuclides leaching from the radioactive glass samples and their migration in compacted backfill materials is greatly appreciated.

This project would not have succeeded without the help of many colleagues from CEA, GRS, SCK•CEN, and other institutes:

- Dr. C. Gatabin (CEA-Saclay, France) for supplying the pre-compacted blocks of the backfill materials for the surface laboratory experiments
- Mrs. S. Kranz and Mr. U. Hertes (GRS-Braunschweig, Germany) for preparation of the samples and gas analyses
- Mr. G. Volckaert (SCK•CEN, Waste and Disposal Expert Group) and Mr. J. Peeters and his team (SCK•CEN, main workplace) for the concept development and (pre)assembly of the test tubes;
- Mr. M. Buyens and his team (SCK•CEN, HADES Underground Research Facility) for the installation and retrieval of the test tubes;
- Mr. W. Claes and his team (Laboratory for High- and Medium-level Activity, SCK•CEN) for the assistance during the assembly and the dismantling of the radioactive test tubes;
- Mr. P. Boven (SCK•CEN, Waste and Disposal Expert Group), for assistance during assembly, operation, retrieval, and dismantling of the test tubes, and for the treatment of glass samples and clay cores;
- Mr. B. Gielen, Mr. K. Penasse†, Mr. W. Verwimp, Mrs. S. Lunardi, and Mrs. R. Vercauter (SCK•CEN, Waste and Disposal Expert Group), for assistance during assembly, operation, retrieval, and dismantling of the test tubes;
- D. Mallants and X. Sillen (SCK•CEN, Waste and Disposal Expert Group) for supporting scoping calculations;
- P. De Cannière and B. Kursten, (SCK•CEN, Waste and Disposal Expert Group) for many scientific discussions and review of the progress reports and detailed SCK•CEN report;
- Mr. P. Antoine, Mr. P. Vandycke, and Mr. H. Maussen (SCK•CEN, Radiation Protection)
- Mr. C. Hurtgen and Mr. F. Verrezen and their team (Laboratory for Low-activity Measurements, SCK•CEN) for radiochemical analyses of low-radioactive samples
- Dr. N. Valle (CRPGL, Luxembourg) and Dr. E. Deloule (CNRS/CRPG Nancy, France) for the SIMS analyses of the non-radioactive glass samples
- Dr. M. Martin, Dr. E. Curti, and Dr. D. Gavillet (PSI, Switzerland) for the SIMS analyses of the radioactive glass samples.

Executive summary

The CORALUS project aimed at assessing and demonstrating the performance of the SON 68 glass – a reference glass simulating the French R7T7 HLW (high-level waste) glass – in conditions that are representative for those expected in a disposal system relying on the use of a clay-based backfill material. More specifically, the objectives of the CORALUS project were:

1. To provide realistic data on and to gain more insights in the dissolution of SON 68 glass – a reference glass simulating the COGEMA R7T7 SON 68 HLW glass – and in the release and the migration of radionuclides and some other incorporated elements into the backfill materials at high density.
2. To estimate the extent of the thermal and radiolytic gas generation in the three backfill materials that are studied in the CORALUS test.
3. To assess, for a Ca-bentonite-based backfill material, the mineralogical alteration upon prolonged heating and gamma irradiation.

In the CORALUS *in situ* tests, four test tubes were placed in the boom clay through the HADES underground research facility at temperatures of 30 or 90 °C, for durations between 1.3 and 10 years. Each test tube consists of three modules, containing non-radioactive and highly alpha-active (^{237}Np, $^{238\text{-}242}$Pu, or ^{241}Am doped) SON 68 glass samples in direct contact with a backfill material with swelling pressure of 2 MPa. Three backfill materials are studied: dried boom clay and two bentonite-based materials, one of them containing 5 weight% of powdered glass frit. The interstitial backfill solution can be sampled through built-in piezometers. The test tubes at 90 °C contain ^{60}Co sources. These two test tubes represent an accidental situation occurring shortly after disposal of the HLW glass, exposing the HLW glass directly to the backfill. The test tubes at 30 °C do not contain ^{60}Co sources. They simulate the normal evolution scenario conditions some 500 years after disposal of the waste, after corrosion of the overpack and glass canister. In addition to the *in situ* tests, supporting laboratory experiments were performed on glass dissolution and thermal gas generation, to allow optimal interpretation of the results of the *in situ* tests.

During the operation of the test tubes, samples of the backfill interstitial solutions were regularly analysed. All solutions were fingerprinted by the slightly oxidised surrounding boom clay: they contained high Na^+, SO_4^{2-}, and Ca^{2+} concentrations. Solutions were furthermore fingerprinted by the type of backfill material. For instance, the Ca-bentonite with 5 weight% of powdered glass frit contained high B and Si concentrations. CO_2 was the most important dissolved gas. Especially at 90 °C, high CO_2 concentrations were produced by thermal and radiolytic decomposition of organic matter. Using flow-through cells, the pH and the redox potential of the backfill interstitial solutions were measured under nearly *in situ* conditions. pH values in the test tubes at 90 °C (5.5-6.5) were by 1 unit or more lower than the corresponding values in the tube at 30 °C (6.2-7.4). This is related to the high concentration of dissolved CO_2. Redox potentials were negative, but tended to be less negative in the test tubes with ^{60}Co sources. The concentrations of hydrogen and methane were low, so that these gases could be dissolved in the interstitial solution, thus presenting no safety problems. In 2004, two of the four tubes (one at 30 °C and one at 90 °C) were retrieved and dismantled, and the glass samples and the clay in contact with the glass samples were analysed.

As to the glass alteration, the results largely correspond with the expectations.

1. The alteration at 90 °C is considerably higher than at 30 °C, with differences in specific daily mass loss of a factor 20. It is thus of high interest to avoid contact between the HLW glass and formation water during the thermal phase.
2. The addition of powdered glass frit to the backfill material diminishes the glass alteration with about two orders of magnitude. Optimisation of the repository performance is thus possible.

3. The alpha-doped glasses behave rather similarly as the inactive ones. Yet, for these systems with glass samples in contact with clay at high swelling pressure and water pressure, we observe slightly thicker alteration layers for the active samples, and the thickness seems to increase with increasing alpha-beta-gamma activity of the samples. Because of the lack of sufficient mass loss data, we cannot conclude that the thicker alteration layers go along with an increased mass loss. As this phenomenon was also observed for the samples of test tube 3 (90° C, ^{60}Co sources), for which the pH was already low and the gamma radiation dose rate high (> 100 Gy/h), we conclude that this effect is probably due to the increasing specific alpha activity.
4. If other processes such as the thermal decomposition of the natural organic matter of the backfill material result in an important decrease of the pH, the contribution of gamma radiation to a lower pH and concomitant decreased initial glass alteration rate may become negligible.
5. From the analysis of the SIMS profiles, we conclude that the dissolution of the SON 68 samples is predominantly selective-substitutional leaching, as observed also in other SON 68 glass alteration tests. Yet, the loss of a distinct part ('layer') of the alteration layer, either because of the sorption of the glass constituents onto the clay (exerting a high swelling pressure) and/or secondary phase formation, or because of the treatment of the glass samples before analysis, can be interpreted as matrix dissolution.
6. Due to the loss of part of the alteration layer, especially for the radioactive samples, the results of the SIMS analyses do not allow to conclude on the retention of radionuclides in the alteration layer. Fortunately, the results of the radionuclide migration enable to calculate radionuclide retention factors which vary between 1 and 3. These values are much smaller than the values normally reported for glass alteration in water in the absence of solids. This is due to the high affinity of the clay-based backfill material for the radionuclides. The loss of part of the alteration layer also impeded the detection of secondary phases.
7. Taking into account the loss of part of the alteration layer of the samples of the *in situ* tests, the results compare fairly well with those of surface laboratory tests and modelling predictions, confirming the high degree of understanding of the glass alteration phenomena.

Also concerning the migration of radionuclides and (stable) U, Cs, Th, Zr, and Pd, the results meet the expectations.

1. Highly compacted clay-based backfill materials with good radionuclide sorption properties are efficient in retarding radionuclide migration. Over a distance of ~5 mm, the specific activity of Np, Pu, and Am decreased by several orders of magnitude.
2. A contribution of colloidal transport of Am and Pu is observed. These are probably radionuclide – organic matter pseudo colloids, which are expected to become unstable over larger distances.
3. The type of backfill material has a very important effect on the general behaviour of the glass: glass alteration, radionuclide leaching, retention, and migration (*e.g.* addition of powdered glass frit, presence of mobile organic matter). Optimisation of the repository performance is thus possible.
4. Zr^{4+}, Th^{4+}, and Pd^{2+} did not migrate far, whereas U and Cs^{+} migrated relatively fast.

The characterisation of the Ca-bentonite with powdered glass frit showed that after ~1.3 years of heating and gamma irradiation the interface between clay and glass (both the glass samples and the glass powder in the backfill) was fully reactive. At the interface, Si had precipitated. Kaolinite and interstratified kaolinite/smectite of the Ca-bentonite had started to become unstable, tending to form non-swelling 7Å minerals. As these reactions may have negative consequences (for instance faster radionuclide migration through non-swelling clay minerals), it may be of interest to include the powdered glass frit within the water-tight engineered barrier ('overpack').

On the basis of all results and observations, we conclude that the CORALUS *in situ* tests largely contribute to the validation of the laboratory tests and modelling predictions, and that they can be considered as a small-scale demonstration test of the performance of a disposal system with SON68 HLW glass surrounded by a high-density clay-based backfill material with high radionuclide sorption properties. The observation of increasing thickness of the alteration layers with increasing specific

alpha-beta-gamma activity, which is possibly due to the increasing alpha activity, demonstrates the need of performing integrated experiments under conditions that are as realistic as possible.

Table of contents

1 Introduction

1.1 Background

The study of the performance of a given radioactive waste form, such as vitrified HLW, in the geological disposal environment requires a continuous interaction between concept development, waste form behaviour studies, near field and far field behaviour studies, and performance assessments and safety studies. The waste form behaviour studies in turn comprise simple to more complex surface laboratory tests (to provide data on basic dissolution processes, radionuclide release behaviour, etc. and to derive parameters for modelling), geochemical modelling (to explain or predict the effect of e.g. secondary phase formation), conceptual or mechanistic modelling (to provide means to extrapolate the glass dissolution over long periods of time), study of natural analogues, etc. As the level of understanding increases, more complex experiments are designed, aiming at an increasing integration of the different compounds and processes that will be present in the final disposal system. These integrated tests are performed to produce the best possible realistic data, which can serve as a basis for comparison with and validation of data from simpler surface laboratory experiments and modelling studies. *In situ* testing provides the possibility to maximise the degree of integration and reality: interaction with the host formation at *in situ* pressure, realistic and relatively easily controllable geochemical conditions, natural shielding against gamma radiation, etc.

As part of the studies on the long-term performance of the French R7T7 HLW glass in a deep underground repository in a clay formation, we have designed and operated during the last 10 years the CORALUS tests (*Corrosion of α-active glass in underground storage*), which are integrated *in situ* tests on the alteration of both non-radioactive and alpha-doped SON 68 reference glass[1] [1, 2]. During the first CORALUS project (performed from 1997 to 2000 under the Fourth Euratom Framework Programme), a first, completely inactive 'dummy' test tube was assembled, installed in the clay, operated, retrieved, and dismantled. During the CORALUS-2 project, which is reported here, we have dismantled two test tubes loaded with radioactive glass samples. We have analysed the glass samples and one of the backfill materials, and we have determined the leaching and the migration profile of active and non-radioactive elements.

1.2 Objectives

The CORALUS project aims at assessing and demonstrating the performance of the SON 68 reference glass in conditions that are representative for those expected to prevail in a disposal system relying on the use of a thick layer of clay-based backfill material. More specifically, the objectives of the CORALUS project are:

1. to provide realistic data on and to gain more insights in the dissolution of SON 68 18 17 L1C2A2Z1 glass – a reference glass simulating one of the main high-level waste glasses in the European Union, namely the COGEMA R7T7 SON 68 HLW glass – and in the release and the migration of the radionuclides and some other incorporated elements into the high-density backfill materials.
2. to estimate the extent of the thermal and radiolytic gas generation in the three backfill materials that are included in the CORALUS test tubes.
3. to assess, for a Ca-bentonite-based backfill material, the mineralogical alteration upon prolonged heating and gamma irradiation.

[1] SON 68 is the abbreviation of SON 68 18 17 L1C2A2Z1, a reference glass with a composition simulating the nominal composition of the COGEMA R7T7 glass that is used for the vitrification of high-level and long-lived radioactive waste. Its main constituents are (wt %) 45.5 SiO_2, 4.9 Al_2O_3, 14.0 B_2O_3, 11.8 Na_2O + Li_2O, 4.0 CaO, 2.9 Fe_2O_3, 2.65 ZrO_2, 2.5 ZnO, 9.65 fission product oxides, 0.85 actinide oxides, 2.25 other elements.

The data obtained from the *in situ* tests are expected to be realistic because the *in situ* dissolution tests they are obtained from are performed under close-to-real disposal conditions, including the presence of inactive and highly alpha-active glass samples, backfill materials exerting a high swelling pressure, contact with the host formation, representative temperature, and alpha and gamma irradiation. The data will be compared with the results on glass dissolution from laboratory experiments, performed under the same or similar conditions, and with the derived modelling predictions. This will give an idea of the reliability of the present long-term predictions, which in turn can contribute to the *acceptability of geological disposal of high-level radioactive waste*.

1.3 Methodology

1.3.1 Contractual and organisational aspects

The overall CORALUS project started as an EC co-funded project on 1 January 1997 and lasted until 30 June 2000 (EC contract N° FI4W-CT96-0035). Partners in the project were SCK•CEN (co-ordinator), CEA-Valrhô (Marcoule, France), and GRS-Braunschweig (Braunschweig, Germany). During this first phase project, the test tubes for integrated *in situ* testing were designed, and a fully inactive dummy ('test tube 1') was successfully assembled, installed in the clay, operated, retrieved, and dismantled. Additionally, two test tubes loaded with radioactive glass samples were to be assembled and installed in the clay. Due to several delays, only one of these could effectively be installed in the clay during the contractual period. The other ('test tube 3') was assembled and installed in the course of the CORALUS-2 project.

Since 1 July 2000, the CORALUS project is also co-funded by NIRAS/ONDRAF, the Belgian Agency for Radioactive Waste and Enriched Fissile Materials (contracts CCHO 98/332, CCHO 2000/0773, and CCHO-2004-2470/00/00). In 1999, a collaboration agreement was signed between the CORALUS partners and JAEA (formerly JNC, Tokai, Japan) on the modellisation of the leaching of radionuclides from the radioactive glass samples and their migration in the compacted backfill materials.

The second-phase project, CORALUS-2, started 1 October 2000 and lasted until 31 July 2005, with the same partners (EC contract N° FIKW-CT-2000-00011). It consisted of eight work packages (WP; see also the flow chart in Figure 1).

WP1 – Assembly and installation of test tube 4 (SCK•CEN) Assembly and installation of test tube 4 (and test tube 3, see above), follow-up of the convergence of the boom clay and the re-saturation of the backfill materials, follow-up of temperature and pore water pressure, installation of the ^{60}Co sources (for tubes 3 and 4), and heating to 30 °C (test tubes 2 and 5) or 90 °C (test tubes 3 and 4).

WP2 – Operation of the test tubes (SCK•CEN + GRS) The operation of a test tube started when the target temperature of 30 or 90 °C was reached. The operation comprised *(i)* the follow-up of the temperature and the pore water pressure, *(ii)* the sampling of the piezometer waters for measurement of alpha activity, ionic composition, and dissolved gases, *(iii)* the online measurement of pH and redox potential, and *(iv)* the measurement of the permeability to water. The operational phase stopped when the heating of the test tubes was stopped.

WP3 – Retrieval and dismantling of test tubes 2 and 3 (SCK•CEN) Towards the end of the CORALUS-2 project, these two test tubes were withdrawn from the boom clay and dismantled, to enable analyses of altered glass and clay samples, and to measure the leaching and migration of Np, Pu, Am, and some non-radioactive elements.

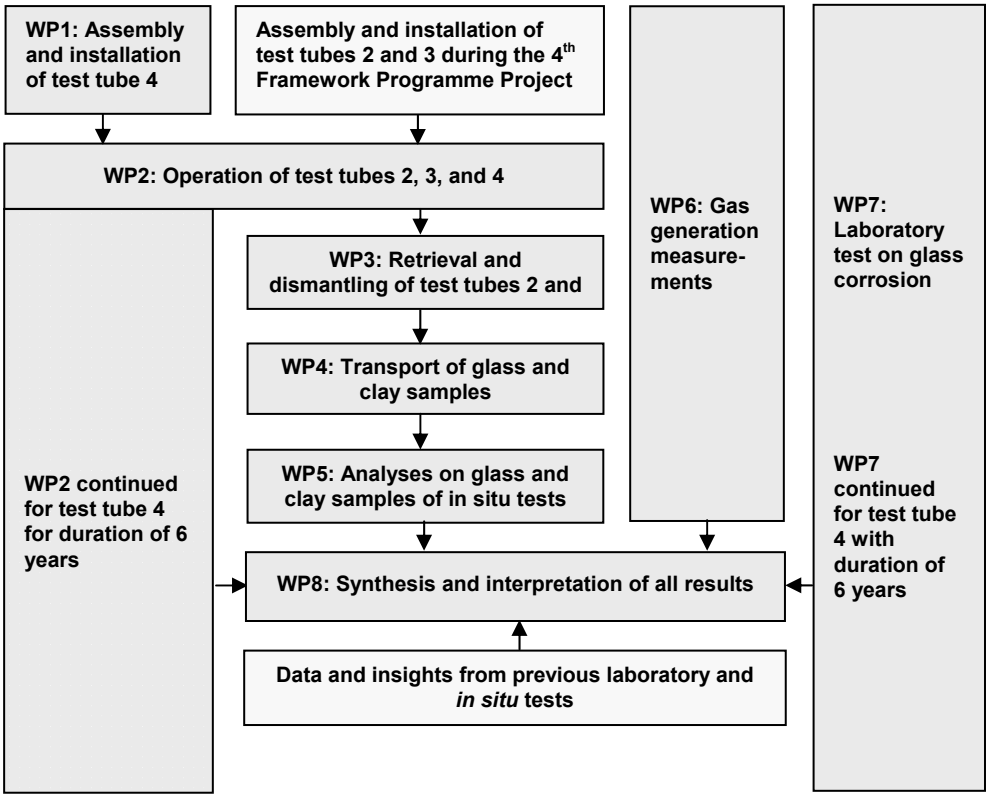

Figure 1 *Schematic representation of the project structure and interrelations.*

WP4 – Transport of the radioactive glass samples and backfill materials of test tubes 2 and 3 (CEA + SCK•CEN) A set of altered glass samples and backfill materials coming from these two test tubes were transported to CEA-Valrhô (Marcoule, France) for further analysis.

WP5 – Analyses on glass and clay samples (CEA and SCK•CEN, with sub-contractors) The bulk glass corrosion was determined by mass loss, and glass dissolution and radionuclide leaching processes were elucidated by surface (SEM, EDS, EPMA) and in-depth (SIMS) analyses. The alteration of one of the three interacting materials after prolonged heating and irradiation was studied by XRD, SEM, and TEM.

WP6 – Gas generation measurements (GRS) In a separate laboratory experiment the thermal gas generation for the three interacting materials was measured at 90 °C for periods up to 1000 days, to help to understand the results on the gas concentration in the piezometers solutions to be obtained under WP2.

WP7 – Laboratory tests on glass corrosion (CEA) The objective of this work package was to perform a surface laboratory test on glass alteration, performed under conditions that simulated as good as possible the *in situ* test conditions, to be able to compare both sets of results. Within the framework of the EC contract, 18 tests with non-radioactive SON 68 glass samples were foreseen: two temperatures (30 and 90 °C), three backfill materials, and three durations (~1, ~2, and ~5 years), however in the absence of gamma radiation.

WP8 – Interpretation of the results (CEA, GRS, and SCK•CEN) At the end of the project, all results were synthesised and interpreted, and compared with those from other laboratory and *in situ* tests, and (for glass dissolution only) with model predictions.

CORALUS integrates the experience of previous *in situ* tests performed at SCK•CEN and other institutes, and the expertise of the two cooperating institutes. CEA provided the non-radioactive and alpha-active

SON 68 glass samples and participated in the analyses on the retrieved glass and backfill specimens. GRS performed the laboratory and *in situ* measurements on gas generation and migration.

1.3.2 The CORALUS in situ tests

The CORALUS *in situ* tests comprise four modular test tubes, installed in the boom clay formation – that is studied as a reference host formation in Belgium – through the HADES underground research facility (URF; Mol, Belgium), for durations between 1.2 and 10 years (Table 1).

Table 1 *Experimental matrix and time-schedule for the four CORALUS in situ test tubes.*

Tube N° *	Temp. (°C)	^{60}Co	Installation **	Operation	Duration (years)
2	**30**	**No**	2000.04.10	2001.02.21 - 2004.06.01	3.3***
3	**90**	**Yes**	2001.04.25	2002.12.05 - 2004.02.20	1.3***
4	**90**	**Yes**	2001.10.25	2003.04.15 - 2009.04.15	6.0
5	**30**	**No**	2003.11.06	2004.09.01 - 2014.08.31	10

* A first, completely inactive 'dummy' test tube was assembled, installed in the clay, operated, retrieved, and dismantled (1997-1999) [1, 2]. Tubes 2 and 5 are installed at 45 ° to bedding plane; tubes 3 and 4 are installed perpendicular to the bedding.

** The long time between installation and operation is due to the slow convergence of the boom clay around the test tube and the slow water saturation of the dry pre-compacted backfill materials.

*** The alteration duration was 1196 days and 442 days, for tube 2 and tube 3, respectively.

Each CORALUS tube consists of three modules. One module comprises an inner support tube and a partially porous outer support tube, and a bottom and a top flange, all made of stainless steel. In each module, 2 inactive and 6 alpha-doped SON 68 glass samples, placed on an inner support tube, are in contact with a backfill material that exerts a design swelling pressure of 2 MPa (20 bar). Each module further contains three piezometers that are in contact with the backfill material. They are connected with thin stainless steel tubes to the valve panel in the URF, to sample interstitial backfill solution. Inside the inner support tube a heating element and – for two of the four test tubes – ^{60}Co sources can be placed. These latter tubes have a larger diameter, with a thicker backfill material. A three-dimensional cut-away view of a large test tube is given in Figure 2, together with a picture of part of a module during its assembly. Details on the test tube design are given in [1]. Dimensions of a module are (diameter × height, mm) 300 × 250 ('large' tubes) and 200 × 250 ('small' tubes). The thickness of the saturated backfill materials is 53 mm (large test tubes) and 34 mm (small test tubes).

Radioactive glass samples contain ~0.85 weight% of $^{237}NpO_2$ (0.22 MBq ^{237}Np per g glass), $^{238\text{-}240}PuO_2$ (27 MBq $^{239/240}$Pu + 8 MBq ^{238}Pu + 0.30 GBq ^{241}Pu + 13 MBq ^{241}Am per g glass), or $^{241}Am_2O_3$ (1 GBq ^{241}Am per g glass) (activity on May 1st, 2000). The active glass samples also contain some impurities such as ^{137}Cs and ^{152}Eu. Together with the increasing alpha activity (Np < Pu < Am), also the beta-gamma activity of the active samples increases (^{237}Np: 1.3 MBq ^{152,155}Eu and ^{233}Pa (beta-gamma) per g glass; $^{238\text{-}240}PuO_2$: 300 MBq ^{241}Pu (beta) and 13 MBq ^{241}Am (gamma); per g glass); $^{241}Am_2O_3$: 1 GBq ^{241}Am (gamma) per g glass; activity on May 1st, 2000). Inactive glass samples contain ~0.37 weight % of $(U,Th)O_2$, and inactive isotopes, or chemically similar elements, of other critical long-lived nuclides such as ^{79}Se, ^{93}Zr, ^{107}Pd, ^{135}Cs. Each module contains 2 inactive samples, and 2 samples of each type of the radioactive glasses. The two replicates are placed side by side (see Figure 2). The modules of test tube 5 contain only 2 non-radioactive samples and 2 samples doped with ^{237}Np.

The backfill materials are (module A) **d**ried **boom clay** ('**DBC**'), (module B) Ca-**b**entonite mixed with **s**and and **g**raphite (60/35/5 wt %; '**BSG**'), and (module C) Ca-**b**entonite mixed with powdered

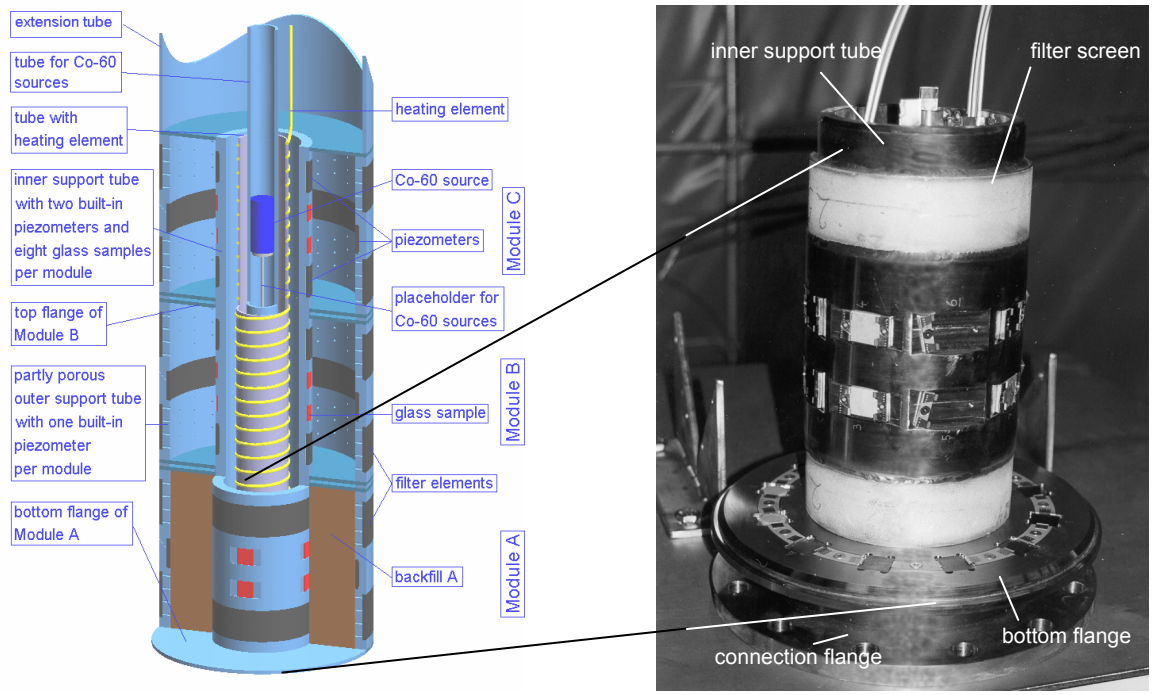

Figure 2 *(left) Three-dimensional cut-away view of a test tube with ^{60}Co sources. (right) Inner support tube, bottom flange, and connection flange of a module. The photo shows the position of the samples (SON 68, other glass types, container materials) on the inner support tube and on the flange, and the filter screens and connecting tubes of the inner piezometers (in grey). The α-doped SON 68 samples were not yet installed when the photo was taken.*

SON 68 **g**lass **f**rit (95/5 wt %; '**BGF**'). The addition of graphite aims at increasing the thermal conductivity of the backfill material during its dry period. The addition of the powdered glass frit aims at establishing high solution concentrations of the main glass constituents, hence decreasing the chemical potential difference of these elements between glass and pore water, and thus slowing down the glass dissolution rate. During assembly of the test tubes, backfill materials were inserted as pre-compacted half-cylindrical blocks in the annular gap between the inner support tube and the partially porous outer support tube. After installation of the test tube and convergence of the boom clay, backfill materials were hydrated by boom clay pore water entering the modules through the partially porous outer support tube.

The CORALUS *in situ* tests integrate many compounds and processes that will be present in an underground repository that relies on the use of swelling clay-based materials to seal the disposal gallery. Therefore, the test tube design integrates different processes that affect the glass dissolution and radionuclide release and migration, and thus creates the conditions for coupled processes to occur: secondary phase formation, sorption, (co-)precipitation, complexation, ion exchange, diffusion.

The test matrix is as follows (Table 1):

- Tubes 2 and 5 are operated at 30 °C during 3.3 and 10 years, respectively, in the absence of gamma radiation. They simulate the normal evolution scenario conditions beyond the thermal period, after advanced corrosion of the overpack and glass canister (after > 500 years).
- Tubes 3 and 4 contain ^{60}Co sources and are operated at 90 °C, during 1.2 and 6 years, respectively. These conditions represent an early failure scenario, occurring ~50 years after disposal of the waste. The gamma radiation dose rate of ~130 Gy/h (start of the operation) corresponds with the one at the glass/backfill interface some 100 years after production of the HLW glass.

2 Scientific and technical results

2.1 Assembly, installation, operation, retrieval, and dismantling of the test tubes, and transport of the radioactive glass and clay samples (WP1, WP2, WP3, WP4) [2]

2.1.1 Assembly and installation of the CORALUS test tubes (WP1)

A detailed description of the assembly of the inactive test tube 1 (the dummy test) is given in [1]. The assembly of the test tubes with radioactive glass samples proceeded similarly, with the additional level of complexity that all actions had to be performed in a ventilated tent, using full protective clothing (PEDI®) with external air supply.

The installation of the radioactive glass samples on the test tube required a low removable contamination on the surface of the samples. For the ^{237}Np-doped and $^{238\text{-}240}$Pu-doped samples, we achieved stable removable alpha contaminations of 1 (= detection limit) to 2 Bq/cm² by cleaning the samples with tissues soaked in ethanol. For the highly active ^{241}Am-doped samples, the removable contamination was never lower than 15-30 Bq/cm², despite repeated ultrasonic treatment with ethanol or acetone. However, four months after cleaning, the removable contamination for the ^{241}Am-doped samples had again increased up to 600 to 2000 Bq/cm². Such values for the ^{241}Am-doped samples were also measured upon reception of the active samples, *i.e.* before cleaning the glass samples. This increase of the removable contamination is attributed to the effect of alpha recoil [3] and the lack of repair mechanisms at the surface [4]. It was not observed for the Np-doped and Pu-doped glass samples.

Due to the recurring high removable contamination measured on the ^{241}Am-doped glass samples, the assembly and installation of test tubes 3 and 4 had to be delayed until this phenomenon could be explained and additional evidence could be provided that the high removable contamination would not increase the risk of contamination of the boom clay surrounding the test tubes. To this purpose, a detailed safety file was prepared, specifically addressing the migration of the radionuclides leached from the active SON 68 glass samples into the backfill materials. This safety file included calculations on the migration of Np, Pu, and Am in dense clay materials. The input parameters for these calculations were derived from the interpretation of the migration profiles of these radionuclides in undisturbed boom clay at 25 °C. Initial values for the Np, Pu, and Am concentrations in the pore water close to the SON 68 glass samples were obtained from different publications describing the leaching of doped SON 68 glass in the presence of clay materials [5-11]. To confirm the retardation factors obtained for undisturbed boom clay, batch type sorption experiments (liquid/solid ratio of 5/1 ml/g, measurements after 7 and 27 days of end-over-end shaking) were performed, to measure the sorption of Pu and Am on the backfill materials at 80 °C under reducing conditions. After 27 days, the Am sorption coefficients varied between 30 000 ml/g (DBC) and 120 000 ml/g (BGF). For Pu, the sorption coefficients varied between 150 000 ml/g (DBC) and 400 000 ml/g (BSG). In conclusion, the safety file indicated that no or only a very low contamination of the surrounding boom clay was to be expected. Also the outer piezometer waters of test tube 2 were analysed (see Section 2.1.2.2). As the specific total alpha activity in the piezometer waters was very low and similar to the value for boom clay pore water (0.3 to 0.5 Bq/l, [12]), the approval was given to proceed with the assembly and installation of test tubes 3 and 4.

The test tubes were installed in the boom clay at a distance of 4 m to 5 m from the gallery wall, after drilling a borehole with an excess diameter of about 10 %. Test tubes 2 and 5 were installed at 45 ° to the bedding plane [1]. Test tubes 3 and 4, which had to host ^{60}Co sources, were installed perpendicularly to the bedding plane. For these two test tubes, the borehole had to be reamed the day after the drilling, due to the presence of large pyrite nodules in the clay, which during the drilling resulted in a deviation of the borehole from the initial axis. This resulted in a larger excess diameter and the removal of boom clay that had already expanded after the first drilling. As a result, more time was needed before the boom clay had completely converged around these test tubes (Table 1).

[2] This part has been described in detail in the detailed report of SCK•CEN.

After installation of a test tube, the annular gap between the extension tube (Figure 2) and the boom clay was sealed. This allowed rinsing the gap between test tube and boom clay daily with argon until the clay had converged, thus limiting the oxidation of the surrounding clay. Due to the presence of radioactive glass samples, the voids within the modules could not be rinsed. However, it is likely that most of the oxygen in the modules was removed by dilution with argon.

For the small test tubes 2 and 5, the boom clay contacted (the upper part of) the test tube about 2 to 3 months after installation. For the larger test tubes 3 and 4, this took about 6 months. For test tubes 2 and 5, it took another six months before the total pressure around the test tube had reached a stable value of approximately 0.5-0.6 MPa (5-6 bar). Data on water pressures of the piezometer waters suggest that this total pressure was essentially due to the water pressure, *i.e.* the total pressure exerted by the expanded boom clay had dropped to almost 0 MPa. During this period of convergence and pressure build-up, boom clay pore water infiltrated the test tube modules through the porous outer support tube, and started to hydrate the backfill materials. This means that shortly after installation of the test tube the glass samples came in contact with humid clay, at a temperature of ~18 °C. Total pressure transmitters built-in in tube 5 revealed that the swelling pressure in module A (1.5-2.5 MPa) was close to the target pressure of 2 MPa. Swelling pressures in modules B and C were between 2.5 and 3.5 MPa. When the backfill materials were fully saturated, the temperature was slowly raised to 30 °C.

Hydration of the thicker layer of backfill material in the large test tubes 3 and 4 proceeded very slowly, and even ~1.5 year after their installation full saturation was not yet achieved. Hence, it was decided to install the ^{60}Co sources and to start the heating to 90 °C, assuming that, in analogy with the results of other tests on backfill material behaviour, about 95 % of the saturation was already achieved [13–15]. Moreover, we expected that the re-saturation would proceed faster at higher temperature, due to the lower viscosity of the pore water.

More details on the type of ^{60}Co sources and the way they were placed in and retrieved from the test tube can be found in [1]. ^{60}Co sources were placed in September 2002 (test tube 3) and March 2003 (test tube 4), respectively. The dose rate at the interface of the glass samples and the backfill materials at the time of installation was calculated to be respectively ~135 Gy/h and 125 Gy/h (Visiplan [3], and assuming 1.145 Sv = 1 Gy). This dose rate is lower than the one previously reported [1, 2], because 1 cm of lead was additionally placed around the central tube that hosts the ^{60}Co sources. It is close to the dose rate (in air) at the surface of a COGEMA canister with high-level vitrified waste with nominal radionuclide inventory, after approximately 100 years of cooling (after ~100 years, the temperature at the surface of the HLW canister is ~90 °C, *i.e.* an internationally applied reference temperature for glass alteration tests at high temperature). According to the same calculations, the dose rate at the end of the test was ~110 Gy/h for test tube 3 (on 20/2/2004), and will be ~60 Gy/h on 1.3.2009 (foreseen retrieval of test tube 4). For both test tubes, the installation of the ^{60}Co sources resulted in a temperature rise of ~4 °C at the inner support tube, due to gamma heating. Thus, the temperature at the interface glass-backfill increased to ~22 °C. After installation of the ^{60}Co sources, the temperature of the test tubes was slowly raised to 90 °C (temperature measured on the inner support tube).

[3] VISIPLAN 3D ALARA (as low as reasonably achievable) dose assessment programme. The code is based on a 3D model including material, geometry, and sources. The Point-kernel dose calculation method, with build-up correction is used. The code allows performing dose assessment for tasks, trajectories, and scenarios. It estimates individual and collective dose. Special tools are available for source sensitivity analysis and source strength determination from measured dose rate sets (www.visiplan.be).

For modules C and – especially – B of tube 3, it then still took another 6 to 8 months before full saturation was achieved. It remains unclear whether at the interface of the glass and the clay small compressed air or argon bubbles remained trapped, which dissolved only slowly in the pore water. This could perhaps explain the smaller glass dissolution and/or the thicker alteration layers (because they are still intact) observed for some glass samples of these modules (see Section 2.2.1).

Dry densities of the pre-compacted blocks, 'reduced' dry densities of the swollen backfill in the test tubes, and calculated pore volume (%) and mass % at full saturation are given in Table 2. The overall relative uncertainty on the 'reduced' dry density in the module is estimated to be less than 1 %.

Table 2 *Dry densities (g/ml) of the backfill materials in the pre-compacted blocks and in the test tube modules ('reduced' dry density), and calculated pore volume% and weight% of water in the backfill materials in the test tube modules at full saturation.*

Backfill material	Dry density of the pre-compacted blocks (g/ml)	'Reduced' dry density (in the module) (g/ml)	Calculated water volume % at saturation	Calculated weight % of water at saturation
A (DBC)	2.17	1.88	30	13.7
B (BSG)	2.17	1.88	30	13.7
C (BGF)	1.88	1.62	40	20.4

DBC = dried boom clay, BSG = bentonite with sand and graphite, BGF = bentonite with powdered glass frit.

2.1.2 Operation of the CORALUS test tubes (WP2)

The operation of the test tubes started when the target temperature was reached. During the operation of the test tubes, the following actions and measurements were (or still are being) performed:

- continuous monitoring of temperature and pore water pressure;
- regular sampling of the piezometer waters, for control for alpha contamination, and for measurement of the chemical composition of the solution and the type and amount of dissolved gases;
- online measurement of the pH and redox potential in the inner piezometer waters;
- measurement of the permeability of the saturated backfill material to water.

2.1.2.1 Evolution of the temperature and pore water pressure in the test tubes

As test tube 2 was installed in a downward angle of 45 ° and contained only one heating element for the entire test tube, the temperature varied with height within the test tube and within one module. The temperature differences within a module increased when the module was positioned higher. Therefore, the power of the heating element was tuned to achieve an average temperature of 30 °C. The corresponding temperatures (°C) on the inner support tube – measured at two different positions close to the glass samples – and on the outer support tube are presented in Table 3. The combined uncertainty on the recorded temperatures is estimated to be 2 °C (95 % confidence). Test tube 5 was also installed in a downward angle of 45 °, but contained three heating elements. This allowed achieving more comparable temperatures for the three modules (Table 3). Yet, due to the inclined position of the test tube, the temperature at the lower part of the module was always lower than in the upper part of the module.

Test tubes 3 and 4 were installed vertically, and contained one heating element per test tube, allowing achieving temperatures close to the target temperature of 90 °C. Yet, also in these test tubes, the temperature was always a little bit lower at the lower part of the module. The average temperatures over the whole operational period is summarised in Table 4. The large difference of ~10 °C between the two inner thermocouples on modules A and C of test tube 3 cannot be explained.

Table 3 *Average temperatures (°C) for test tube 2 (25.02.2001 to 08.04.2004) and for test tube 5 (04.07.2004 to 28.02.2006), measured on the inner support tube at two positions close to the glass samples, and on the outer support tube.*

Position on the test tube	**Module A: DBC (Bottom)**		**Module B: BSG (Centre)**		**Module C: BGF (Top)**	
	Tube 2	**Tube 5**	**Tube 2**	**Tube 5**	**Tube 2**	**Tube 5**
0 ° (non-radioactive samples*)	27 ± 2	32 ± 2	31 ± 2	33 ± 2	35 ± 2	32 ± 2
180 ° (Pu-doped samples*)	27 ± 2	28 ± 2	28 ± 2	27 ± 2	31 ± 2	28 ± 2
Outer support tube	25 ± 2	26 ± 2	26 ± 2	26 ± 2	26 ± 2	26 ± 2

DBC = dried boom clay, BSG = bentonite with sand and graphite, BGF = bentonite with powdered glass frit.
* The temperature close to the Np-doped and Am-doped samples (placed respectively at 90 ° and 270 °) is comprised between the two temperatures reported for each module.

Table 4 *Average temperatures (°C) for test tube 3 (05.12.2005 to 20.02.2004) and test tube 4 (for modules A and B, 15.04.2003 to 28.02.2006; for module C, 01.05.2003 to 28.02.2006), measured on the inner support tube at two positions close to the glass samples, and on the outer support tube.*

Position on the test tube	**Module A (DBC)**		**Module B (FSG)**		**Module C (BGF)**	
	Tube 3	**Tube 4**	**Tube 3**	**Tube 4**	**Tube 3**	**Tube 4**
Inner support tube, TC1	90 ± 2	88 ± 2	91 ± 2	89 ± 2	91 ± 2	92 ± 2
Inner support tube, TC2	82 ± 2	91 ± 2	89 ± 2	92 ± 2	80 ± 2	88 ± 2
Outer support tube	65 ± 2	66 ± 2	74 ± 2	71 ± 2	64 ± 2	66 ± 2

TC = thermo-couple.

After saturation of the backfill materials, the (relative) pore water pressure in the modules was around 0.7 MPa (7 bar) for the lower positioned module A, 0.65 MPa for the central module B, and 0.6 MPa for the higher positioned module C. For test tubes 2 and 5, the increase of the temperature to 30 °C resulted in a pore water pressure increase of 0.15 to 0.2 MPa because of the thermal expansion of water. During the following weeks, the pore water pressure decreased again to the normal values due to the dissipation of pore water into the surrounding boom clay. For test tubes 3 and 4, the increase of the temperature to 90 °C resulted in a pore water pressure increase of 0.5 to 0.8 MPa. Also for these test tubes, the expanded pore water was slowly dissipated in the surrounding boom clay, resulting in a decrease of the pore water pressure to values of about 0.9 MPa for test tube 4, and to values of 0.3-0.5 MPa for module A (DBC) of test tube 3. These values are lower than the expected values of 0.6-0.7 MPa for this depth, and suggest that the pore water around this test tube was flowing to another sink at low pressure. Indeed, the installation of test tube 3 necessitated repeated drillings, resulting in large volumes that had to be re-filled. Additionally, the highly expanded boom clay probably presented a preferential pathway for water flow towards the gallery (Section 2.1.1). Only towards the end of the operational duration, the pore water pressure in this module seemed to have reached a stable value.

In contrast to the dried boom clay in module A of test tube 3, the bentonite-based backfill materials in modules C and – especially – B were not saturated when heating started. The pressure increases due to the heating were much lower than for module A. During the following months, the pressures remained low and sometimes negative, indicating under-pressure due to suction, and showed a deviating behaviour (*i.e.* slow and unexpected response to pressure drops and increases) (Section 2.1.1).

During the operation of the test tubes, piezometer waters were regularly sampled (see next Section). Depending on the sampling method, this resulted sometimes in an important pore water pressure drop, which was also observed in the surrounding piezometers. Especially in the bentonite based backfill materials of modules B and C, it took several weeks or months – depending on the sampling method –

before the pressure had increased again to the normal values.

2.1.2.2 Sampling of the piezometer waters and online measurement of pH and redox potential

2.1.2.2.1 Sampling of the piezometer waters

The sampling of the piezometer waters had/has three purposes:

1. to measure the total alpha activity in the solution that surrounds the radioactive glass samples. These data are required by the Radiation Protection Service of SCK•CEN, as they are important with regard to a possible contamination of the surrounding boom clay.
2. to measure the type and amount of gases generated and released by heating and gamma radiation, and dissolved in the water. Based on the experience with the CERBERUS project [16], we did not expect a separate gas phase.
3. to measure the chemical composition of these solutions. These results give an indication of the composition of the pore water close to the glass samples.

In essence, the sampling consists of displacing the piezometer water through the outgoing tube towards a Teflon coated sampling container or a septum bottle by applying a gas pressure through the ingoing tube. During the operation of test tubes 2, 3, and 4, several variants of the sampling method have been applied. All these alternatives aimed at minimising the perturbation of the geo-chemical conditions at the level of the corroding glass samples, and at optimising the usefulness of the obtained results.

To minimise the perturbation upon sampling, the sampled piezometers were often re-filled with synthetic solutions that were prepared on the basis of the measured composition of the previously sampled pore waters. However, since the ionic composition of synthetic and pore water always differed, we decided in 2003 to stop re-filling the piezometers with synthetic solution, but to allow filling the piezometer with small amounts of pore water. We kept the volume of piezometer water to be sampled to a minimum of about 30 ml per sampling, to avoid or minimise the disturbance of the glass alteration and radionuclide leaching process.

When it was important to measure the type and amount of dissolved gases, the piezometer waters were displaced towards Teflon coated sampling containers that were repeatedly filled with nitrogen or argon, and evacuated afterwards (to ~0.005 MPa absolute), to remove the gases in the container prior to the sampling. Sampling of the piezometer waters through septum bottles (applied from 2003 onwards for determination of the chemical composition) resulted in a pore water pressure drop, and for test tubes 3 and 4, possibly in some loss of dissolved CO_2.

2.1.2.2.2 Online measurement of pH and redox potential

The pH and redox potentials were measured ‘online’ by means of flow-through cell (FTC) units that were connected to the piezometers [1]. We used combination electrodes that are filled with the solid Xerolyt polymer reference system (Mettler Toledo) – enabling to work at the *in situ* pore water pressure – and that have an open junction. The pH electrodes were calibrated (before measurement) and verified (after measurement) against Orion certified perpHect buffers pH 7 and 10, at atmospheric pressure, and at a temperature of 20 °C, that is the temperature in the underground laboratory. The redox electrodes were tested on their proper functioning using Orion certified perpHect buffers pH 7 and 10 to which quinhydrone was added. The solution in the piezometers in which the pH and redox potential was measured was either an (equilibrated) synthetic solution, or the real pore water. It took up to several weeks to reach, after an initial drop, a more or less stable value. At the end of the ~2 months measurement campaigns, drifts of the pH electrodes appeared to be relatively small, and varied between ~0.01 to ~0.15 pH units. Also redox electrodes were tested on their proper functioning after the measurement campaign. No malfunctioning electrodes were detected.

For all but one (test tube 4, 2005.05.05) measurements, the piezometer waters were circulated every hour during 12 minutes within the piezometer. This resulted in an important leakage of KCl and organics into the solution. The high K^+ concentrations might have affected the pH of the solutions (apparently lower pH values) by K^+-Ca^{2+} ion exchange with the surrounding clay and subsequent $CaCO_3$ precipitation ($Ca^{2+} + HCO_3^- \rightarrow CaCO_3 + H^+$; [17]). It is difficult to estimate the extent of this effect on the pH, but based on a comparison of the results for test tube 3 (with re-circulation) and test tube 4 (without re-circulation), we expect an effect of 0.1 pH units at most.

For test tubes 3 and 4, the temperature of the piezometer water decreased from 90 °C at the level of the test tube to 20 °C at the level of the electrodes. Due to practical and financial constraints, it was impossible to maintain for all inner piezometer waters of test tubes 3 and 4 the temperature at 90 °C over the whole measurement loop. We estimate that in the piezometer waters at 90 °C the pH was about 0.3 pH units lower than the measured values.

The results of the pH and E_h measurements are discussed in Section 2.1.2.5, together with the results of the analyses of the piezometer waters.

2.1.2.3 Total alpha activity of the piezometer waters

The total alpha activity of the sampled piezometers solutions was always below or just around the detection limit, demonstrating that after saturation the swelled backfill materials indeed constitute an effective seal for radionuclide migration. Alpha spectrometry revealed the presence of very small concentrations of ^{241}Am (0.26 Bq/l) and $^{238\text{-}239}$Pu (0.01 Bq/l) in the outer piezometer waters sampled before the start of the operation of tube 2, *i.e.* when the clay had not yeat sufficiently swelled to fill the initial small gaps between the backfill blocks.

Alpha spectrometry of the outer piezometer waters of test tube 2, sampled shortly before the retrieval of this test tube – scheduled February 2004 – revealed that the piezometer water A3 had a total alpha activity of 1.6 Bq/l, with 1.5 Bq/l of ^{241}Am and/or ^{238}Pu. It is very likely that this small but significant contamination in the outer piezometer was due to preferential flow during the re-filling of this piezometer with interstitial backfill water after the sampling of that piezometer. It is thus unlikely that the surrounding boom clay was contaminated (see Section 2.1.3.1).

2.1.2.4 Dissolved gases (GRS) [4]

2.1.2.4.1 Experimental aspects

When the specific total alpha activity of the piezometer waters was below the detection limit, the Teflon coated sampling containers were sent to GRS (Braunschweig, Germany) for measurement of the dissolved gases. Also samples of the synthetic solutions that were injected in the piezometers were analysed. The gases dissolved in the piezometer waters first had to be released into a larger volume of nitrogen at atmospheric pressure. This was achieved by repeated heating at 90 °C. Samples of the nitrogen gas phase, containing the released gases, were then injected into the gas chromatograph for qualitative and quantitative determination of the type and amount of dissolved gases. After each gas sampling, the rest of the residual volume was flushed with fresh nitrogen. The extraction was repeated three to four times, until the gas concentration released into the residual volume was less than 10 % of the concentration after the first heating. Despite the repeated extraction, it is likely that the total amounts of dissolved CO_2, being a reactive gas in water, were underestimated.

[4] This part has been described in detail in the detailed report of GRS.

2.1.2.4.2 Results

The most important dissolved gases in the piezometer waters were carbon dioxide, methane, and hydrogen. Additionally, hydrogen sulphide (almost below the detection limit of 0.2 litre gas per 1000 kg of solution), and further sulphur components were seen in the gas chromatograms. The water and the gases extracted from the different piezometers had a smell similar to hydrogen sulphide or mercaptans. Also oxygen was found, in varying concentrations. This is related to the different sampling methods applied, the residence time of the solution in the piezometer prior to the sampling, the use of argon during the first stage of the operation of the test tube (the gas chromatography system of GRS cannot distinguish between argon and oxygen), and possibly to oxygen intrusion during sampling, transport of the sampling containers, and handling in the laboratory. The results on the dissolved contents of CO_2, CH_4, and H_2 in the different piezometer waters of test tubes 2, 3, and 4 are summarised in Table 5.

Table 5 *Ranges of dissolved contents of CO_2, CH_4, and H_2 (expressed as litre gas dissolved per 1000 kg of solution), measured in the piezometer waters of test tubes 2, 3, and 4.*

		Tests tube 2 (30 °C)	Test tubes 3 and 4 (90 °C)
Module A (DBC)	**CO_2**	83 – 639	311 – 1029
	CH_4	1.0 – 105	< D.L. – 4.6
	H_2	< D.L. – 0.5	< D.L. – 2.2
Module B (BSG)	**CO_2**	23 – 141	194 – 600
	CH_4	< D.L. – 76	< D.L. – 2.1
	H_2	< D.L. – 0.1	2.0 – 26
Module C (BGF)	**CO_2**	36 – 165	125 – 466
	CH_4	< D.L. – 0.8	< D.L. – 2.0
	H_2	< D.L. – 0.4	< D.L. – 69

DBC = dried boom clay, BSG = bentonite with sand and graphite, BGF = bentonite with powdered glass frit.

The results in Table 5 show high variations, especially for CH_4 and H_2. These were caused by:

1. Different degrees of dilution as a result of the removal of the piezometer waters and the subsequent renewal of the extracted volume with synthetic or pore water, in combination with different equilibration times (different time periods between the different samplings).
2. Diffusion of the gases from the area close to the heater into the surrounding host rock, again in combination with different time periods between the different samplings.
3. Insufficient gas tightness of the different compounds used in the measurement chain (piezometer valves, sampling container and sampling container valves, etc.), as evidenced by the sometimes high oxygen concentrations.
4. Microbial activity in the piezometer waters of test tube 2, especially affecting the methane concentration.

These variations hamper the interpretation of the results. Yet we can make some conclusions.

CO_2 was the most important gas, both in test tube 2 (30 °C) and in test tubes 3 and 4 (90 °C and gamma radiation). The differences between the lower and the upper values were relatively small, on the average about a factor of 5. The contents in the solutions of module A (DBC) were (in most cases) considerably higher than in the solutions from the modules filled with the Ca-bentonite based backfill materials (BSG and BGF). In addition, CO_2 concentrations in test tubes 3 and 4 were a factor 2 to 5 higher than the amounts dissolved in the piezometer waters of test tube 2. These two observations are related to *(i)* the fact the partial CO_2 pressure in boom clay is $10^{-2.42}$ atm. (3800 Pa) [17], and *(ii)* – especially for test tubes 3 and 4 (90 °C, ^{60}Co sources) – the thermal and the radiolytic decomposition of the organic matter (kerogen fraction) in the (dried) boom clay (host formation and backfill) and graphite (module B, BSG) [18-20]. The importance of the thermal CO_2 generation was confirmed by the surface laboratory experiment on thermal gas generation (Section 2.3).

Based on these amounts of dissolved CO_2, and using the equations and equilibrium constants at 20 °C and 100 °C for carbonate equilibria published in [21], the partial CO_2 pressure in a sampled solution can be calculated as a function of the pH in that solution. The results for the solution sampled from piezometer A1 in test tube 3 on 2003.08.06 (674 litre per 1000 kg of solution, or: 361 mg/l or 30 mM inorganic C), and for a few typical pH values are summarised in Table 6 below (for the calculations at 100 °C, we have assumed that the pH at 100 °C is 0.3 pH units lower than the pH measured on line at 20 °C, see Section 2.1.2.2.2). It is seen that especially at 100 °C the partial CO_2 pressure reaches very high values, exceeding 1 atm. As a result, opening the piezometer valves will result in a pressure drop and in some release of dissolved CO_2. This may have a pH increasing effect when the pH is measured at atmospheric pressure, as was the case for the pH measurement for test tube 4 (see Section 2.1.2.5).

Table 6 *Partial CO_2 pressure as a function of pH for a total amount of dissolved CO_2 of 674 litre per 1000 kg of solution (or a total amount of inorganic carbon of 361 mg/l or 30 mM), at 20 °C and 100 °C (based on equations and data in [21]).*

pH	Log (partial CO_2 pressure)	Partial CO_2 pressure (atm.)
Temperature = 20°C		
6.0	-0.263	0.55
6.5	**-0.477**	**0.33**
7.0	-0.825	0.15
Temperature = 100°C		
5.7	0.347	2.22
6.2	**0.225**	**1.68**
6.7	-0.025	0.94

The data in bold are the most realistic values (that is, based on the pH value measured on line; see Section 2.1.2.5).

In contrast to CO_2, the CH_4 contents in the waters differ widely, up to a factor 100. For test tube 2 (30 °C), it is likely that methane is produced by methanogenic bacteria which grow in the piezometers, and which consume hydrogen and dissolved CO_2. This might – at least partially – explain the differences observed for the dissolved gas contents for test tube 2, and possibly also some of the differences observed for the ionic composition (see Section 2.1.2.5). Such influence of bacterial activity on the ionic composition and on the type and amount of dissolved gases in piezometer waters was also reported for the Mont Terri pore water chemistry experiment [22]. Recent experimental results reported by Ortiz and co-workers provide evidence for the transformation of hydrogen by bacteria in boom-clay slurries [23]. These typically anoxic bacteria were presumed to be naturally present in the boom-clay formation, which is a marine sediment. Microbial activity could have taken place during sedimentation of the boom clay, as suggested by the rather high natural organic matter and pyrite contents of the clay (both up to 5 weight %). However, the metabolic rates of these bacteria are supposed to be very low in undisturbed compact boom clay because of space and water restrictions. It is unlikely that methanogenic bacteria are present in the piezometer waters of test tubes 3 and 4, because of the high gamma radiation dose rates (> 100 Gy/h) and the high temperature (90 °C). The hydrogen contents were mostly very low. This is in agreement with the results of the CERBERUS experiment, where the results indicated that no separate hydrogen gas phase was formed in the clay around the gamma radiation field [16].

2.1.2.5 Composition of the piezometer waters

After sampling, part of the piezometer waters were filtered over a 0.45 µm membrane filter and analysed by ICP-AES[5], IC[6], ion selective electrode (F^-), and total DOC/IC[7] measurement. The 95 % uncertainties on the results typically are 10 % for ICP-AES and ion-selective electrodes, 5 % for IC, 8-12 % for total DOC, and 10 % for total DIC. The range of concentrations of the different elements and substances in the *representative* sampled piezometer waters is given in Table 7 (for instance, the composition of the solutions containing high KCl concentrations from the pH and E_h measurements was not considered). The table also comprises the data on the estimated (calculated) HCO_3- concentration and on pH and redox potential (see Section 2.1.2.2.2). It is important to note that the results in Table 7 apply to the piezometer waters. It is very likely that the composition of the pore water at the glass/clay interface differed from these solutions. This will be especially the case for the elements that are also present in the SON 68 glass samples.

Table 7 *pH, E_h, and ranges of concentrations (meq/l) of major cations and anions and total organic carbon (TOC) in the inner piezometer waters. Except for $B(OH)_3$ and $Si(OH)_4$, the higher concentrations were usually measured in the early phase of the tests, whilst the lower concentrations were usually found towards the end of the test. The first pH value was measured at the beginning of the test, the second value at the end of the test.*

	Tube 2 (30 °C, no ^{60}Co sources)			**Tube 3 and 4 (90 °C, ^{60}Co sources)**		
	module A	**module B**	**module C**	**module A**	**module B**	**module C**
Na^+	50–117	15–20	11–31	47–84	12–26	23–48
K^+	3.1–4.7	0.3–0.4	0.1–0.3	3.5–4.3	0.2–0.4	0.3–0.4
Mg^{2+}	14–31	2.1–2.8	1.6–2.6	10–22	0.7–2.6	0.2–0.7
Ca^{2+}	16–25	19–25	22–31	13–18	4.8–23	6.1–30
$B(OH)_3$	1.1–1.8	<0.2–2.6	43–56	3.5–4.1	0.2–2.8	88–211
$Si(OH)_4$	0.1–1.4	<0.5–0.2	0.5–0.7	0.2–0.3	0.2–0.3	0.9–2.8
F^-	0.1–0.1	<0.01–0.04	0.04–0.3	0.04–0.09	0.05–0.11	0.02–0.1
Cl^-	3.2–5.8	3.0–3.8	3.3–4.1	2.4–3.5	1.0–8.0	2.9–8.3
SO_4^{2-}	73–153	33–41	30–47	90-103	11–29	32–65
$HCO3^{-*}$	9.7–13	0.3–2.4	1.2–3.7	3.9–6.7	1.8–4.3	0.4–3.5
total DIC**	10–14	0.3–2.7	<0.1–4.0	0.7–8.7	<0.1–5.2	0.5–2.0
total DOC	6.5–56	1.5–5.8	1.1–23	29–55	8.8–11	1.7–13
pH (20 °C)	7.9 → 7.4	7.3 → 7.4	6.8 → 6.2	6.4 → 6.1	5.9 → 5.5	6.6 → 6.6
pH (90 °C)$^{\$}$	–	–	–	6.1→ 5.8	5.6 → 5.2	6.3 → 6.3
E_h	-340 – -360	-310 – -170	-200 – -250	-40 – -80	0 – -80	-80 – -80

* Derived from total DIC and from data on dissolved gas contents.
** Data are less reliable because of degassing of the solution before analysis.
$ assuming that the pH at 90 °C is 0.3 pH units lower than the value at 20 °C.

From Table 7, it is seen that the composition of the pore waters of all three backfill materials is fingerprinted by the high Na_2SO_4 concentration occurring in the partially oxidised surrounding boom clay. Oxidation of pyrite, which in boom clay is present in 1-5 wt %, finally results in the production of SO_4^{2-}, $FeCO_3$, FeOOH, and H^+. The thus generated protons in turn dissolve calcite, and the released Ca^{2+} ions ion exchange with Na^+, K^+, and Mg^{2+} on the solid phase [16, 24, 25]. In module A, with DBC, this effect of pyrite oxidation is of course more pronounced. The sulphate concentrations in test tube 3 (90 °C) are not so much higher than in test tube 2 (30 °C). Therefore, if sulphate is formed by radiolysis of the boom clay, as considered in [16], this contribution of radiolytically formed sulphate is small compared to the

[5] ICP-AES = inductively coupled plasma – atomic-emission spectrometry.
[6] IC = ion chromatography.
[7] Total DOC/IC = total dissolved organic carbon/inorganic carbon. We define here the total dissolved organic and inorganic carbon content as the concentration in the filtered solutions (< 0.45 µm).

amount produced by oxidation of pyrite due to exposure to oxygen. The thiosulphate concentration was usually below the detection limit (results not shown), but this is probably linked to the instability of this species. Thiosulphate is important regarding the pitting corrosion of stainless steel [16, 25, 26], and deserves therefore more attention in future analyses. For both test tubes 2 and 3, the $B(OH)_3$ and $Si(OH)_4$ concentration in module A (DBC) was higher than in undisturbed boom clay. Also in the CERBERUS project, higher concentrations of $B(OH)_3$ and $Si(OH)_4$ were observed for oxidised and heated boom clay, compared to undisturbed boom clay [16,25]. This is due to the liberation of initially unavailable $B(OH)_3$ upon heating of boom clay, which is a marine sediment (the boron concentration in seawater is 4×10^{-4} M [21]).

For modules B and C, with a bentonite-based backfill material, the composition of the piezometer waters is the result of the interaction between the backfill material itself and the percolating oxidised boom clay water. The piezometer waters contain high concentrations of Na^+ and SO_4^{2-} originating from the oxidation of the surrounding boom clay, and possibly from the oxidation of (small amounts of) pyrite during the pre-treatment of the Ca-bentonite after excavation (drying and grinding) and/or during the re-saturation phase [27]. The higher Na_2SO_4 concentration and the lower pH in module C, with 95 wt % of Ca-bentonite, is in line with this (backfill BSG in module B contains only 65 wt % of bentonite). In addition to this, the higher Na^+ concentration in module C than in module B can be due to the dissolution of the powdered glas frit, containing 7.2 wt % of Na_2O (see below). Na^+-Ca^{2+} ion exchange with the Ca-bentonite may (partially) account for the high Ca^{2+} concentration. The dissolution of gypsum may also have contributed to the high concentrations of Ca^{2+} and SO_4^{2-}.

The piezometer waters from module C, with the Ca-bentonite with powdered glass frit, contain also very high concentrations of $B(OH)_3$, higher concentrations of Na^+ and Ca^{2+}, and a slightly higher total Si concentration, compared to the solutions from module B, with the Ca-bentonite with sand and graphite. The higher B and Si concentrations, and possibly also (partially) the higher Na^+ and Ca^{2+} concentrations, originate from the dissolution of the powdered glass frit in the backfill of module C. The powdered glass contains 58.7 wt % SiO_2, 18.3 wt % B_2O_3, 7.2 wt % Na_2O, 5.4 wt % CaO, and has a large specific surface (> 87 cm²/g, if we assume spheres with diameter of 0.25 mm and density of 2.75 g/ml), enabling high dissolution rates. For module C of test tube 2, it should be noted that still higher B and Si concentrations were measured in small scale integrated tests performed in a surface laboratory (30 °C), using the same type of backfill material (BGF) [28]. These higher concentrations are probably due to the fact that these integrated tests were closed systems, whereas the CORALUS integrated tests were open systems, enabling dissolved B and Si to diffuse into the surrounding boom clay. The higher B and Si concentrations in module C of test tube 3 compared to test tube 2 is due to the fact that the dissolution of the powdered glass frit is much higher at a temperature of 90 °C.

HCO_3^- contents were calculated on the basis of (*i*) the amount of 'dissolved CO_2' (as measured by GRS; see Section 2.1.2.4) or the total DIC content (determined at SCK•CEN) and (*ii*) the pH dependent speciation distribution of H_2CO_3 – HCO_3^- – CO_3^{2-} at 25 °C (test tube 2, 30 °C) and 100 °C (test tubes 3 and 4, 90 °C), as calculated from the equations and equilibrium constants for carbonate equilibria published in [21], using the pH values that were measured online (for test tubes 3 and 4, these values were corrected for the temperature difference). Due to the uncertainties on the various input values, the uncertainty on these HCO_3^- contents is high, and the values are probably underestimated. In fact, they can only be used to demonstrate the higher amount of dissolved inorganic carbon – especially dissolved CO_2 – in the DBC (module A) of both test tubes, with very high values for test tube 3. These high values are due to the thermal and radiolytic decomposition of boom clay organic matter.

The pH values are corrected for the drift of the pH electrode. The uncertainty on the pH measurements is not exactly known, but probably does not exceed 0.5 pH unit. The uncertainty on the redox potential measurements is not known, and the measured values give only an indication of the redox conditions in the piezometers. Negative redox potentials therefore suggest that reducing conditions prevailed in these piezometer waters. This is not surprising given the omnipresence of stainless steel (piezometer, connecting tubes) in the system. Hence, care has to be taken in concluding on the redox conditions within

the modules. Yet, it is likely that shortly after full saturation of the backfill materials all dissolved oxygen was consumed by reaction with backfill constituents, stainless steel of the test tube, and, for test tube 2, microbial activity. For test tube 3, redox potentials were less reducing, which is in line with the lower pH (see below), and which is perhaps also due to the net production of oxidising radicals in these closed systems.

For test tube 2 (30 °C), the pH of the piezometer waters varied from slightly alkaline for module A (DBC, 7.9 to 7.3) and module B (BSG; 7.3 to 7.4)) to slightly acidic for module C (BGF; 6.8 to 6.2). For the dried boom clay, the pH was slightly lower than for undisturbed boom clay, which is due to its partial oxidation. During the test, the pH in module A tended to decrease further, indicating that the oxidation of the dried boom clay continued. The oxidation of traces of pyrite in the Ca-bentonite in modules B and C – during the excavation stage of the bentonite [27] and/or during the re-saturation phase during the test – may account for the relatively low pH in these modules. The higher amount of Ca-bentonite in module C (BGF, 95 wt % Ca-bentonite) could thus explain the lower pH in this module compared to module B (BSG, 65 wt % Ca-bentonite). The lower pH in module C than in module B is possibly also due to the dissolution of B_2O_3 in the powdered glass frit. Simple geochemical calculations with the CEA LIXIVER 1 code [29] show that addition of $B(OH)_3$ to pure water at 30 °C (pH 5.7) decreases the solution pH with 0.5 units (for 600 mg/l $B(OH)_3$, as for test tube 2) to 0.6 units (for 1200 mg/l $B(OH)_3$, as for test tubes 3 and 4). Yet, the dissolution of glass is generally known to increase the pH due to the reaction $SiONa + H_2O \rightarrow SiOH + Na^+ + OH^-$ [30]. A similar reaction can be written for $(SiO)_2Ca$ groups, with the hydrolysis of these groups proceeding slower due to the stronger binding of the bivalent Ca^{2+}. This apparent discrepancy can be explained by the almost two times higher B/Na ratio in the powdered glass frit (B/Na = 2.26) than in the SON 68 glass (B/Na = 1.23; see Section 2.1) for which the pH increase is always reported. In combination with the high specific surface of the powdered glass frit (> 87 cm²/g, if we assume spheres with diameter of 0.25 mm and density of 2.75 g/ml), this results in a faster dissolution of the powdered glass frit than the SON 68 glass, and in a subsequent high release of B (for Si, this is less clear because of the precipitation and secondary phase formation involving Si) and, to a smaller extent, Na^+ and Ca^{2+}. Also in small scale integrated tests performed in a surface laboratory (30 °C) and using the backfill material with 95wt % Ca-bentonite and 5 wt % powdered glass frit, the pH of the pore water had a tendency to decrease from ~8.2 at the start of the glass dissolution test to ~7 after two years [28]. The pH in module C (BGF) of test tube 2 tended to decrease during the test, which is to be ascribed to the continuing dissolution of the powdered glass frit.

For test tube 3, pH values were still lower, due to the generation of CO_2 upon thermal and radiolytic decomposition of organic matter (especially in DBC) and carbon (in BSG) [18–20]. The real pH values at 90 °C were even ~0.3 units lower, due to the lower ionic product of water (the log*K* of pure water ($[H^+].[OH^-]$) decreases from 14 at 25 °C to ~12.4 at 90 °C). Taking into account the relationships between dissolved CO_2 and pH as published by Stumm and Morgan [21], we can conclude that the results on the dissolved CO_2 agree fairly well with the results of the on line pH measurements.

The pH values obtained for tube 4, using a slightly adapted procedure (no re-circulation of the piezometer water, which was moreover at atmospheric pressure) yielded values that were slightly higher than for test tube 3 (6.3 for DBC, 6.3 for BSG, and 7.0 for BGF; for 20 °C). This is likely due to the release of dissolved CO_2 from the solutions, which were calculated to be oversaturated in CO_2 (Table 6). Also the lower K^+ concentrations in these solutions, and the related lack of acidification due to K^+/Ca^{2+} ion exchange and subsequent $CaCO_3$ precipitation (see Section 2.1.2.2.2), may have contributed to a higher pH value. In contrast, redox potentials are much less negative: this is likely due to the intrusion of oxygen from the septum bottle.

For test tube 3, the solutions contained also very small concentrations of oxalate (0.05-0.2 mM, with the higher values for DBC, and the lower values for BSG and BGF). Oxalate was most probably formed by the radiolysis of humic substances (decarboxylation of carboxylic functional groups and recombination of the $^{\bullet}COO^-$ radicals [31]). Oxalate, a dicarboxylic anion, can form complexes with many radionuclides. Stable complexes of oxalate with radionuclides could increase the solubility and reduce the sorption of

these radionuclides, subsequently increasing their migration. Experimental and theoretical studies [32-34] demonstrated that the complexing capacity of oxalate is small in solutions that are normally to be considered in geological disposal studies (with high concentrations of competing ligands such as OH^-, HCO_3^-, organic ligands, etc.), and that there is no or only a small negative effect of oxalate to be expected.

2.1.2.6 Effective permeability of the backfill materials to water [8]

From the water pressure build-up curves obtained after closure of a piezometer following previous release of the initial water pressure, the effective permeability to water can be derived [35]. For test tube 2, module B (BSG), the permeability to water measured at the end of 2003 (that is, after about three years of operation), was 2×10^{-18} m². The values for modules A (DBC) and C (BGF) of this test tube were more or less the same, but the uncertainty on these values was somewhat higher. These values are about three times higher than the value of 6×10^{-19} m² measured for module A of test tube 1 [1]. This latter test tube was heated for three months at 90 °C. The difference between these two values possibly gives an indication of the uncertainty on the permeability values. The effective permeability to water of slightly disturbed boom clay is also about 5×10^{-19} m² [36]. Values for the bentonite-based materials were of the same order of magnitude. In any case, these values are low, and they demonstrate the good sealing properties of pre-compacted clay materials.

The water pressure build-up curves for the three modules of test tube 3 could not be interpreted satisfactorily, so that the permeability to water for the backfill materials in these test tubes is not known. We will repeat the test in the future with the piezometers of test tube 4.

2.1.3 Retrieval and dismantling of test tubes 2 and 3 (WP3)

2.1.3.1 Retrieval of the test tubes

Alpha spectrometry of the outer piezometer waters of test tube 2, sampled shortly before the retrieval of this test tube – scheduled February 2004 – revealed that the piezometer water A3 (DBC) had a total alpha activity of 1.6 Bq/l, with 1.5 Bq/l of ^{241}Am and/or ^{238}Pu. Even if it was unlikely that the surrounding boom clay was contaminated, it was decided to implement extra safety measures to prevent that during the overcoring of the test tubes the underground research facility would be contaminated. As a result, the retrieval of the test tubes, scheduled in February and April 2004, respectively, had to be postponed to May-June 2004.

It was agreed to drill away the clay around the 4 m long extension tubes by means of the overcoring technique. For the removal of the clay around the test tube, a specially designed ‘twisted drill’ was used. This implied that this drill had to be withdrawn frequently to remove the clay adhering on it. In addition, to be able to keep under control any release of radioactivity, these manipulations were performed in a ventilated tent, constructed around the drilling machine. Especially for the large test tube 3, the drilling of the clay proceeded very slowly. Nevertheless, we succeeded in retrieving this test tube after five days of drilling. The retrieval of the smaller test tube 2 was achieved after two days of drilling.

[8] This part has been described in detail in the detailed report of GRS.

2.1.3.2 Dismantling of the test tubes

The dismantling of the test tubes took place in a ventilated tent with continuous monitoring of the radioactivity in the air. All actions were performed by a team of two persons, protected by means of an overpressure suit with external clean air supply. Per intervention, the maximum working time was 2 hours. Outside the tent, a third person provided assistance and supervision.

By means of a stationary drilling machine, cores were taken of the backfill material in contact with glass samples. The diameter of the cores was 19 mm, the length was ~30 mm for the small test tubes and ~45 mm for the large test tubes. For module A (DBC), we succeeded in sampling the complete cores, *i.e.*, the clay detached nearly completely at the glass/clay interface. For the bentonite-based backfill materials in module B (BSG) and module C (BGF), the bentonite in contact with the glass surface remained stuck on the glass.

Next, the outer support tube was cut in two half-cylindrical parts and removed. The remaining backfill material was then cut in pieces that were stepwise taken away from the module. Macroscopically, the backfill materials appeared to be very homogeneous, and had filled the complete module. Yet, for test tube 3, and especially for the Ca-bentonite-based backfill materials, the re-saturated backfill fell easily apart in the initial pre-compacted blocks, with the original pattern of the edges still visible. These backfill materials were relatively dry, and therefore probably too stiff to creep to achieve a backfill material with a homogenous water content and density. Similar observations were made during the dismantling of the OPHELIE[9] mock-up, which was a surface test to prepare the *in situ* testing of a full scale disposal gallery, backfilled with a bentonite-based material, in boom clay [39].

The water contents (volume % and weight %) as calculated from the particle density and the dry density of the swollen backfill material (*i.e.* the reduced dry density) and the water content measured at the end of the test are summarised in Table 8. It is seen that the measured water contents are always lower than the calculated water contents. This is especially the case for the bentonite-based backfill materials of module B (BSG) and C (BGF), and the difference is higher for test tube 3. As at the end of the test the backfill materials in all modules were saturated (see Section 2.1.2.1), this means that there was not sufficient space to accommodate the (calculated amount of) water. Consequently, the dry density of the backfill material in the centre of the module (that is, in the core of the pre-compacted bricks, where the samples for the measurement of the dry weight where taken from) was higher than the expected 'reduced' dry density (see Table 2). Dry densities were determined by weighing according to the Archimedean principle on the clay samples that were used for the measurement of the dry weight. The results are summarised in Table 9. In this table, also the dry density of the pre-compacted backfill and the theoretical 'reduced' dry density of the swollen backfill are given, together with the respective calculated water contents. It is seen that the measured dry densities fall between the dry density of the pre-compacted bricks and the target 'reduced' dry density. Thus, there seems to be some gradient of denser backfill material in the centre and lower density material towards the borders of the module (which could swell more because of the initial gap between the pre-compacted backfill blocks and the surrounding test tube module). Due to the lack of data, we do not know the pattern of this gradient. Probably, the clay at the borders has a density that is slightly below the target reduced dry density. This is important for the determination of the radionuclide migration profiles (see Section 2.2.3). The measured water content agrees qualitatively with the calculated values, but the difference between both values is sometimes large. This is especially the case for module C (BGF), with 5 wt % of powdered glass frit. Possibly, the dissolution of the powdered glass frit during the test resulted in changing parameters (average particle density, dry density).

[9] OPHELIE = on-surface preliminary heating simulation experimenting later instruments and equipments.

Table 8 *Calculated and measured water contents of the re-saturated backfill materials.*

	'Reduced' dry density (g/ml) *	Calculated volume% of water at saturation	Calculated weight % of water at saturation	Measured weight % of water	Measured/ calculated weight % of water
	Test tube 2 (30 °C, no ^{60}Co)				
A (DBC)	1.88	29.6	13.7	12.2	0.89
B (BSG)	1.88	29.6	13.7	9.3	0.68
C (BGF)	1.62	41.5	20.4	15.1	0.74
	Test tube 3 (90 °C, with ^{60}Co)				
A (DBC)	1.88	29.6	13.7	11.1	0.81
B (BSG)	1.88	29.6	13.7	9.2	0.67
C (BGF)	1.62	41.5	20.4	11.2	0.55

DBC = dried boom clay, BSG = bentonite with sand and graphite, BGF = bentonite with powdered glass frit.
* The reduced dry density is the density in the module (after swelling of the pre-compacted backfill material).

Table 9 *Calculated water contents of the pre-compacted backfill materials, and comparison with the measured water content at the end of the test.*

	Pre-compacted brick		Experimental value		Target values (full saturation)	
	Dry density[1] (g/ml)	water content (weight %)	Dry density (g/ml)	water content (weight %)[2]	Dry density[3] (g/ml)	water content (weight %)
Test tube 2 (30 °C, no ^{60}Co)						
A (DBC)	2.17	7.9	2.12	8.9 / 12.2	1.88	13.7
B (BSG)	2.17	7.9	1.99	11.3 / 9.3	1.88	13.7
C (BGF)	1.88	14.1	1.84	11.8 / 15.1	1.62	20.4
Test tube 3 (90 °C, with ^{60}Co)						
A (DBC)	2.17	7.9	2.08	9.6 / 11.1	1.88	13.7
B (BSG)	2.17	7.9	1.99	11.3 / 9.2	1.88	13.7
C (BGF)	1.88	14.1	1.69	18.3 / 11.2	1.62	20.4

DBC = Dried boom clay, BSG = Bentonite with Sand and Graphite, BGF = bentonite with powdered glass frit.
[1] The dry densities measured on the backfill material agreed very well with these target values (that were taken from literature [37, 38]).
[2] Two values are given: the theoretical value (determined from the particle density and the measured dry density), and the measured water content.
[3] This is the reduced dry density (see Table 8).

After removal of the backfill material, the glass samples could be retrieved. Especially for the bentonite-based materials, part of the clay remained stuck on the glass samples. Most of the samples were broken, some of them in two or three pieces only, but other samples in more pieces. Some of the glass samples that were not broken (at least not at first sight) broke during further manipulations.

At the end, cores were also taken from the half-cylindrical backfill blocks that were removed from the test tube (before the removal of the outer support tube, a small hole was drilled into the backfill to indicate the position of the respective (duplicate) glass samples). However, this sampling of the clay after removal of the glass sample often resulted in fissuring of the clay during the insertion of the sampling tube, because the backfill was no longer confined.

Each glass sample was placed in a polystyrene container with a wet paper tissue – separated from the glass sample by means of an aluminium sheet – to prevent the alteration layer from drying out. Per module, these small containers were stored in a larger container that in turn was packed in a plastic bag.

The sampled clay cores were closed with of a protective cap with wet paper tissue, tightly packed in plastic foil, and afterwards double-packed in two plastic bags. The ^{237}Np-doped and $^{238\text{-}240}$Pu-doped glass samples and the clay cores were stored in a refrigerator (~4 °C). The highly radioactive ^{241}Am-doped glass samples were stored at ambient temperature in a lead-shielded box.

2.1.4 Transport of the radioactive glass and clay samples

Part of all the radioactive glass samples could be sent without problems to CEA-Valrhô (France). Part of the clay samples in contact with the non-radioactive glass were sent to CEA-Cadarache (France). The preparation of the transport of part of the radioactive glass samples to PSI (Switzerland) was much more complicated. It took several months before all documents permitting this transport were available. This contributed largely to the overall delay of the CORALUS-2 project.

2.2 Treatment and analysis of the glass and clay samples (WP5) [10]

2.2.1 Treatment and analysis of the glass samples

2.2.1.1 Treatment of the glass samples

After dismantling of the test tubes, the glass samples were treated to remove the adhering clay. In general, there was little clay on the surface of the glass samples in contact with the dried boom clay (module A). The bentonite-based backfill material, especially the one with 95 wt % of Ca-bentonite (BGF), adhered stronger on the glass samples (Figure 3).

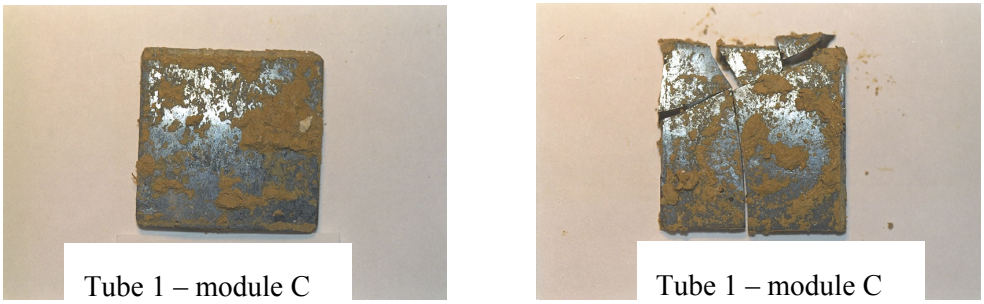

Figure 3 *Non-radioactive glass samples after retrieval from module C (BGF) of the dummy test tube 1 (3 months at 90 °C), with bentonite-based backfill still sticking on it. On the left an intact glass sample (no clay sampling), on the right a broken glass sample (the clay in contact with the glass sample was sampled before: the circular impress of the sampling tube is still visible).*

For some glass samples, cleaning with a mild spray of de-ionised water was sufficient. For other samples, the clay was removed with a soft paint brush. These samples were afterwards also rinsed with a mild water spray. All useful (sub)samples were carefully dried with paper tissue before being stored again in small plastic containers that contained a humid tissue, separated from the glass sample by means of an aluminium sheet. Samples that – at least at first sight – were still intact were gently rinsed with ethanol and allowed to dry about ten minutes in a ventilated box before weighing.

Finally, the intact glass samples and the large sub-samples were broken into smaller sub-samples for further analysis. For the non-radioactive samples, the bottom part of the sample was sawn to a depth of ~1.5 mm (the alteration layer was not touched). The sample could then easily be broken in rectangular sub-samples. The radioactive samples were broken with a hammer and a chisel, after putting the glass sample on a concave support with the alteration layer below, and after having carved the bottom part of the sample with a glass cutter. With this technique, it was possible to produce useful small sub-samples

[10] This part has been described in detail in the detailed reports of SCK•CEN, CEA-Valrhô, and CEA-Cadarache.

without generating a lot of dust that would have been produced by sawing the samples. However, during microscopic examination of these glass samples, it appeared that they were heavily fissured.

The glass samples were then submitted to a detailed characterisation programme. The samples in contact with the DBC and BSG were analysed by the SCK•CEN, the glass samples in contact with the BSG backfill material were analysed by the CEA-Valrhô.

2.2.1.2 Mass loss

The results of the mass loss of the unbroken glass samples (including those in contact with module C, with BGF) are expressed as specific daily mass loss (Table 10). These few results should be interpreted with caution, because *(i)* on all glass samples very small quantities of clay (as a thin 'film' layer) were still present (the results for the glass samples in module C (BGF) of test tube 2 may give an indication of the weight of this clay film), and *(ii)* we cannot exclude that very small glass fragments split off during the test or manipulations. However, in case the two duplicate samples were not broken (n=2), the difference between the two values was smaller than 15 %. This may indicate that the results are possibly still fairly reliable. The value for the Np-doped glass in DBC of test tube 2 is not realistic.

Table 10 *(Average) specific daily mass loss (g/m²/day) of the SON 68 glass samples.*

		Test tube 2	Test tube 3			Test tube 2	Test tube 3
DBC	**U+Th**	0.0093 (n = 2)	no data	**BSG**	**U+Th**	0.0075 (n = 2)	no data
DBC	**Np**	0.0008 (n = 1)	no data	**BGF**	**U+Th**	-0.0019 (n = 2)	no data
DBC	**Am**	0.0143 (n = 1)	0.301 (n = 2)	**BGF**	**Np**	0.0013 (n=1)	no data

DBC = dried boom clay. BSG = Ca-bentonite with sand and graphite. BGF = Ca-bentonite with powdered glass frit.

The results in Table 10 allow making the following two observations that are fully in agreement with the expectations. First, the specific daily mass loss is considerably higher (about 20 to 30 times) at 90 °C than at 30 °C. Second, the addition of powdered glass frit to the backfill material reduces significantly (a factor of ~10) the glass corrosion rate. The specific daily mass loss for BSG is fairly similar to the value for DBC. The difference between active and inactive samples, if significant, is small. The results of Table 10 are discussed in more detail in Section 2.5.

2.2.1.3 SEM-EDS [11] of surface and cross-section

The surface and the cross section of all glass samples was analysed by SEM and EDS. For the U/Th-doped samples in contact with DBC (module A) and BSG (module B) at 30 °C, SEM of the surface revealed that the surface was homogeneously covered with isolated spots of limited alteration (Figure 4). Polishing lines were still visible, as well as a few small cavities that are remainders of gas bubbles occluded during the casting of the glass. The radioactive samples appeared to be more severely altered. Traces of the polishing lines were no longer visible. The alteration of the samples in contact with BGF (module C) at 30 °C was, as could be expected, very limited. At 90 °C, the glass samples from modules A (DBC) and B (BSG) were much more altered, and no difference could be seen between non-radioactive and radio-active samples (Figure 5). The alteration layers of these samples were heavily fractured, most likely due to drying out during the preparation of the samples for SEM-EDS. At several spots, the alteration was locally more important, with resulting loss of part of the alteration layer (this occurred most probably due to manipulation of the sample). For the samples of module C (BGF), the surface alteration was, just as for 30 °C, very limited.

[11] SEM-EDS = scanning electron microscopy – energy-dispersive X-ray spectrometry.

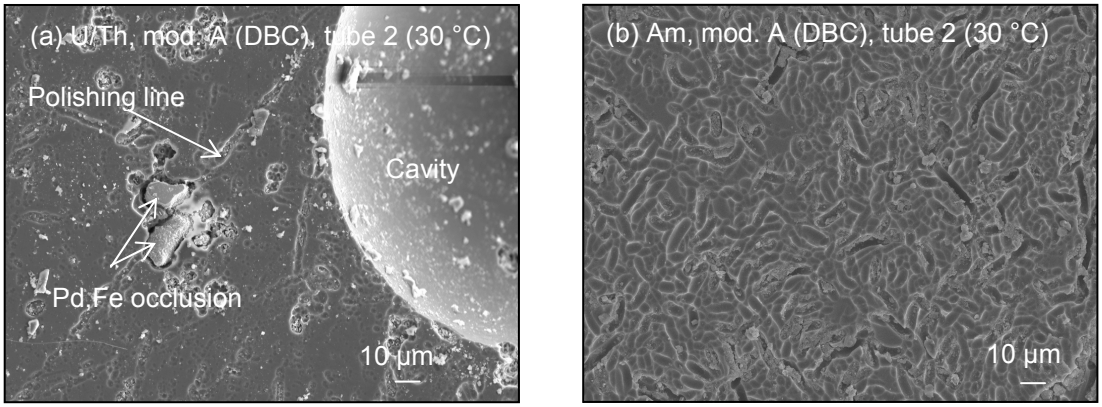

Figure 4 *SEM observation of the surface of in situ corroded U/Th-doped (left, a) and Am-doped (right, b) SON 68 glass sample of module A (DBC) after 3.3 years at 30 °C; magnification 500×.*

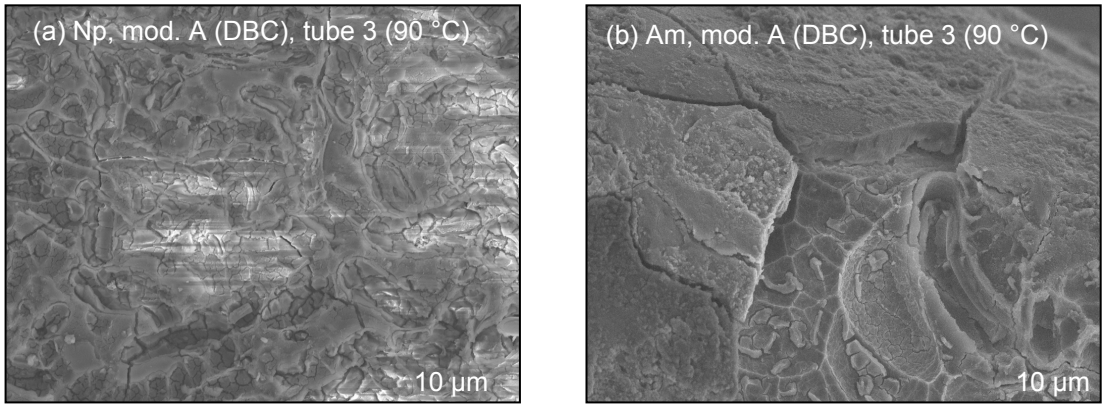

Figure 5 *SEM observation of the surface of in situ corroded Np doped (left, a) and Am-doped (right, b) SON 68 glass sample of module A (DBC) after 1.3 years at 90 °C; magnification 500×. The horizontal whitish lines and/or shade on figure (c) are the result of the scanning of the surface of the sample for element profiling. The picture in figure (b) is taken from an oblique angle and clearly shows the cracked alteration layer that partly disappeared, with locally a deeper alteration.*

EDS of the altered surface and of the cross section gave no evidence for the presence of radionuclide containing secondary phases. It is possible that such phases had formed, but that they were lost during retrieval and treatment of the samples. The normal spectra contained (B [12]), O, Na, Si, Al, Zr, Ca, and Fe, and smaller quantities of Ru, Nd, Ni, Zn, and Cs. The peaks for Na^+ were generally smaller than in the spectra for the pristine glass, pointing to the leaching of this element. Especially for the glass samples from tube 3 (90 °C), K^+ and Mg^{2+} were present in the alteration layer, pointing to inwards diffusion due to interaction with clay and pore water. Besides the 'normal' spectra, phases enriched in Pd/Fe, Ru/Pd/Th, Th/U, Np/K, Fe/S (test tube 2, 30 °C) and Ru/Rh/Pd, Fe/Ca/K, Nd/Ce/La, Nd/Ce/Pr, and Nd/Am (test tube 3, 90 °C) were found at the surfaces of the altered glass samples.

Besides the small and sometimes larger gas bubbles present due to the casting of the glass (see for instance Figure 4-a), SEM of the non-radioactive samples of tube 2 (30 °C) also revealed the presence of very small voids spread over and within the sample. These small voids seemed to have formed – during waste glass production – around inclusions of noble metals (Pd, Rh, Ru) and/or U/Th (see Figure 4-a, Figure 6-a, Figure 7-a). Similar inclusions, as well as inclusions of REE (La, Ce, Nd, Pr) were evidenced by EDS for the non-radioactive samples of tube 3 (90 °C). The radioactive samples contained similar

[12] Because it is a light element, it is more difficult to attribute the observed peaks to boron.

inclusions, in some samples at a high frequency, in other samples, however, at a much lower frequency.

SEM analysis of the polished cross section of the glass samples confirmed that the whole sample surface was altered (Figures 6 and 7). The alteration degree varied sometimes considerably from one place to another, probably due to local heterogeneities in the glass (*e.g.* inclusions, polishing lines) and/or in the backfill (*e.g.* bentonite – sand – graphite (module B) and bentonite – glass powder (module C)). This is reflected in the variation of the alteration layer thicknesses per sample, reported in Table 11. For a few samples, the alteration layer was almost completely lost, most likely due to manipulations. For all the other samples, there is strong evidence that part of the alteration layer was missing. This is likely an inherent part of the corrosion process (see Section 2.5).

For modules A (DBC) and B (BSG), the alteration layers of the radioactive samples were thicker than for the inactive samples, the difference being a factor 4 at most. The increase of the thickness seemed to be related to the increasing specific alpha-beta-gamma activity. There are no clear indications that the alteration layer is different in DBC and BSG. The alteration layer of the Np-doped sample in contact with module B of test tube 3 (90 °C) was thick and almost intact (see Annex 1, detailed SCK•CEN report). We hypothesise that this is due to the fact that at that place the glass alteration started only later

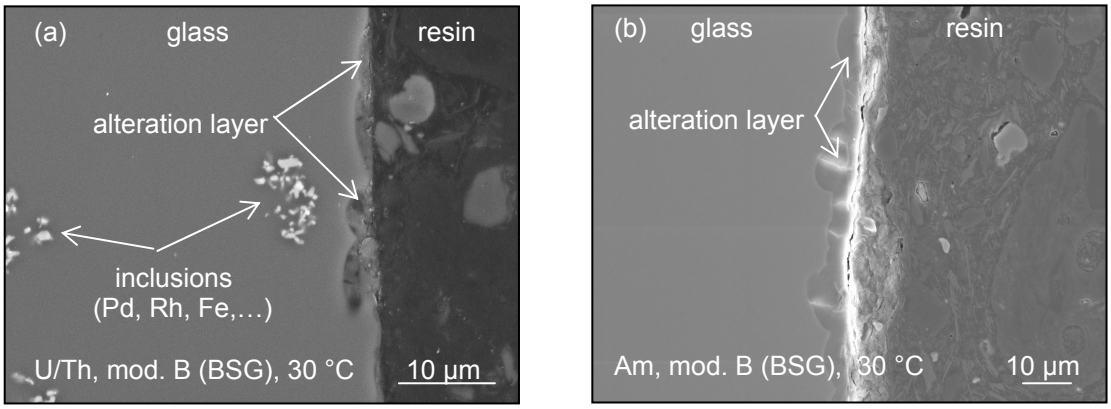

Figure 6 *SEM observations of the polished cross section of in situ corroded SON 68 glass samples of module B (BSG) after 3.3 years at 30 °C. (a) U/Th-doped, magnification 2500×, (b) Am-doped, 1000×. It is seen that the whole glass surface is attacked (alteration layer is present over the whole length of the glass surface on the photos). There are spots of deeper alteration and at some places (part of) the alteration layer is missing.*

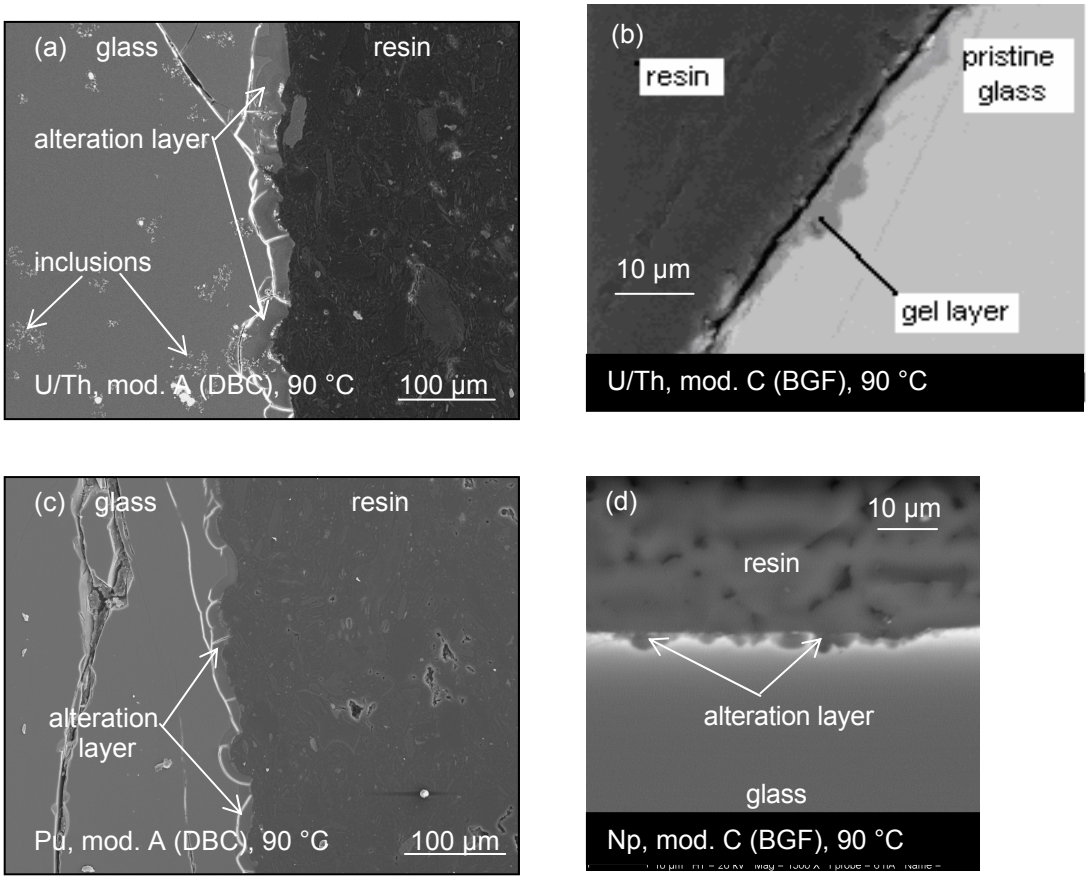

Figure 7 *SEM observations of the polished cross section of in situ corroded SON 68 glass samples of module A (DBC; (a) and (c)) and module C (BGF; (b) and (d)) after 1.3 years at 90 °C. (a) and (b) U/Th-doped, magnification 800× and 2000×, (c) Pu-doped, 250×, (d) Np-doped, 1500×. The white or grey lines and curves in the figures are due to the fissuring of the dried alteration layer and/or the glass. It is seen that the whole glass surface is attacked (alteration layer is present over the whole length of the glass surface on the photos). There are spots of deeper alteration.*

Table 11 *Alteration layer thicknesses (µm) measured on the glass samples of the in situ tests.*

	Tube 2 (30 °C, no ^{60}Co, 3.3 years)			**Tube 3 (90 °C, ^{60}Co, 1.3 years)**		
	Module A (DBC)	**Module B (BSG)**	**Mod. C (BGF)**	**Module A (DBC)**	**Module B (BSG)**	**Module C (BGF)**
U/Th	0.5 < 1.5±0.5 < 5	0.5 < 2.3±0.3 < 5	0.2±0.1	10 < 25±3 < 55	15 < 20±5 < 50	1 < 2.5±0.5 < 5
Np	3 < 3.7±0.3 < 6	2 < 3.5±0.5 < 10	<0.5	30 < 35±3 < 50	55 < 80±10 < 130	1 < 2.6±0.5 < 5
Pu	3 < 3.5±0.5 < 12	2 < 3.0±1 < 12	<0.5	30 < 40±10 < 50	45 < 50±5 < 55	2.3<2.8±0.5<3.3
Am	5 < 6±0.5 < 12	3 < 4.0±1 < 15	<0.5	40 < 45±3 < 55	45 < 50±10 < 90	gel layer lost

The lower and upper values give the range of thicknesses observed per sample. The central value gives the estimated average thickness, with an estimate of the uncertainty on this average.

during the test, due to the slow re-saturation of the backfill material in this module (see Sections 2.1.2). The alteration layers for the samples in contact with module C (BGF) were very thin. For the samples from test tube 2 (30 °C), the thickness of the alteration layer of the radioactive samples was even below the detection limit. Hence, no effect of the increasing specific alpha-beta-gamma activity on the thickness of the alteration layer could be evidenced for this test case. For the samples at 90 °C, the alteration layers were somewhat thicker, and there seemed to be a tendency to slightly thicker alteration layers with increasing specific alpha-beta-gamma activity.

A few samples were submitted to a mapping analysis by EDS, providing in a quick way information on the thickness and the composition of the reaction layer. Figure 8 shows the results for the lower part of the U/Th-doped sample of Figure 7-a. Care has to be taken when interpreting these results. Indeed, each colour gives the intensity of a given element relative to that of the other mapped elements *in a particular location*. Since both the density and the elemental composition of the alteration layer differ from that of the pristine glass [40-42], a more intense colour of a given element in the alteration layer does not necessarily mean that the absolute concentration of that element is higher in the alteration layer. In Figure 8, one can clearly distinguish the alteration layer from the pristine glass. This alteration layer contains the same elements as the pristine glass, but the different intensities indicate that the elemental composition and/or the density of this layer differ from the pristine glass. The alteration layer contains relatively more Al, Si, Fe, and Zr, whilst the Ca^{2+} content is relatively the same in the glass and in the alteration layer. The alteration layer contains also K^{+} and Mg^{2+} that are stemming from the contact with the clay (water). Ru seems to be localised in a Ru containing phase with stable elemental composition and density in the pristine glass and in the alteration layer.

2.2.1.4 SIMS [13] analyses of the surface

The surface of all glass samples was analysed by SIMS. SIMS profiling allows to analyse the variation in chemical composition over the reaction layer, and therefore to obtain information on the dissolution mechanism. The SIMS analyses of the U/Th-doped glass samples of modules A and B were performed at the Laboratory for Materials Analysis of the Gabriel Lippmann Public Research Centre in Luxembourg. Per glass specimen, the element profiles were measured at three different positions, and these proved to be in most cases similar for all three positions. In some cases, however, there was an important difference in thickness of the alteration layer and, related with this, the element profiles. Obviously, this is due to the big variations of the thickness of the alteration layers (due to loss of (part of) the alteration layer), as discussed in the previous section. SIMS analyses on the U/Th-doped glass samples of module C were carried out at CRPG in Nancy, France. SIMS analyses of the radioactive samples were performed at the Laboratory for Materials Behaviour of the Paul Scherrer Institute (PSI) in Switzerland. Per glass specimen, the element profiles were measured at two different positions, and they proved to be in most cases similar for the two positions.

[13] Secondary ion mass spectrometry.

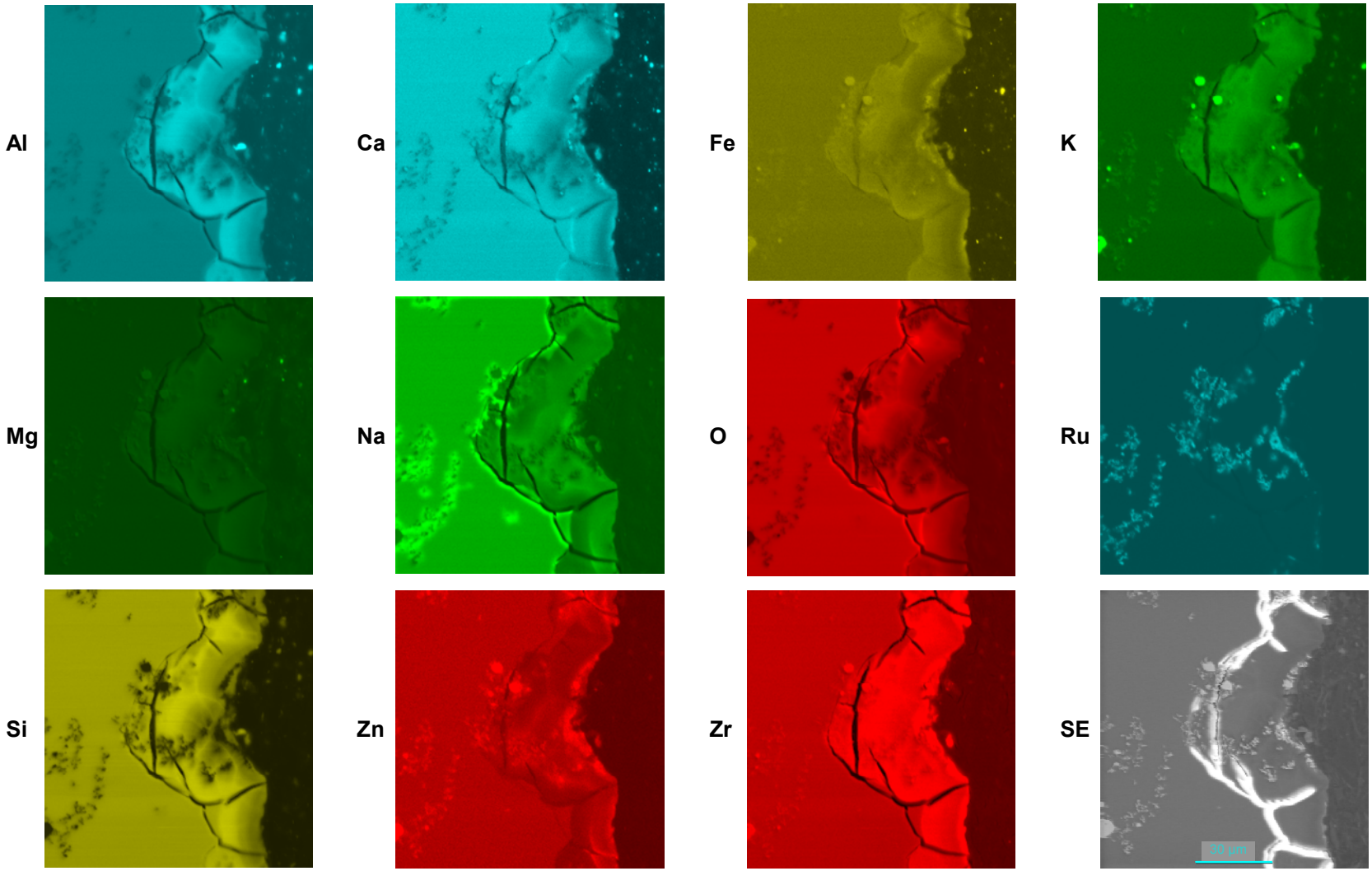

Figure 8 *Mapping of part of the polished cross section of an U/Th-doped SON 68 glass sample from module A (DBC) after 1.3 years at 90 °C (magnification 800×; see also Figure 7-a).*

2.2.1.4.1 Thickness of the alteration layer

As already discussed, the alteration layer was in most cases partly lost upon retrieval of clay and glass from the test tube due to the intense contact between the glass sample and the backfill material. Further treatment of the glass samples sometimes resulted in further removal of (part of) the alteration layer. Furthermore, especially for the radioactive glass samples, we cannot exclude that shrinkage and/or (partial or complete) loss of the alteration layer due to its drying out may have contributed to the unexpectedly low thicknesses of the alteration layer. For reasons discussed before (Sections 2.1.1, 2.1.2, and 2.2.1.3), the alteration layers of the samples from module B (BSG) of test tube 3, especially the Np-doped samples, seemed to be more intact. In conclusion, only in a few cases (mostly for the thinner alteration layers) more or less complete profiles were obtained.

For the non-radioactive glass samples, the thickness of the erosion crater was measured with a profilo-meter when the signals for different elements (B, Si, Al, …) had attained a (sometimes more or less) stable value. The values obtained this way agreed well with the values that were derived from the SEM analysis of the cross section, taking into account the (partial) loss and the big variations of the thickness of the alteration layer. For the radioactive samples, the thickness of the alteration layer was estimated on the basis of the erosion speed for the pristine glass and the time needed to obtain more or less constant signals for the glass elements. Because the density of the alteration layer is smaller than that of the pristine glass, the thickness of the alteration layer estimated this way underestimates the real thickness. Complementary measurements will be performed to measure the thickness of the alteration layer with a profilo-meter, to obtain better estimates of the thickness.

2.2.1.4.2 Profiles

To interpret the results, we have applied a normalisation procedure that is based on the general observation that Zr (the glass samples contain 1 wt % ZrO_2) is a rather immobile element, so that its volumetric concentration in the glass and in the alteration layer is rather stable. Only towards the glass/clay interface, the Zr intensity sometimes sharply increased or decreased. By following the evolution of the ratio of the concentration of an element to that of Zr in the alteration layer to the same ratio in the pristine glass, we can discuss the SIMS profiles in a semi-quantitative way:

$$\frac{C}{C_0} = \frac{\left.\frac{I(^{m}X)}{I(^{90}Zr)}\right|_{gel}}{\left.\frac{I(^{m}X)}{I(^{90}Zr)}\right|_{\substack{pristine\\glass}}}$$

In this equation, C and C_0 refer to the concentration in the alteration layer and in the pristine glass, respectively. A ratio C/C_0 equal to 1 indicates the same element concentration in the gel and in the glass (with respect to Zr, which is thus assumed to have a constant concentration). If this ratio is greater than 1, the gel is enriched with the element with regard to the pristine glass. If the ratio is less than 1, the opposite is true. Considering that there is some uncertainty on the absolute value of the signal intensity of each element, and hence on the ratio C/C_0, we consider C/C_0 ratios between ~0.8 and ~1.2 as equal to 1, *i.e.* no (important) leaching or enrichment with respect to Zr. The normalised profiles of the glass samples are given in the detailed reports of SCK•CEN and CEA-Valrhô, respectively (Annexes 1 and 2 to this report). By way of example, some normalised profiles are given in Figure 9.

Before discussing the profiles, an important remark applies to the ^{24}Mg and ^{39}K profiles measured by PSI for the radioactive glass samples. The measurement technique used by PSI is sensitive to isobaric molecule interferences. Taking into account the chemical composition of the glass, probable isobaric interferences occur at mass 24 with $^{16}O_3^{++}$ ions, and mass 39 with $^{23}Na^{16}O^{+}$ ions. Because Mg^{2+} and K^{+}

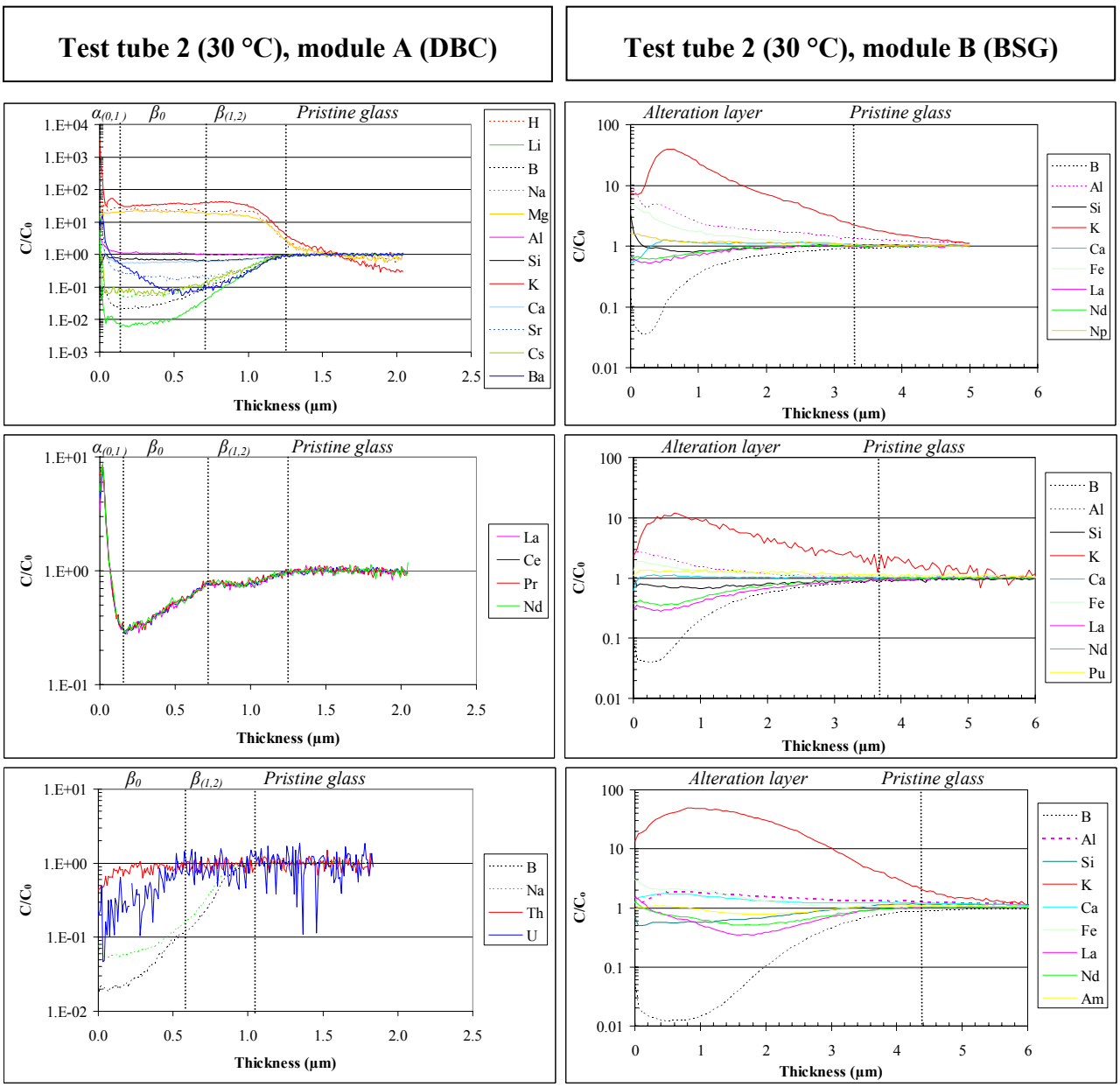

Figure 9 *(Left) SIMS profiles of an U/Th-doped SON 68 glass sample of module A (DBC) after 3.3 years at 30 °C. The profiles in the top and the centre picture were obtained at the same position; the profiles in the bottom picture (U, Th) were taken at a different position with apparently a slightly thinner alteration layer. Note the different scales of the Y-axis. (Right) SIMS profiles of Np-doped (top), Pu-doped (centre), and Am-doped (bottom) SON 68 glass samples of module B (BSG) after 3.3 years at 30 °C. The C/C_0 ratios for Al, Si, Fe, Ca, La, Nd, and Np – Pu – Am are only less than 10 times higher or lower than 1. Note that the thickness of the alteration layer may be underestimated (see text).*

are not components of the SON 68 glass, the high signal intensities measured for masses 24 and 39 (between 103 and 105 cps, counts per second) can be hardly interpreted as due only to ^{24}Mg and ^{39}K, respectively. In particular, the high intensities in the bulk of the glass make it difficult to explain these signals as due to K and Mg in-diffusion from the clay. Thus, although in the plots the curves for 24 and 39 amu (atomic mass units) were labeled as ^{24}Mg and ^{39}K, it should be kept in mind that these profiles most probably represent also other complex ions.

In almost all cases, the elemental profiles met very well the expectations on the basis of other tests exposing SON 68 glass samples to clay [e.g. 43-46]:

1 A strong to very strong leaching of B, Li^+, Na^+, and Cs^+. These species are neutral ($B(OH)_3$) or monovalent cations, which are not or poorly retained in the (altered) glass network, and which do not (co)precipitate. The leaching profiles were less steep than expected for Na^+ in module A (DBC) and B in module C (BGF), because of the high solution concentration of these elements (see Section 2.1.2.5).

2 A strong leaching of Sr^{2+} and Ba^{2+}, and to a smaller extent Ca^{2+}. These are bivalent elements, which are stronger retained in the (altered) glass network than the monovalent species, and which might also (co-)precipitate. The smaller leaching of Ca^{2+} (in some cases, the C/C_0 ratio for this element remained stable) is related to the high solution concentrations (see Section 2.1.2.5). The re-increase of the Ca^{2+} and Ba^{2+} profile in some cases is possibly related to precipitation with carbonate and/or sulphate.

3 In most cases almost flat profiles for Si, Al, and Fe, sometimes increasing towards the glass/clay interface. This indicates that these elements leach out predominantly through matrix dissolution, and that the β layer is generated by selective leaching of easily leachable glass compounds (M^+, M^{2+}, *etc.*). Si seemed to be somewhat more mobile than Al. For the Am-doped sample in contact with module C (BGF) of test tube 3 (90 °C), and in contrast to the Np- and Pu-doped glass samples, the Si, Al, and Ca profile decreased towards the glass/clay interface. Since all glass samples in tube 3 were gamma irradiated at high dose rates (> 100 Gy/h), it is unlikely that this different behaviour of Si and Al is due to the gamma radiolysis by Am, which could depolymerise the silicated gel network. Therefore, we cannot explain this observation, which not observed for the other test cases.

4 Influx of H^+, K^+, and Mg^{2+}, which are not present in the SON 68 glass. These elements originate from the pore water in contact with the backfill materials.

5 Moderate leaching of La, Ce, Pr, and Nd. The profiles for these four elements were always remarkably similar. This is somewhat surprising, given the expected different valencies (La(III), Ce(IV) (also Ce(III) is possible, but this is less likely), Pr(IV) or Pr(III), and Nd(IV) or Nd(III) (Nd(II) is also possible, but less likely). It is also possible that they have more or less the same solubility. In any case, these elements seem to be strongly retained in the alteration layer. In some cases, the concentrations tended to increase again towards the glass/clay interface. It is important to note that the La and Nd profiles in the radioactive samples (SIMS analyses performed at PSI, Switzerland) sometimes show a smaller decreasing tendency than in the non-radioactive samples.

6 Th seems to be very immobile (or: 'inert'), with a behaviour that closely resembles that of Zr. Towards the glass/clay interface, a small and probably insignificant depletion or enrichment – depending on the test case – could be noticed. Th occurs in the glass and in the alteration layer in the tetravalent form (Th(IV) [47], which is the only stable form of Th, and which can strongly sorb onto the alteration layer and/or can easily hydrolyse to the poorly soluble $Th(OH)_4$.

7 U seems to be somewhat more mobile, with its behaviour often resembling that of La, Ce, Pr, and Nd (Nd, Neodymium, is the 'lanthanide analogue' of U: they both occur in the VIIb series). This higher mobility of U is possibly because in the glass it occurs for 80% as U(VI) (and for 20% as U(IV)) [48], which occurs as uranyl UO_2^{2+}, with a lower sorption affinity and a higher solubility than in the tetravalent oxidation state. At the glass/clay interface, it may form *e.g.* negatively charged – and therefore unretained and more mobile – $UO_2(CO_3)_3^{4-}$ species. The tetravalent form of U is, just like Th and other tetravalent elements, easily hydrolysed to the poorly soluble $U(OH)_4$. Since the local redox conditions are not known, this interpretation about oxidation state and speciation of U in the alteration layer and in the contacting backfill and interstitial backfill solution remains speculative.

8 There are no useful profiles for Np for module A. For module B (BSG) of tube 2 (30 °C), it has a behaviour that is close to that of Zr^{4+}, with some tendency to enrichment towards the glass/clay interface. For module B (BSG) of tube 3 (90 °C), it showed more or less the same behaviour as La and Nd, with some depletion in the alteration layer, and some enrichment towards the glass/clay interface (note that the alteration layer of the Np-doped sample is unusually thick, probably because of the lack of long and/or intense contact with the backfill). In the glass, Np occurs in the pentavalent form (Np_2O_5, [47]). In the hydrous alteration layer, it can occur as $Np(V)O_2^+$, which as a monovalent species is only poorly retained in the glass lattice and in the alteration layer. The solubility of pentavalent Np is also higher than that of tetravalent Np. Upon contact with the pore water, it may exist as $Np(V)O_2^+$ or it may form negatively charged and therefore unretained complexes such as $Np(V)O_2CO_3^-$ and $Np(V)O_2(CO_3)_2^{3-}$ *etc.* In reducing conditions, it may be reduced to the tetravalent

form, with a behaviour that resembles that of Th(IV) and Pu(IV) . As in our tests the Np behaviour in module B of test tube 2 (30 °C, BSG) closely resembles that of Zr(IV) and Th(IV), it is possible that Np indeed occurred as Np(IV). Just like for U, this interpretation is speculative, since we do not know the local redox conditions.

9 Pu showed more or less the same behaviour as La(III) and Nd (presumably present as Nd(III)) in modules A (DBC) and C (BGF). In module B, Pu behaved as Th(IV). It was stronger retained than La and Nd, with an almost constant ratio over the whole thickness of the alteration (*i.e.* no depletion nor enrichment), and with a slight increased retention towards the glass/clay interface. In the glass, Pu occurs as Pu(IV) [49]. Its behaviour in the alteration layers of the glasses in contact with BSG (module B) suggests that it remained in the tetravalent oxidation state, thus reacting as Th(IV). The behaviour of Pu in the alteration layer of the glass samples in contact with DBC (module A) might suggest that Pu occurred in the trivalent form. A similar behaviour of Pu and Am was also observed in percolation experiments with these radionuclides in boom clay [50]. According to the thermodynamic database that is used, Pu is predicted to occur mainly in the tetravalent or in the trivalent oxidation state in boom clay; the exact oxidation state of Pu in boom clay is still not clear yet [51]. According to recent thermodynamic calculations on the speciation of Pu in boom clay pore water, using different codes and thermodynamic databases, Pu(III) is the predominant species at intermediate pH values and $Pu(OH)_4$ (aq) predominates at pH values above 8.3 [52]. Also for Pu, our interpretation in terms of oxidation state of Pu is speculative.

10 For module A, no useful Am profiles were available, because in all cases the alteration layer was lost. The profiles of the small remaining alteration layer close to the pristine glass (< 1 µm) suggest a behaviour that is similar to Nd and La. For modules B (BSG) and C (BGF), Am followed more or less the behaviour of La and Nd, with a very slight depletion in the alteration layer, and a slight accumulation at the glass/clay interface. Am occurs in the very stable trivalent oxidation state in both the glass and the clay [49]. It forms easily complexes with carbonate ($AmCO_3^+$, $Am(CO_3)^{2-}$) and mixed complexes with carbonate and organic matter.

For the profiles of complete alteration layers (*i.e.* no loss of (part of) the alteration layer), we can attempt to distinguish the layers that have been identified and reported before [*e.g.* 43–46], namely:

A precipitation layer α , which probably consists of *an outer 'clay' precipitation layer* α_0 (formed upon precipitation and secondary phase formation reactions with elements stemming mainly from the backfill material) and *an inner 'glass' precipitation layer* α_1 (formed upon precipitation and secondary phase formation reactions with elements stemming mainly from the glass). The inner 'glass' precipitation layer typically shows variations of the Si, Al, Zr, and, Fe signal intensities (increase or decrease, depending on test case; in our case, Zr seemed to be the most stable). Because especially for the radioactive samples, except for the Np-doped sample of module B (BSG) of test tube 3 (90 °C), the outer part of the alteration layer was lost, the SIMS profiles do not allow to detect any radionuclide accumulation at the surface of the alteration layer. Therefore, we have to rely solely on the results from the radionuclide migration to conclude on the radionuclide retention in the alteration layer (see Sections 2.2.3 and 2.5).

A depletion zone β_0 , where the concentration of easily leachable elements is constant (or where the slope of the profile is less steep than deeper in the glass), and at its lowest value. Major components of the glass are depleted in this area, and elements that are present in the interstitial clay water but not in the glass (such as H^+, K^+, Mg^{2+}) have infiltrated into the altered glass.

A zone where the slopes of the element profiles is the steepest. In the literature [*e.g.* 43–46], reference is made to *a gradient zone* β_1 *and a diffusion zone* β_2. *The gradient zone* β_1 is characterised by depletion of alkali and alkali earth components of the glass, and by influx of backfill elements (in our case, H^+, K^+, Mg^{2+}). *The diffusion zone* β_2 would be similar to the gel layer that initially forms on glasses during simple leaching tests. The zone is characterised by depletion in Li^+ from the glass and enrichment of H^+ from the solution. We cannot systematically distinguish these two zones in our profiles, and consider these therefore as a combined $\beta_{(1,2)}$ layer.

It is important to note that we have not applied quantitative criteria to fix the transition between the different layers in Figure 9. The indicated transitions between the zones were drawn arbitrarily, on the basis of the information regarding different zones as described above. The $\beta_{(1,2)}$ layer integrates also a 'mixed zone', due to the fact that the angle between the primary ion beam and the sample is never 90°. We cannot exactly quantify this effect.

Taking into account the nearly complete elimination in B and the alkali metals in the β_0 layer of the SIMS profiles, we conclude that the dissolution of the SON 68 samples is predominantly selective-substitutional leaching, as observed for other SON 68 glass alteration tests [25, 42, 44, 46]. Yet the loss of a distinct part ('layer') of the alteration layer, either because of the sorption of the glass constituents onto the clay and/or secondary phase formation or because of the treatment of the glass samples (meaning that this part of the layer is very fragile), can be interpreted as some kind of matrix dissolution.

2.2.2 Characterisation of the altered clay in module C (BGF) of test tube 3 [14]

The clay in contact with the U/Th-doped glass of module C (BGF) of test tube 3 (90 °C, 1.3 year) was analysed by ESEM[15], SEM-EDS, TEM[16], XRD[17], and FTIR[18]. The characterisation of the altered clay showed that after ~1.3 years of heating and gamma irradiation the interface between clay and glass was still fully reactive. ESEM and EDS showed that at the interface of the U/Th-doped glass sample and the clay, Si had precipitated either as spherical flaky nodules, or in larger layers on the clay surface, as chalcedony (microcrystalline quartz, SiO_2) and (amorphous) opal ($SiO_2.nH_2O$) (Figure 10).

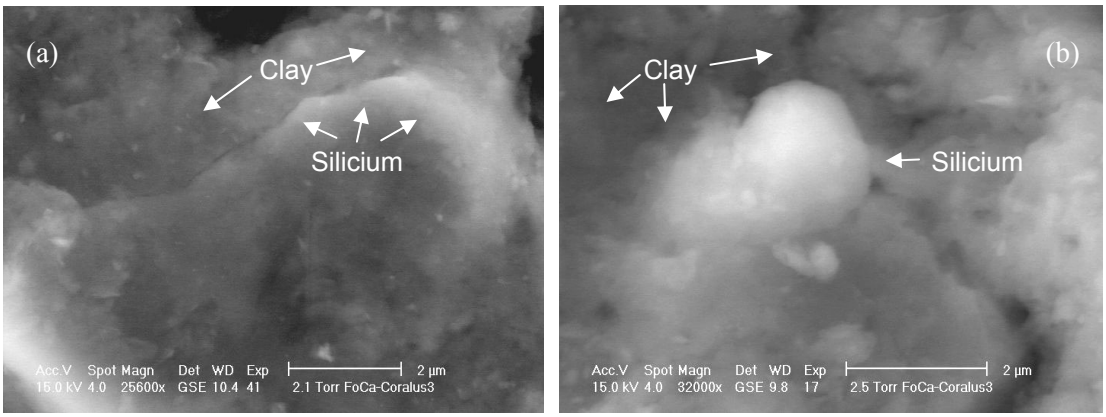

Figure 10 *ESEM pictures of the clay formerly in contact with the U/Th-doped glass sample of module C (BGF) of test tube 3 (90 °C), showing the Si enrichments. (a) Layer of Si precipitate on top of clay, magnification 25600×, (b) Si sphere on top of clay, magnification 32000×.*

XRD showed that the peaks related to quartz increased with respect to the original material, especially in the zone close to the glass/clay interface. SEM-EDS revealed that all over the clay Si precipitates were present both close to the glass fritt and in the bulk of the clay. These precipitates were clearly neo-formed, and their structure seemed to be amorphous (Figure 11). SEM-EDS in the BSE[19] mode showed a significant enrichment in Si and Na throughout the clay (no gradient was observed). This is related to the dissolution of the powdered glass fritt. Na^+ leached from the glass frit and from the pore water had ion exchanged with Ca^{2+} and Mg^{2+} on the cation exchange sites of the clay minerals. The fate of Si could not

[14] This part has been described in detail in the detailed report of CEA-Cadarache.
[15] ESEM = environmental scanning electron microscopy.
[16] TEM = transmission electron microscopy.
[17] XRD = X-ray diffraction analysis.
[18] FT-IR = Fourier-transformed infrared spectrometry.
[19] BSE = backscattered electron.

be ascertained: it can either be present in Si phases and/or in newly formed clay minerals.

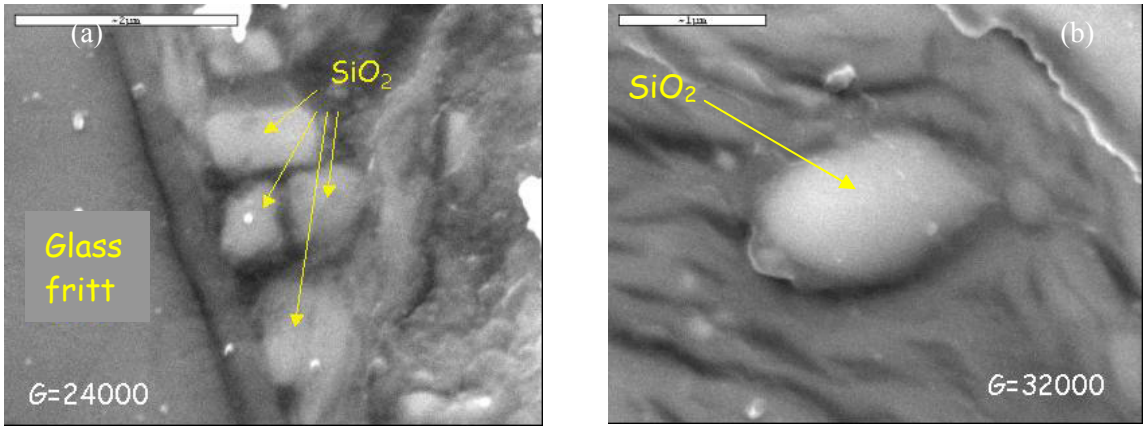

Figure 11 *SEM pictures of the bulk of the clay from the clay core formerly in contact with the U/Th-doped glass sample of module C (BGF) of test tube 3 (90 °C), showing the Si precipitates (a) close to a glass fritt grain (magn. 24000×) and (b) in the bulk of the clay (magn. 32000×).*

As no substantial Zr concentration increase could be demonstrated with ESEM-EDS, we must conclude that Zr remained and/or precipitated in the alteration layer of the glass or in the clay that remained stuck on the glass (see Sections 2.1.3.2 and 2.2.1.1), and that the surface of the clay core that was in contact with the glass did not contain part of this alteration layer. ESEM-EDS also revealed that the surface of the clay core (in contact with glass) was covered with enrichments of small grains of calcite. Although the original backfill material contains 1.2-1.6 wt % of calcite [53], results of XRD and FTIR spectrometry of both the altered clay from test tube 3 and the original backfill material confirmed that the calcite found close to the glass sample precipitated during the test.

XRD analysis indicated that kaolinite and interstratified kaolinite/smectite minerals had become unstable due to the high temperature and/or pH variation due to the glass dissolution and CO_2 production. The degree of alteration increased towards the glass/clay interface. In addition, a distinct 7 Å clay phase seemed to have formed. FTIR spectrometry gave further evidence for the gradual disappearance of kaolinite. TEM analysis of the clay formerly in contact with the glass sample confirmed that kaolinite gradually disappeared due to important dissolution of this mineral (Figure 12-a).

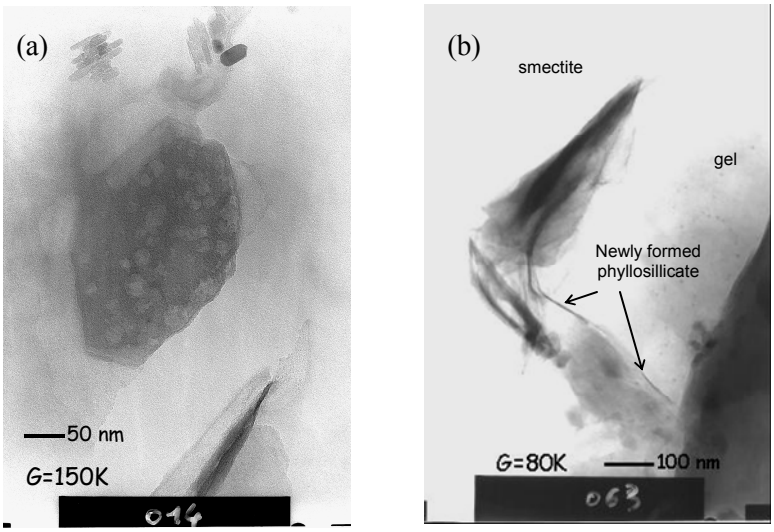

Figure 12 *TEM pictures of (a) altered kaolinite (magnification 150,000×) and (b) a smectite clay mineral with gel and newly formed phyllosilicates (magnification 80,000×). The borders of the kaolinite mineral in figure (a) are clearly dissolved, which point to an important alteration.*

The TEM analysis further revealed the presence of minerals consisting of very small-sized sheets, which are well crystallised and which have a periodicity that is much smaller than that of the Ca-bentonite in the backfill material (Figure 12-b). These newly formed phyllosilicates contain more Mg^{2+} than the Ca-bentonite (4 to 6 % instead of 0.5 to 1 %), and their Si/Al is lower than in the Ca-bentonite (1.4 instead of 1.6 to 1.7). All this information suggests that the newly formed phases are of the non-swelling 7 Å – serpentine type minerals ($Mg_3Si_2O_5(OH)_4$), with Mg^{2+} coming from (degrading) interstratified minerals and from the (boom clay) pore water. The destabilisation of interstratified kaolinite/smectite was also described for the same material under thermal gradient by Latrille *et al.* [53]. The formation of Fe-containing (instead of Mg^{2+}) non-swelling 7 Å minerals has also been observed in iron/clay interaction tests [55].

2.2.3 Leaching and migration of Np, Pu, Am, U, Th, Cs, Zr, and Pd [20]

2.2.3.1 Experimental aspects

The clay cores sampled from the backfill materials were cut in 0.3-0.5 mm thick slices, taking maximum precautions to prevent cross contamination. Clay samples were dried in a dessicator (silica gel) until constant dry weight. This drying procedure yielded results that were close to the dry weight determined after heating to 105 °C during several days. The thickness of the clay slices was calculated on the basis of their dry weight, the internal diameter of the sampling tube, and the dry density of the clay. We estimate the uncertainty (95 % confidence interval) on the thickness to be ~10 % for the slices close to the glass sample, and 0.5 % for the slices further from the glass (> 2 to 4 mm).

Migration profiles for ^{237}Np and ^{241}Am were established by gamma spectrometry. The relative uncertainties (95 % confidence) on the specific activity were ~15 % (^{241}Am) and ~10 % (^{237}Np) for the higher and intermediate activities, and up to ~70 % for the lowest activities (close to the detection limit of ~0.75 Bq/g for ^{241}Am, and ~0.25 Bq/g for ^{237}Np). For Pu, the activity on the clay was measured by alpha spectrometry after an extraction procedure with 10 M HNO_3 and 15 % H_2O_2 at 80 °C with a reproducible extraction yield of ~90 %. The relative uncertainty (95 % confidence interval) on the specific activity was ~10 % for the higher activities, and ~20 % for the lower activities. The detection limit was ~0.02 Bq/g clay.

[20] This part has been described in the detailed report of SCK•CEN.

The 'extractable' amount of U, Th, Zr, Cs, and Pd was determined by extraction during 3 hours at 80 °C with a mixture of 7 M HNO_3 *pro analysi* and 3.5 % H_2O_2 . This method yielded similar results, but also a better repeatability, than extraction with *aqua regia*. The extraction solutions were afterwards analysed by ICP-MS [21]. Control experiments showed that the sum of the extractable concentration and the concentration in the residue left after extraction equalled, within experimental error, the total element concentration.

2.2.3.2 Results and discussion

2.2.3.2.1 Leaching of Np, Pu, and Am from the glass

The total radionuclide activity in the clay can be related to the total activity in the glass, and can be calculated either as a 'leached fraction' (the relative amount of the activity that has leached), as an 'equivalent glass thickness' (the thickness of the glass layer that needs to be dissolved to release the leached activity), or as a retention factor (defined as the ratio of the mass loss and the normalised radionuclide release). The results are summarised in Table 12. The uncertainty on these results is high due to the 10-20 % uncertainty (95 % confidence) on the specific activity of the most active clay slices and the uncertainty on the fraction of clay that remained stuck on the glass surface. The results for module B (BSG) – tube 3 (90°C) show a high variation, which we attribute to incomplete saturation of the backfill during part of the test, and the resulting delayed start of the radionuclide leaching process (see Sections 2.1.1, 2.1.2, and 2.2.1). They are not considered in the interpretation of the results.

The results in Table 12 clearly show the strong decrease of the glass alteration, and the related radionuclide leaching, by the addition of powdered glass frit (module C, BGF): at 90 °C, a reduction of about two orders of magnitude is observed. The results also show the strong increase of the alteration at higher temperature. The conclusions that can be drawn from the results in Table 12 are in agreement with the present understanding of radionuclide leaching from radioactive glasses [56–65, and references therein].

[21] Inductively coupled plasma – mass spectrometry.

Table 12 *Results on Np, Pu, and Am leaching and migration, expressed as leached fraction (%) and equivalent thickness (µm), and thicknesses as calculated from the mass loss of the altered glass samples (see Table 10) (µm).*

Test case	Nuclide	% leached *	Equivalent thickness (µm) *	Calculated thickness (µm)	Retention factor RF *
2-A (DBC) (30°C)	**Np**	0.17 – 0.19	4.8 – 5.6	4.05 (U/Th) to 6.2 (Am)	not reliable
	Pu	0.17 – 0.20	5.0 – 5.8		no data
	Am	0.16 – 0.19	4.7 – 5.4		1.1 – 1.3
2-B (BSG) (30°C)	**Np**	0.09 – 0.10	2.6 – 3.0	3.30 (U/Th)	no data
	Pu	0.03 – 0.03	0.8 – 1.0		no data
	Am	0.04 – 0.05	1.1 – 1.3		no data
2-C (BGF) (30°C)	**Np**	0.006 – 0.007	0.17 – 0.20	~0 (U/Th) to 0.6 (Np)	2.9 – 3.3
	Pu	0.002 – 0.003	0.06 – 0.07		no data
	Am	0.003 – 0.004	0.10 – 0.11		no data
3-A (DBC) (90°C)	**Np**	0.85 – 0.98	25 – 28	48 (Am)	no data
	Pu	0.64 – 0.74	19 – 22		no data
	Am	0.92 – 1.07	27 – 31		1.6 – 1.9
3-B (BSG) (90°C)	**Np**	**0.03 – 0.03**	**0.8 – 1.0**	**no data**	**no data**
	Pu	**0.25 – 0.29**	**7.1 – 8.3**		**no data**
	Am	**0.10 – 0.12**	**3.0 – 3.5**		**no data**
3-C (BGF) (90°C)	**Np**	0.012 – 0.013	0.33 – 0.39	no data	no data
	Pu	0.004 – 0.005	0.12 – 0.14		no data
	Am	0.004 – 0.004	0.11 – 0.12		no data

* The two values are obtained by using two different factors to correct for the activity on the clay that was not sampled with the stainless steel tube, the lower value being the best estimate.

(i) All three actinides are to some extent retained in the alteration layer. Indeed, in all cases the 'equivalent glass thickness' is smaller than the calculated thickness of the glass layer that is dissolved corresponding to the mass loss (thus using the density of the pristine glass; see Table 18 in Section 4.3). Accordingly, the retention factor is larger than 1. However, the retention factors are much lower than the values reported for R7T7 glass alteration in water in the absence of solids (5-10 for Np, 50-100 for Pu, and 500-1000 for Am), and also lower than the values reported for glass alteration in 'diluted' boom clay suspensions (3 for Np, 10 for Pu, and 40 for Am; [57, 61]). Lemmens *et al..,* for glass corrosion tests in contact with dense clay (Ca-bentonite with or without boom clay), report a retention factor for Np of about 1, meaning that there was (almost) no retention of Np in the alteration layer [64]. The low retention factors measured in our tests confirm that in contact with clay, especially at high swelling pressure (resulting in a very intense contact between the clay and the glass), released actinides, as well as leached glass constituents, will strongly sorb onto these clay materials and/or onto secondary phases formed at the interface between the glass and the clay [56-64, and references therein]. These processes act as a sink for the released actinides, thus increasing the actinides leaching from the glass, and possibly decreasing the actinides sorption on the alteration layer. The results of the SIMS analyses might be in agreement with the results on radionuclide leaching; unfortunately, we do not know the SIMS profiles in the part of the alteration layer that is lost (see Section 2.2.1.4).

(ii) The retention of actinides in the alteration layer depends on the type of interaction material, the boom clay being the more 'aggressive' one [56,61]. The fraction leached radionuclide is considerably higher for dried boom clay than for the modules with a Ca-bentonite based backfill material, indicating that the (dried) boom clay has a stronger affinity for these radionuclides. This is probably due to the high amount of immobile organic matter in this backfill material, with strong radionuclide complexation properties. It is also to be noted that the radionuclides leaching follows the order DBC (module A) > BSG (module B) > BGF (module C) (Table 12), whereas the degree of glass alteration (mass loss and thickness of the alteration layer) follows the order DBC (module A) ≈ BSG (module B) > BGF (module C) (Tables 10 and 11). This highlights the strong radionuclide affinity of the boom clay.

(iii) The retention factor in the alteration layer for Np is smaller than for Pu and Am. For module B (BSG) of test tube 2 (30°C), and for module C (BGF) of test tubes 2 and 3, the leached fraction and the equivalent thickness are always distinctly higher for Np, indicating that Np is less well retained than Pu and Am. For module A, the trivalent Am is leached to the same extent as Np.

2.2.3.2.2 Migration of Np, Pu, and Am

The results for the different test cases represented in Figure 13. Data points coincide with the position of the half thickness of the clay slice. For tube 3 – module B (90 °C, ^{60}Co, BSG), the activity profiles of Np and Pu decrease unexpectedly rapidly. We attribute this to the fact that the clay close to these glass samples was not fully saturated during part of the test, as already discussed in previous Sections. This hypothesis is corroborated by the deviating values of the leached fraction and the equivalent thickness for this module (Table 12).

For all test cases, the specific radionuclide activity drops by several orders of magnitude over the first few mm of clay. This demonstrates the good properties of the high-density backfill materials with high radionuclide sorption capacity for retarding radionuclide migration. It has to be noted that in a first stage, when the pre-compacted clay was not yet fully re-saturated, the radioactive glass samples were during several months in contact with a loose clay sludge (filling the gap between the glass samples and the pre-compacted bricks) rather than with a dense saturated clay (except for BSG, 90 °C). This may have resulted in a fast dispersion of the radionuclides in the first few mm of clay.

Despite the strong decrease of the specific activity over the first few mm of clay, the specific activity of Pu and Am in module A (DBC) and B (BSG) further away from the glass remains substantially higher than the background. This is especially the case for Am. Although we took great care to clean after each cutting the clay sampling tube and the cutting tool, we cannot exclude that this is due to a small (but with an important effect, given the big activity gradient over the first few mm) cross contamination with clay particles from the more active slices. If, however, the high specific Am (and, to a smaller extent, Pu) activities are not due to such cross contamination, these results demonstrate that a small but important fraction of these radionuclides migrates relatively rapidly through the clay. This is discussed further below.

The sharp increase of the Am specific activity at ~13 mm (test tube 2) and ~17 mm (test tube 3) in the DBC and BSG clay cores is most probably not due to a cross contamination. These peaks are likely caused by the rapid advection-driven migration of an Am front in the partly hydrated backfill material during the re-saturation phase. Indeed, based on the experience with the RESEAL tests [13], we know that the re-saturation of the pre-compacted backfill materials proceeds from the borders to the central

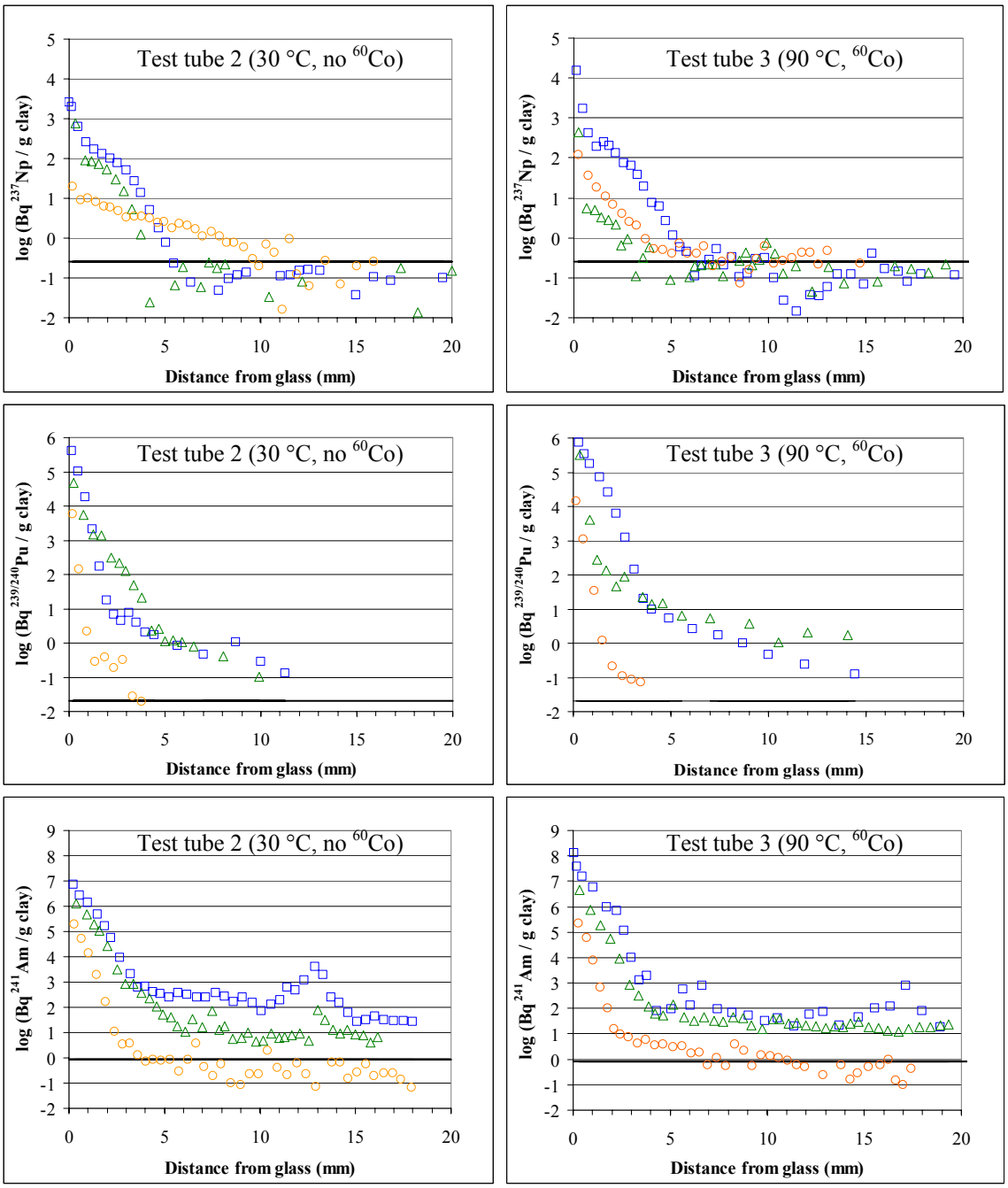

Figure 13 *Radionuclide migration profiles for Np (top), Pu (centre), and Am (bottom). Left: test tube 2 (3.3 years 30 °C, no ^{60}Co sources); Right: test tube 3 (13 years 90 °C, with ^{60}Co sources); (□) DBC, (△) BSG, (○) BGF. The horizontal black line represents the detection limit (0.25 Bq/g for ^{237}Np, 0.02 Bq/g for Pu, and 0.75 Bq/g for ^{241}Am).*

part. Consequently, there must have been in the re-saturation phase a small advective flow of pore water from the surroundings of the glass samples – with, for the Am-doped samples, already an important leached activity – to the centre of the pre-compacted bricks. A distance of ~13 mm (test tube 2) and ~17 mm (test tube 3) corresponds with a little bit less than half the thickness of the pre-compacted bricks (34 mm for test tube 2; 52.5 mm for test tube 3). This is in line with the fact that the more important advective flow during the re-saturation phase is from the partial porous outer support tube (see Figure 2) towards the centre of the pre-compacted backfill materials.

In all cases the order of specific activity at the glass/clay interface is: DBC ≥ BSG >> BGF. This sequence agrees with the higher degree of alteration of the SON 68 glass, with thicker glass alteration layers, found for DBC and BSG (see Section 2.1.1). Activities are always higher for test tube 3, operated at 90 °C, but for a shorter duration. This is fully in agreement with the glass alteration increasing strongly with temperature. The difference is less pronounced for BGF, with addition of powdered glass frit.

When expressed as specific molar adsorption, the higher values (this is for tube 3 – DBC, and for the clay slice in contact with the glass sample) are (^{237}Np) ~2.3 µmol/g clay, ($^{239/240}$Pu) 0.4-1.3 µmol/g clay (depending on the ratio of ^{239}Pu to ^{240}Pu), and (^{241}Am) 4.3 µmol/g clay. These concentrations are far below the cation exchange capacity of the backfill materials (~230 µeq/g for (undisturbed) boom clay and ~700 µeq/g for 100 % Ca-bentonite), so that it is unlikely that these radionuclides precipitated. Yet, it is possible that at the glass – clay interface (part of) the leached radionuclides did (co-)precipitate.

The radionuclide migration profiles are very complicated and function of different mechanisms: dissolution rate of the glass, (co-)precipitation, sorption, colloid formation and transport. As already mentioned, a fast dispersion of the radionuclides in the first ~2 to ~4 mm of clay might have taken place when the pre-compacted clay was not yet fully saturated. The extent of the contribution of colloids depends on the radionuclide and on the colloid forming conditions, such as type of backfill material, temperature, pH, and E_h. [61 and references therein]. Both real colloids (formed from hydrolysis and polymerisation of dissolved actinides) and pseudo colloids (formed by adsorption of radionuclides onto existing colloids in the backfill pore water, or onto freshly formed glass alteration products) can be involved. Especially for Am, the profile in DBC and BSG suggest a contribution of colloidal transport.

Am is very succeptible to complexation by humic acids [61], and the resulting pseudo colloid formation could be invoked to explain the high activities deeper in the DBC, with a high total organic carbon content in the pore water (see Section 2.1.2.5). Also in BSG, with a lower total organic carbon content in the pore water, the specific Am and Pu activity remains high, indicating that this complexation of Am by humic acids is very strong. The same conclusion was drawn from migration experiments with ^{241}Am and ^{14}C-labelled boom clay 'natural organic matter' (NOM) in undisturbed boom clay cores [66, 67]. Upon contacting the ^{241}Am-^{14}C-NOM mobile complexes with boom clay, the major part of Am became almost instantaneously dissociated and immobilised, while only a small fraction persisted as a 'stabilised complex' which migrated along with the mobile NOM. This resulted in an apparent constant concentration release of 10^{-13} to 10^{-12} M Am. However, by increasing the travel time in the clay, the recovery of these 'stabilised complexes' decreased, indicating a slow but significant dissociation of these 'stabilised' mobile complexes. This decrease could be fitted to a first order kinetic model with a rate of 8×10^{-8} per second. Although not always so clearly visible in the Am migration profiles in Figure 13, we can expect that the specific Am activities in the backfill materials of the CORALUS tests would decrease to very low values if the backfill materials were sufficiently thick.

For Np in tube 2 and – but less clear – tube 3, the profile for BGF has a different shape than for DBC and BSG. Possibly, this is linked to a different oxidation state and/or speciation of Np. Np occurs in the SON 68 glass as Np(V) and is released as neptunyl (NpO_2^+), which is slowly reduced to Np(IV) [61]. Because of its low electric charge, $Np(V)O_2^+$ is more soluble and less strongly hydrolysed and complexed than Np(IV). Our results could suggest that Np occurs as Np(IV) in modules DBC and BSG, and as NpO_2^+ in BGF. If this would indeed be the case, we can only speculate about the reason for this different behaviour (the backfill materials BSG and BGF both contain Ca-bentonite).

The heating of test tube 3 to 90 °C in combination with the gamma irradiation has resulted in a 3 to 5 times increased content of dissolved carbon dioxide in the solution, compared to tube 2 (30 °C) (see Section 2.1.2.5). Accordingly, the pH decreased, especially for DBC and BSG (decrease of ~1.5 units). It is very likely that the variation of these two parameters will have influenced the radionuclide speciation. Thermo-dynamical modelling is necessary to estimate the respective contributions of pH decrease and increase of dissolved carbon dioxide (related to the total inorganic carbon content). Unfortunately, this was not foreseen in the CORALUS-2 project.

2.2.3.2.3 Migration of U, Th, Cs, Zr, and Pd

The evolution of the extractable concentrations of U, Th, Cs, Pd, and Zr as a function of distance in the clay is graphically represented in Figure 14 (U and Cs) and Figure 15 (Th, Zr, Pd). Data points coincide with the position of the half thickness of the clay slice. Detection limits are plotted as horizontal lines, in the colour of the respective test case. For all elements, except for Zr in module C (Zr present in the powdered glass frit of BGF), we observe the same tendencies as for Np, Pu, and Am: the extractable concentrations are considerably higher at higher temperature, and the extractable concentrations generally decrease in the order DBC > BSG > BGF. The degree of decrease of element concentration as a function of depth varies for the different elements. We can roughly distinguish two groups: U and Cs, which seem to be more mobile, and Th, Zr, and Pd, wich appear to be rather immobile.

Making abstraction of the variability of the results, we can somehow detect slightly higher extractable U concentrations close to the U/Th-doped glass samples of the different backfill materials of test tube 2 (30 °C). The increase is small, in agreement with the limited glass alteration observed for this test tube (see Section 2.2.1). Within 1 to 2 mm, the extractable concentration decreases again to the background value. The picture is quite different for DBC (module A) and BSG (module B) of test tube 3 (90 °C). Especially for DBC, the extractable concentration at the glass/clay interface is high, and U seems to have migrated over about 10 mm (5 mm for BSG). On the basis of E_h-pH speciation diagrams of U for boom clay pore water [51,52,66], and taking into account the lower pH and E_h and the higher dissolved CO_2 concentration in the DBC system, we hypothesise that U is present in the hexavalent form, as a $UO_2(CO_3)_2^{2-}$ (lower pH) or $UO_2(CO_3)_3^{4-}$ (higher pH). These negatively charged species are not retarded in the DBC backfill material, which explains their rapid migration. For module B (BSG) of test tube 3 (90 °C), the same species might have occurred. For module C (BGF) of test tube 3, with (almost) no visible U migration, it is more difficult to comment on the result. The flat profile can be the result of the very low glass alteration and the related low leaching of U. But it is also possible that in this test system U occurs as the less mobile $U(OH)_4$ (aq). Of course, thermo-dynamical calculations for the specific test conditions are necessary to ascertain these hypotheses.

Just like Na^+, Cs^+ is a very soluble element that leaches easily and congruently from the altering glass (see Section 2.2.1). It is well-known that trace concentrations of Cs^+ are very strongly and specifically retained on the so-called Frayed Edge Sites of clay minerals like illite and vermiculite [68, 69]. Under given conditions (ratio of the concentrations of the monovalent K^+ and Na^+ to the bivalent Ca^{2+} and Mg^{2+}, application of wetting-drying cycles), traces of Cs^+ can also strongly adsorb on collapsed interlayers of montmorillonite and bentonite clay minerals [70]. The capacity of these high affinity sites is, however, fairly low, a few µeq/g of clay. At slightly higher Cs concentrations, caesium also sorbs on the regular cation exchange capacity of clay minerals and organic matter, where it has to compete with other monovalent and bivalent cations (Na^+, K^+, Mg^{2+}, Ca^{2+}) [71, 72]. The relatively high concentration of Cs^+ in the U/Th-doped glass samples (1.1 wt %) in combination with the high Na^+ concentration in the pore water (competing strongly with Cs^+) may explain the relatively weak specific sorption of Cs^+, and hence its high migration (~15 mm in DBC of test tube 2, 30 °C, and ~25 mm in DBC of test tube 3, 90 °C). The lower migration of Cs^+ in the bentonite based backfill materials suggests that in these materials more high affinity sites were available to assure the strong sorption of Cs^+.

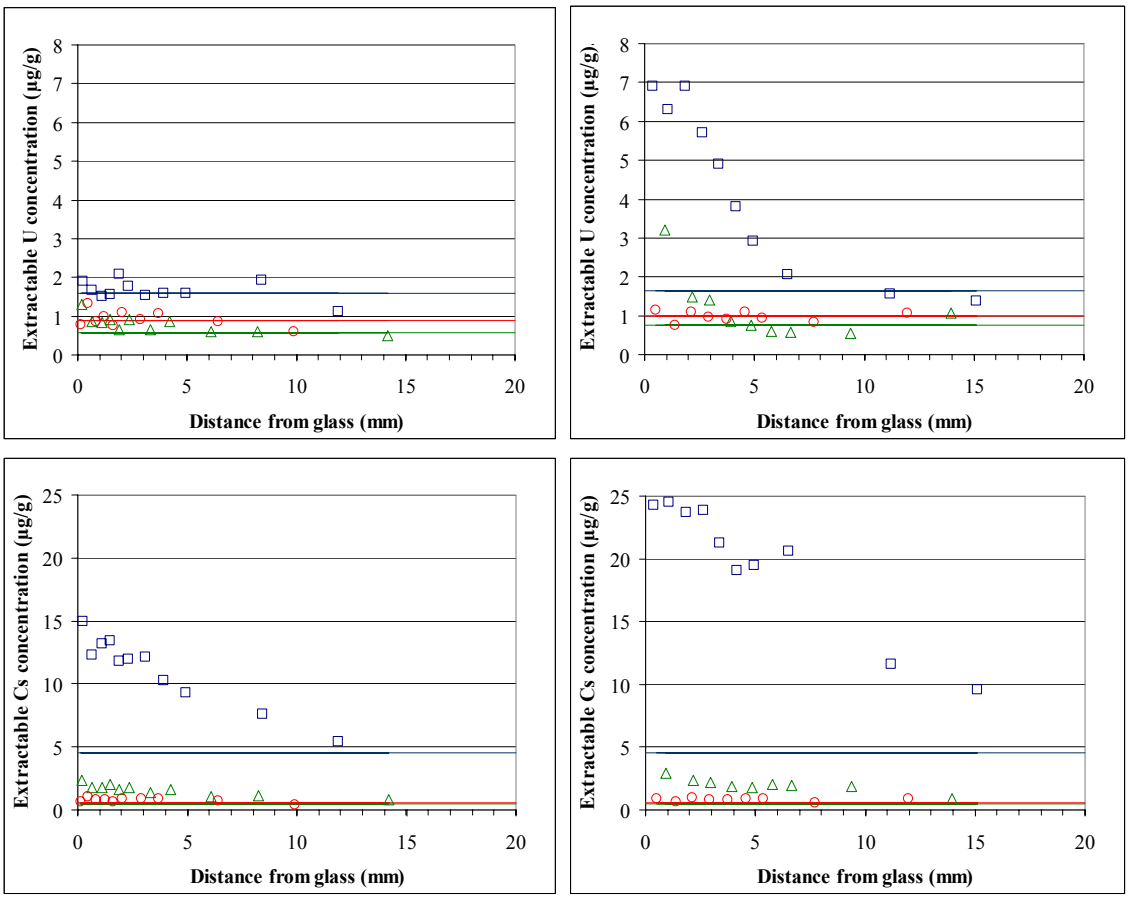

Figure 14 *Migration profiles for U (top) and Cs (bottom). Left: test tube 2 (30 °C, 3.3 years); Right: test tube 3 (90 °C, ^{60}Co sources, 1.3 years); (□) DBC, (△) BSG, (○) BGF. The horizontal coloured lines represent the background values or the detection limit for the respective test cases.*

The only stable oxidation state of Th is Th^{4+}. It has a high tendency to hydrolyse to the poorly soluble $Th(OH)_4$, with the $Th(OH)_4$ (aq) species in the pore water. Th^{4+} also strongly adsorbs on the solid phase (clay, immobile organic matter). The strong sorption in combination with the low solubility results in a very low migration of Th^{4+} in all three backfill materials (as well as in the glass alteration layers).

As can be expected, the behaviour of Zr^{4+} strongly resembles that of Th^{4+}. Zr^{4+} is both in the alteration layer (Section 2.2.1) as in the backfill material almost immobile, due to its strong sorption and low solubility. The situation is of course different for module C (BGF). The presence of 0.7 wt % of ZrO_2 in the powdered glass frit results in high and varying extractable Zr concentrations in BGF. For test tube 2 (30 °C), we can still distinguish a small increase of the extractable Zr concentration at the glass-clay interface. This is no longer the case for test tube 3 (90 °C). For DBC, the extractable Zr^{4+} concentration at the glass-clay interface is very high, indicating an important glass alteration in this backfill material with a strong Zr immobilisation at the glass/clay interface.

For Pd^{2+}, the extractable concentration was in most slices below the detection limit of 0.2 to 0.3 µg/g. Only in the first clay slice(s) of DBC and BSG (these slices were in contact with or very close to the altered glass sample), higher extractable Pd^{2+} concentrations were measured. Pd^{2+} is thus very immobile, which is of course linked to the fact that in the glass it was present in the poorly soluble metallic form (see Section 2.2.1 and Figure 6-a).

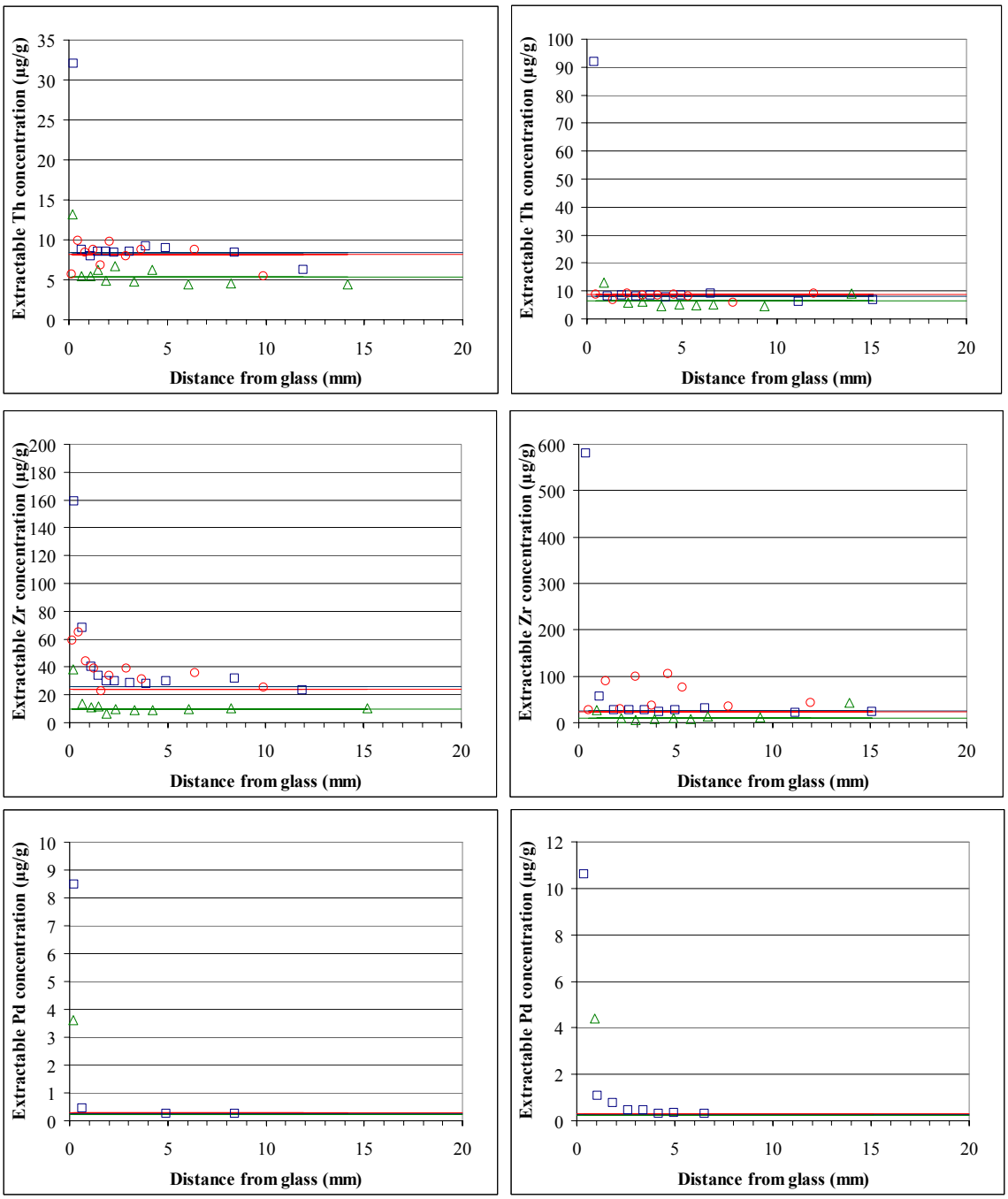

Figure 15 *Migration profiles for Th (top), Pd (centre), and Zr (bottom). Left: test tube 2 (40 months 30 °C, no ^{60}Co sources); Right: test tube 3 (15 months 90 °C, with ^{60}Co sources); (□) DBC, (△) BSG, (○) BGF. The horizontal coloured lines represent the background values or the detection limit for the respective test cases.*

2.3 Laboratory tests on thermal gas generation (WP6) [22]

In a separate laboratory experiment, the thermal gas generation for the three backfill materials was measured at 90 °C for periods up to 1000 days, to help to understand the results on the gas concentration in the piezometer waters obtained under WP2. The backfill materials were heated in specially designed glass recipients to which degassed water was added to achieve the calculated water content of the saturated backfill materials in the *in situ* tests, and with nitrogen in the residual volume.

[22] This part has been described in detail in the detailed report of GRS-Braunschweig.

The results, which are the average of three measurements, are presented in Figure 16. Results are expressed as m^3 of gas produced per 1000 kg of oven-dry material. As expected, carbon dioxide is the only gas which was released in large amounts: up to 0.95 m^3 per 1000 kg from backfill A (DBC), up to 0.30 m^3 per 1000 kg from backfill B (BSG), and up to 0.06 m^3 per 1000 kg from backfill C (BGF). The amount was still increasing with time, especially in backfill A and backfill B. Carbon dioxide is generated by thermal decomposition of organic matter in all three backfill materials, and by thermal decomposition of the graphite, even at 90 °C, in backfill B (see Section 2.1.2.4). The Ca-bentonite clay has a low content of organic material which results in lower generation of carbon dioxide from the backfill B and C. Additionally, carbon dioxide might also have been generated by thermal decomposition of calcium carbonate (calcite) in the clay. Both the boom clay and the Ca-bentonite contain about 1 wt % of calcite.

Hydrogen was generated up to 0.08 m^3 per 1000 kg from backfill A (DBC) and up to 0.006 m^3 per 1000 kg from backfill B and C within 1 to 3 days of heating. Later on, its amount decreased by oxidation and back reaction. Below the combustible concentration of oxygen and hydrogen, calm reactions take place, generating hydrogen peroxide and hydrogen oxygen radicals which decompose at elevated temperature [73, 74].

Methane was only detected in the systems with backfill B (BSG) and in the systems with backfill C (BGF) when heating lasted longer than 100 days. The released amount was up to 0.0008 m^3 per 1000 kg. Further hydrocarbons and further gases were below the detection limit of the gas chromatograph and therefore do not seem to be of importance.

For long-term safety aspects, the amounts of the generated and released hydrogen and of the hydrocarbons are not of importance, because they will be dissolved in the interstitial water of the clay. The boom clay and the buffer materials contain at least 300 litre of water per 1000 kg. The Bunsen coefficient (solubility of the gas in water at 20 °C and 1 bar or 0.1 MPa) is 0.035 litre per kg water for methane and 0.0178 litre per kg water for hydrogen. Consequently, with a water content of 300 litre per 1000 kg clay, up to about 10 litre of methane and up to about 5 litre of hydrogen can be dissolved. These values are much higher than the amount of gas generated within 1000 days.

Carbon dioxide is a reactive gas in water, and therefore the Bunsen coefficient of 0.87 litre per kg water cannot simply be used for calculation of the total amount of carbon dioxide that can be dissolved in the pore water. The calculations reported in Section 2.1.2.4 suggest that the partial CO_2 pressure can exceed 1 atmosphere (~1 bar), but with pore water pressures of the order of 20 bar (0.2 MPa), as in undisturbed boom clay at a depth of 220 m, the CO2 generation would not result in the formation of a separate gas phase.

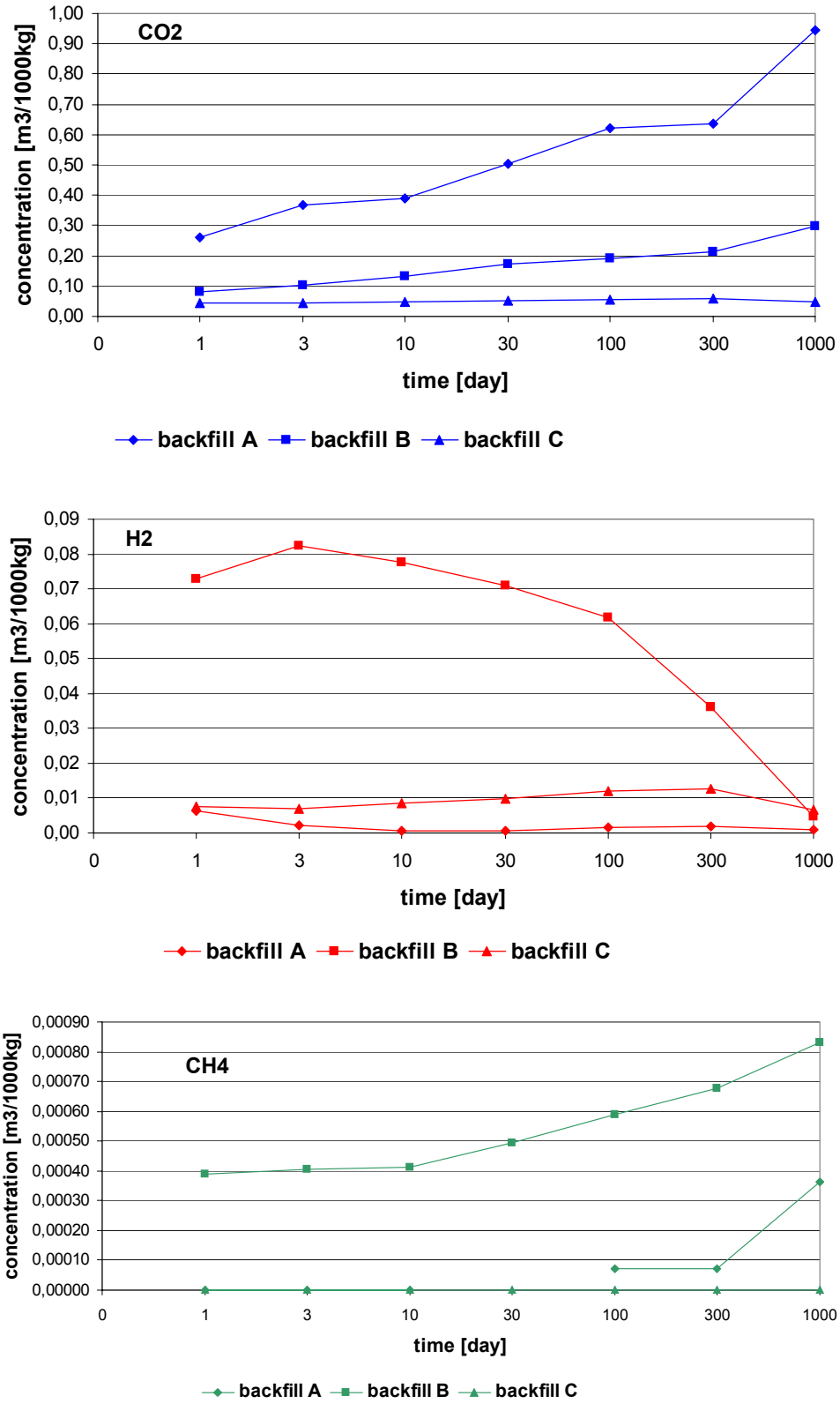

Figure 16 *Evolution of the release of carbon dioxide (top), hydrogen (centre), and methane (bottom) from the different backfill materials upon heating at 90 °C (closed systems with nitrogen in the residual volume). Backfill A = Dried boom clay, backfill B = FoCa clay with sand and graphite, and backfill C = FoCa clay with powdered glass frit.*

2.4 Laboratory test on glass alteration (WP7) [23]

To compare the results of the *in situ* test, glass corrosion tests were performed in a surface laboratory, under the same specific CORALUS test conditions (30 or 90 °C, three backfill materials at high density, contact with boom clay pore water). Within the framework of the EC contract, 18 tests with non-radioactive SON 68 glass samples were started: two temperatures, three backfill materials, and three durations (between 1 and 10 years), however in the absence of gamma radiation.

2.4.1 Experimental aspects

The tests were performed in small stainless steel reactors allowing to contact 'inactive' U/Th-doped glass samples with pre-compacted backfill materials that after re-saturation with partially oxidised boom clay water would have the same density as in the *in situ* test tubes. Before addition of the partially oxidised boom clay water, under pressures between 4 to 8 MPa, the reactors were several times evacuated and flushed with hydrogenated argon. About 1 month was necessary for the resaturation of the backfill materials, and about 0.15 ml of solution was injected per gram of clay. Reactors were then placed in an oven at 30 °C or 90 °C for periods listed in Table 13.

Table 13 *Test durations for the surface laboratory glass corrosion tests.*

Temperature	Duration 1	Duration 2	Duration 3*
30 °C	1 year	2 years	10 years
90 °C	1 year	16 months	6 years

* See also Table 1.

2.4.2 Results and discussion

During the project, the glass corrosion tests of duration 1 and 2 were retrieved and dismantled. For all test systems, the backfill materials appeared to be wet, and all glass samples were broken. This could suggest that the re-saturated clay must have exerted at least some swelling pressure. However, it is equally possible, or even more likely, that the glass samples were already broken because of the high gas pressure applied to inject the leaching solution. The surface and the polished cross section of the altered glass samples have been characterised by SEM-EDS.

Similarly as for the *in situ* tests, the surface of the alteration layer of the glass samples in contact with DBC (module A) and BSG (module B) in test tube 3 (90 °C) was cracked due to drying of the alteration layer. This was not the case for the thinner alteration layer for the sample in contact with BGF (module C) of this test tube, and only small holes were observed at the surface of the gel of this sample. SEM of the polished cross section of the glass samples revealed that, in contrast to the samples from the *in situ* tests, the alteration layer on the samples was intact (*i.e.* no partial nor complete loss of the alteration layer), just as for the Np-doped sample in contact with BSG (module B) of test tube 3 (90 °C) (see Sections 2.1.1 and 2.2.1). This could perhaps be due to the fact that the total pressure exerted by the clay and the pore water on the glass alteration layer, was lower than for most test cases in the *in situ* tests. The SEM and EDS analyses of the polished cross section further showed a very dense zone of ~6 µm, composed of nodules of Si, Al, Ca, Fe and REE [24], outside the alteration layer of the glass sample in contact with DBC, after 16 months at 90 °C (Figure 17-a). Also on top of the alteration layer of the glass sample in contact with BSG after 16 months at 90 °C, many crystals were present. They were made of P, Ca, and REE. Below these crystals, phyllo-silicates were observed, as well as nodules inside the gel layer (Figure 17-b).

[23] This part has been described in detail in the detailed report of CEA-Valrhô.
[24] Rare earth elements.

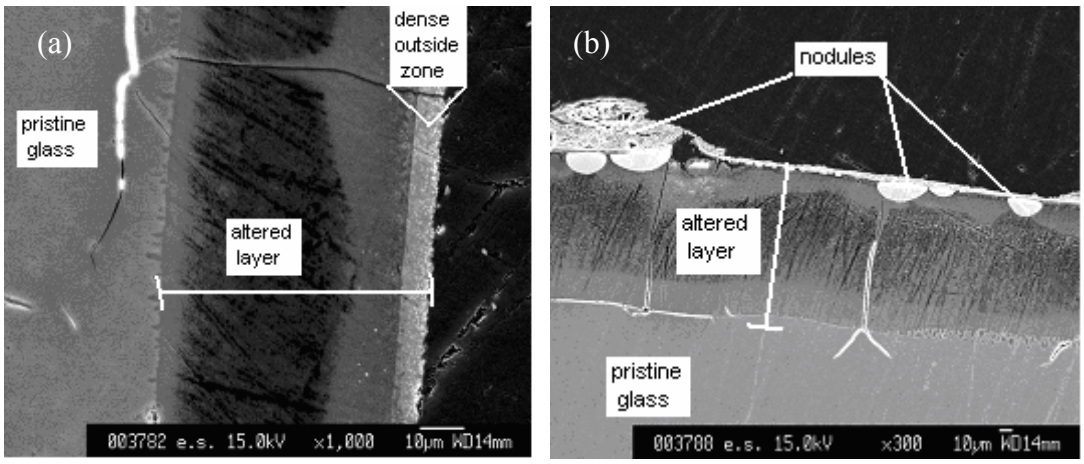

Figure 17 *SEM observations of glass samples altered during 16 months at 90 °C in contact with DBC (a; magnification 1,000 ×) and BSG (b; magnification 300 ×) (surface laboratory tests, no ^{60}Co).*

The thickness of the alteration layer of the different samples is summarised in Table 14. The experimental data confirm the difference between the different interacting materials: the glass alteration is up to two orders of magnitude higher in contact with DBC (module A) than in contact with BSG (module C). As expected, the glass alteration at 30 °C is at least two orders of magnitude lower than at 90 °C. There are two deviating values: for module A (DBC) after 1 year of alteration at 30 °C, and for module B (BSG) after 2 years of alteration at 30 °C. Despite these results, no anomaly was observed when the test systems have been opened: the backfill materials in contact with the glass samples were wet. However, we do not know if the glass samples of these test systems were during the whole test duration in contact with the backfill. It is possible that, similarly as for module B of test tube 3 (see Sections 2.1.1 and 2.2.1), the glass came in contact with the clay during the test, and not before the test started. Such behaviour could be due to a slow re-saturation in combination with the occlusion of compressed gas (hydrogenated argon) between the glass and the backfill and/or solution.

Table 14 *Gel thicknesses (µm) measured on the U/Th-doped glass samples of the surface laboratory tests.*

	30 °C, no ^{60}Co			**90 °C, no ^{60}Co**		
	Backfill A (DBC)	**Backfill B (BSG)**	**Backfill C (BGF)**	**Backfill A (DBC)**	**Backfill B (BSG)**	**Backfill C (BGF)**
12 months	< 0.1	0.5<1.0±0.2<1.5	< 0.1	50<55±3<60	65<70±5<75	0<0.1±0.05<0.2
16 months	-	-	-	55<70±5<90	90<95±5<100	0.3<0.5±0.1<0.8
24 months	0.5<1.0±0.2<1.5	0.2<0.3±0.1<0.3	0<0.05±0.05<0.1	-	-	-

The lower and upper values give the range of thicknesses observed per sample. The central value gives the estimated average thickness, with an estimate of the uncertainty on this average.

2.5 Synthesis and interpretation of all results (WP8)

2.5.1 Representativeness of the tests

The CORALUS tests aimed at studying the corrosion of SON 68 glass and the leaching and migration of incorporated radionuclides in conditions that are representative for those expected to prevail in a geological repository based on the use of clay as a backfill material. The design of the *in situ* test tubes integrates different factors and processes that affect the glass dissolution and radionuclide release and migration, thus creating the conditions for coupled processes to occur: temperature and temperature gradient; radiolysis; radioactive glass in contact with a backfill material exerting a high swelling pressure; geochemical conditions that are partially controlled by the surrounding host formation; leaching, sorption, (co)precipation and secondary phase formation of radionuclides and glass

constituents; radionuclide complexation. Moreover, the tests were performed in the best possible conditions, with amongst other, a calibration of the whole measurement chain for temperature and pressure measurements, follow-up of the hydration of the backfill materials, and regular analysis of the pore water of the different backfill materials. The *in situ* tests thus (will) provide(d) a set of realistic and reliable data that can be used for comparison with and validation of data from surface laboratory experiments and modelling studies. It is important to note that due to a slow re-saturation of the pre-compacted backfill, the data obtained for module B (BSG) of test tube 3 (90 °C) are not reliable. The same applies possibly for some test cases of the surface laboratory glass corrosion experiments (see Section 2.4.2).

There are also several parameters and processes that are not included in the design. The tests at 30 °C simulate the normal evolution conditions beyond the thermal period, after advanced corrosion of the overpack and glass canister (after > 500 years). It is well-known that the backfill material that will come in contact with the glass in these conditions will have been altered by prolonged heating and irradiation. If the backfill material contains powdered glass frit, additional reactions involving leached glass constituents will take place, as confirmed by the results of the analysis of backfill C (BGF) from test tube 3 (90 °C, ^{60}Co; see Section 2.2.2). The same remark applies to some extent to the tests at 90 °C. In addition, the anaerobic corrosion of the steel used in the engineered barriers (containers, overpacks, disposal tube) will result in the presence of corrosion products such as magnetite. The backfill materials used in the CORALUS tests, both at 90 °C and 30 °C, did not undergo an 'alteration' pre-treatment (combined heating and irradiation at high pressure), nor were iron corrosion products added to the backfill material. The rationale behind this decision was that *(i)* the effect of clay or corrosion products on the glass alteration is similar, and adding a layer of corrosion products would have made the design and the assembly of the test tubes much more complex, and *(ii)* the effect of the mineralogical alteration on the glass corrosion and radionuclide leaching and migration is likely smaller than the effect of the type of backfill material (for instance with or without addition of powdered glass frit). Of course, this is subject to discussion, and the reality is much more complex and interrelated. In any case, despite these shortcomings, we believe that the tests were in general performed in realistic conditions.

The geochemical conditions prevailing in the three backfill materials were/are the overall result of different processes and interactions:

- the contact, through the partially porous outer support tube, with the partly oxidised surrounding boom clay, containing high Na_2SO_4 and Ca^{2+} concentrations;
- (for DBC, module A) the oxidation of the dried boom clay backfill material, resulting in high Na_2SO_4 and Ca^{2+} concentrations, and in decreasing pH values (pH going from 7.9 to 7.3 in DBC of test tube 2, 30 °C, 3.3 years).
- (for BSG and BGF, modules B and C) the interaction of the infiltrating partly oxidised boom clay water with the Ca-bentonite, resulting in high Na_2SO_4 and Ca^{2+} concentrations.
- (for BGF, module C) the dissolution of the powdered glass frit in the backfill material, resulting in high B and Si concentrations, and in a decrease of the pH to a value of 6.2 at the end of the test (test tube 2, 30 °C, 3.3 years).
- (for test tube 3, especially modules A and B) the production of high amounts of CO_2 due to the thermal and radiolytic decomposition of the organic matter in the different backfill materials and the surrounding boom clay, and (for module B, BSG) due to the radiolytic decomposition of the graphite, resulting in a sharp decrease of the pH (values between 5.5 and 6.5 for the three modules) and in high dissolved $CO_2 – HCO_3^-$ contents.

Geochemical modelling is very useful to better understand the results, but was unfortunately not foreseen in the CORALUS-2 project.

Besides CO_2, also methane (especially in test tube 2, 30 °C) and hydrogen (more in test tube 3, 90 °C, ^{60}Co sources) were present in low to moderately low concentrations in the interstitial solution. The concentrations of these gases were sufficiently low, so as not to create a separate gas phase and related

problems.

The fact that no important contamination was found in the piezometer waters around the glass samples demonstrates that these backfill materials with good radionuclide adsorption properties, at sufficiently high density, indeed constitute an effective seal against radionuclide migration. The low hydraulic conductivity, being only about 3 times higher than that of undisturbed boom clay, gives further evidence for this. Upon retrieval and dismantling, it appeared that all initially pre-compacted backfill materials of test tube 2 (30 °C) had well swollen and become one homogeneous mass of dense humid clay. In contrast, the backfill materials from the modules in test tube 3, especially the bentonite-based backfill materials, fell apart into the initial pre-compacted bricks. This behaviour was also observed in another test using pre-compacted backfill materials. It is very probably due to the low water content of the high-density pre-compacted backfill material. For the surface laboratory test systems, the total pressure – that is the sum of the swelling pressure of the backfill material and the pore water pressure – on the glass was probably lower than in the *in situ* test systems, since the alteration layers of the corroded glass samples were still intact, and thicker than for the *in situ* tests. A similar observation was made for the Np-doped glass samples – and to a smaller extent for the Pu-doped and Am-doped glass samples – of module B of test tube 3 (90 °C, ^{60}Co). For this module, we observed a very long re-saturation phase (even during the heating phase), resulting in a very low pore water pressure.

2.5.2 Glass alteration and radionuclide leaching

2.5.2.1 Results of the in situ and surface laboratory tests: general observations

The results of the glass alteration tests are the outcome of many interacting processes. To interpret the data, a good understanding of the underlying processes and their coupling is necessary, as well as the application of different analytical techniques (mass loss, SEM, EDS, SIMS, *etc.*). In our tests, the lack of sufficient data on mass loss of the altered glass samples hampers the interpretation of the observations. We have to rely more on the thickness of the alteration layers and the results of the SIMS analyses. Yet, the partial loss of the alteration layer of the glass samples of the *in situ* tests, both by processes inherent at the glass corrosion process and by treatment of the glass samples, limits also the use of these data.

In any case, the results of the glass alteration tests respond fully to the expectations and allow making the following conclusions.

1. The glass alteration at 90 °C is considerably higher than at 30 °C. As far as data are available and reliable, we measure differences in specific daily mass loss by a factor of 20.

2. The addition of powdered glass frit to the backfill material has a beneficial effect: it diminishes the glass alteration considerably, probably with about two orders of magnitude, or even more. Optimisation of the repository performance is thus possible. The effect of powdered glass frit occurs most probably through the rapid establishment of high solution concentrations of the main glass constituents, and by concomitant rapid saturation of sorption sites on the backfill material and the production of precipitates and secondary phases close to the surface of the radioactive waste glass.

3. The alpha-beta-gamma doped glasses behave rather similarly as the inactive ones. Yet, we observe slightly thicker alteration layers for the radioactive samples, and the thickness seems to increase with increasing alpha-beta-gamma activity of the samples. This is less clear for the samples of module C, with BGF, because of the low glass alteration. Because of the lack of sufficient data, we cannot conclude that this goes along with an increased mass loss. The SEM analysis of the surface of the glass samples also indicates a higher alteration degree for the radioactive samples. If there would be an effect, it would be small (a factor of ~1.5). The observation of thicker alteration layers for the radioactive samples was also made for the samples from test tube 3 (90 C, with ^{60}Co sources), for which the pH was already considerably lower, and for which the gamma radiation dose rate was already very high (~130 Gy/h) and similar for both inactive and radioactive samples. Therefore, we

conclude that this effect is partly due to the alpha activity of the samples. As this conclusion differs from the conclusions from glass alteration tests in water or suspensions with samples doped exclusively with alpha emitters, the reason for our observations has probably to be looked for in the high water and/or swelling pressures prevailing during the glass alteration, in combination with the increasing alpha-beta-gamma activity of the samples.

4. The results of the SIMS profiles agree well with the results of previous tests. For most profiles, we can distinguish (some of) the layers often reported in literature (precipitation layer, main alteration layer, and diffusion layer). SIMS profiles – normalised to Zr, which proved to be rather stable in both pristine and altered glass – showed the leaching of Li^+, B, Na^+, Cs^+, and – but less pronounced – Sr^{2+}, Ba^{2+}, and REE; influx of H^+, K^+, and Mg^{2+} from the clay (pore water), and the stability of Si, Al, Fe. Ca^{2+} proved to be rather stable, probably because of the high Ca^{2+} pore water concentration. Also Si and Al were stable, in some cases their intensity even increased towards the top surface. The profiles of Th, Np, Pu, and Am showed that these elements were stable in the alteration layer. U, in contrast, seemed to be more easily leached. Enrichments or depletions with respect to Zr were small and probably not significant. The loss of part of the alteration layer did not allow concluding whether these elements were selectively retained in the alteration layer. Taking into account the nearly complete elimination in B and the alkali metals in the alteration layer of the SIMS profiles, we conclude that the dissolution of the SON 68 samples is predominantly selective-substitutional leaching, as observed for other SON 68 glass alteration tests. Yet, the loss of a distinct part ('layer') of the alteration layer, either because of the sorption of the glass constituents onto the clay and/or secondary phase formation, or because of the treatment of the glass samples, can be interpreted as matrix dissolution.

5. EDS of the altered surface and of the polished cross section of the samples did not clearly reveal the presence of radionuclide containing secondary phases. Possibly, such secondary phases had developed, but were removed together with the clay during the retrieval and cleaning of the glass samples.

2.5.2.2 Comparison of the results with results of other tests and modelling predictions

2.5.2.2.1 Mass loss

Inactive glass samples

For DBC (module A), the results presented in Table 10 – except for Np, which is probably an outlier – correspond with the values obtained from integrated surface laboratory tests for the same conditions in undisturbed boom clay (*i.e.*, 0.01 g/m²/day at 30°C, and 0.2–0.3 g/m²/day at 90°C, but without gamma irradiation; test duration up to 2.5 years) [75-77]. The good agreement of the mass loss data at 90 °C for the tests with and without gamma irradiation might suggest that, at least for dried boom clay heated at 90 °C, there is no (important) effect of gamma radiation. This is in contradiction with the assumption that the decreased glass alteration as reported in [25, 78] is due to the gamma irradiation, which would have lowered the pH. However, the decrease of the pH can also be provoked *(i)* by the high CO_2 production upon decomposition of boom clay organic matter at high temperature (see Sections 2.1.2.4 and 2.1.2.5), *(ii)* possibly, by the radiolysis of water, and *(iii)* the high CO_2 production due to the thermal decomposition of the boom clay mineral assembly. An important inherent prerequisite is that the test systems are closed, so that the produced CO_2 cannot escape. In this regard, it is possible that the higher pH values of the control test systems in the work reported in [78] (~8.8 for the control test systems against ~7.5 for the irradiated test systems) is to be related to the different test containers used. Indeed, the test systems that were gamma irradiated were contained in sealed glass ampoules – forcing CO_2 to dissolve and acidify the solution – whereas the unirradiated control tests systems were contained in Teflon recipients that were likely less airtight – thus allowing the generated CO_2 to escape, resulting in higher pH values and higher glass corrosion [76].

The (expected) mass loss for the 'inactive' U/Th-doped SON 68 samples from module A (DBC) in test tube 3 (90 °C, gamma irradiation), *i.e.* 0.2–0.3 g/m²/day, is lower than the values obtained from the

former 'first generation' *in situ* glass corrosion experiments at 90 °C exposing, amongst other, SON 68 glass samples to (partially oxidised) boom clay [26]. The specific daily mass loss data for three test durations are summarised in Table 15. We cannot explain these differences. They are presumably related to differences in pH and/or temperature. Also, we have no idea about the uncertainty on these values.

Table 15 *Specific daily mass loss (g/m²/day) for SON 68 glass samples in contact with boom clay at 90 °C for different time periods (from [26]).*

Nominal test duration (years)	Duration of exposure at 90°C (days)	Effective test duration (years)	Mass loss (g/m²)	Specific daily mass loss (g/m²/day)
2	643	1.8	370	0.58
3.5	1593	4.4	702	0.44
7.5	2545	7.0	2060	0.81

In the frame of the CERBERUS test (Control Experiment with Radiation of the Belgian Repository for Underground Storage), the alteration of SON 68 glass samples in contact with boom clay was studied at 80 to 85 °C, under gamma irradiation. After 1778 days (almost 5 years) of alteration, the average mass loss was 501±168 g/m² (n = 2), giving a specific daily mass loss of 0.282 g/m²/day [25]. This specific daily mass loss, which is in agreement with our results, is considerably lower than the values for the 'first generation' *in situ* corrosion tests reported in Table 15. The reason for the lower values was attributed to the lower pH values prevailing in the systems with gamma irradiation (7.2 instead of 8.2) and/or the slightly lower temperature in the CERBERUS test (80 to 85 °C). From the discussion above, we might conclude that the lower mass loss value was probably more due to the lower temperature (80-85 °C instead of 90 °C) and the related less low pH, than due to the gamma irradiation.

The value for module B (BSG) is realistic: it is a little bit lower than the value for DBC, which is known to be a very aggressive clay towards glass corrosion. The values for module C (BGF) show the expected very low glass dissolution in the backfill with powdered glass frit.

Radioactive glass samples

The difference in mass loss between the U/Th-doped and Am-doped samples (with ~1×10^9 Bq/g ^{241}Am, giving per g glass 1×10^9 alpha and 0.4×10^9 gamma per second) of module A (DBC) of test tube 2, if significant, is very small: a factor 1.5. If significant, this result is qualitatively in line with results from leaching experiments in pure water (6 years, 90 °C) with laboratory-made active SON 68 type glass of nominal radioactivity (1.6×10^9 Bq/g beta-gamma and 3.8×10^8 Bq/g alpha) [62]. The results of this study showed that both the (higher) initial and the (3 – 4 orders of magnitude lower) long-term glass alteration rate were similar to values for non-radioactive glass samples. However, the time necessary for the highly radioactive samples to reach the low final glass alteration rate was longer for the active glass, resulting in a ~5 times higher amount of dissolved glass. The results for module A (DBC) of test tube 2 could thus be in agreement with this (the radioactive samples contain also beta-gamma emitters; see Section 2.1.1).

As such effect of activity on the glass alteration had not been observed in leach tests in distilled water with glass samples doped exclusively with alpha emitters [5, 6], the authors stressed the importance of beta-gamma radiation. Beta-gamma irradiation would have resulted in an increased interconnectivity in the gel (with a less protective effect of the gel) and/or an increased contribution of ion exchange reactions due to a decreased pH (with a slightly larger altered depth of the glass) [62]. Unfortunately, we have no sufficient mass loss data for the samples of test tube 3 (90 °C, ^{60}Co-sources), for which the contribution of the beta-gamma dose rate of the radioactive samples (< 1 Gy/h) is negligibly small compared to the high gamma dose rate from the ^{60}Co sources (> 100 Gy/h), and for which the pH in the different piezometer waters was already low. The results of the SEM analysis of the surface of the glass samples of test tube 2 (30 °C) might support the conclusion of higher mass loss for the radioactive samples, with an increasing tendency as the alpha-beta-gamma activity of the glass samples increases (see

Figure 4). Yet, it is also possible that for the radioactive samples a relatively thicker part of the alteration layer was lost during manipulations (because the alteration layer itself was thicker). Anyhow, the difference between active and inactive glass samples, if significant, is small for the studied time periods.

2.5.2.2.2 Thickness of the alteration layer
Radioactive glass samples

The observation that the thickness of the alteration layers increases (slightly) with the alpha-beta-gamma activity does not necessarily mean that also the mass loss of the active glass is higher than for the inactive glass. We simply have too little data on mass loss to make conclusive statements on this (see previous Section). As to the thicker alteration layers for the samples with higher alpha-beta-gamma activity, one hypothesis is that this is because the pH at the glass-clay interface is locally lower due to alpha-beta-gamma irradiation by the embedded radionuclides. A lower pH would result in lower glass corrosion, resulting in a lower contribution of the matrix dissolution process [25, 44, 62, 78] (this is only valid for the initial glass corrosion rate regime). As a result, the ion exchange reaction (H^+ with Na^+, Li^+,...) becomes more important, *i.e.* more incongruent alteration, with a thicker gel [60,79]. This mechanism could be invoked to explain the observed effects at 30 °C. However, for test tube 3 (90 °C, with ^{60}Co sources), the pH in modules A and B is already considerably lower (Table 9), and the gamma radiation dose rate high (> 100 Gy/h) and similar for both inactive and radioactive samples. It is questionable whether there is an additional pH decreasing effect due to the alpha-beta-gamma irradiation of the radioactive sample. Still, we observe (slightly) thicker alteration layers for the radioactive samples. From this, we conclude that for the conditions in which the CORALUS *in situ* tests were performed (with, amongst other, a high water pressure and the glass samples in contact with a clay-based backfill material exerting a very high swelling pressure), there is a small effect of the alpha activity on the thickness of the alteration layer.

It is unlikely that the thicker alteration layers for the radioactive samples are related to the increasing removable alpha contamination observed for the ^{241}Am-doped glass samples (see Section 2.1.1). The highest measured removable contamination (~2000 Bq/cm²) corresponds with a glass layer thickness of less than 100 Å (0.01 μm). This is far below the average thickness of the alteration layers. Yet, it is not impossible that both phenomena (high removable contamination and thicker alteration layers) are caused by the same feature, namely the high specific alpha activity of the samples. One can imagine that, due to alpha decay (He production) and alpha recoil, and in combination with the high water and/or swelling pressure, *(i)* H^+ ions can more easily penetrate into the glass, thus resulting in thicker alteration layers, and *(ii)* glass constitutive elements at the surface of the glass, in average, are less strongly bond to the bulk glass matrix, thus being more easily removed from the glass surface by precipitation and/or sorption onto the clay.

Inactive samples: comparison between in situ tests and surface laboratory tests

A remarkable observation from the study of the thickness of the alteration layers is that the alteration layers of the inactive glass samples from the surface laboratory tests were intact [25], whereas the alteration layers of samples from the *in situ* tests were in almost all cases partially lost. Only for the samples of module B (BSG) of test tube 3 (90 °C, ^{60}Co) – but to a smaller extent for the U/Th-doped samples of this module – the alteration layer was almost completely intact. As the re-saturation of the backfill material in this module proceeded very slowly (see Section 2.1), resulting in a low swelling and water pressure during a major part of the test, we hypothesise that this different behaviour is due to differences in the swelling and/or water pressure exerted on the alteration layer. The total pressure is the sum of the water pressure and the swelling pressure of the backfill material. For the saturated backfill materials in the *in situ* tests, total pressures may have been as high as 2.5-4.5 MPa. For test tube 3, heated at 90 °C, the total pressure may have been even much higher, due to the thermal expansion of water in the backfill material.

[25] See Section 2.4.2 and detailed report by CEA.

The differences in thickness and shape of the alteration layers of the samples of the surface laboratory tests and the *in situ* tests make it difficult to compare these values.

The thickness of the alteration layer of the glass samples of the surface laboratory tests (from Table 14) and the *in situ* tests (from Table 10) are graphically represented in Figure 18. It is seen that for the samples corroded at 30 °C, and apart from the two 'outliers' for the surface laboratory tests (see Section 2.4.2) the thicknesses of both experiments agree very well. For the samples corroded at 90 °C, the agreement is less satisfactorily. The alteration layer thickness of the samples from modules A (DBC) and B (BSG) of test tube 3 (90 °C, ^{60}Co) are smaller than the respective values for the surface laboratory tests. This is at least partly due to the fact that part of the alteration layer is lost during the glass corrosion process and due to the treatment of the glass samples before analysis. It is very likely that for module B of test tube 3, the glass alteration of the glass samples started later during the test, due to the slow re-saturation of the backfill material, contributing to a lower alteration layer thickness. In contrast, the thickness of the *in situ* corroded sample from module C (BGF) of test tube 3 is considerably higher than the thickness of the alteration layer of the samples of the surface laboratory tests. We cannot explain this difference.

Based on the mass loss data (Table 10), we can estimate the thickness of the alteration layer. To this purpose, we must make a few assumptions. First, we can distinguish two cases: isovolumetric alteration (*i.e.* the initial volume of the glass sample is constant) and non-isovolumetric alteration (*i.e.* the initial volume of the glass sample is not constant; the volume of the pristine glass decreases, but the volume of the alteration layer, with a lower density than the pristine glass, is larger than the volume of corroded glass; furthermore, part of this alteration layer can be 'consumed' by the clay). In the first case, the thickness of the alteration layer 'e_{gel}' (μm) is obtained from equation (1):

$$e_{gel} = \Delta m / (d_{glass} - d_{gel}) \qquad (1)$$

in which Δm refers to the specific mass loss (g/m²) and d_{glass} and d_{gel} to the density (g/cm³) of the pristine glass and the alteration layer, respectively. In the second case, the thickness of the alteration layer 'e_{gel}' (μm) is obtained from equation (2):

$$e_{gel} = e_{glass} \times d_{glass} / d_{gel} = \Delta m / d_{gel} \qquad (2)$$

in which e_{glass}, d_{glass}, d_{gel}, and Δm refer respectively to the thickness of the layer of corroded glass (based on its initial density d_{glass}), the density of pristine glass (2.75 g/cm³), the density of the alteration layer (1 or 1.4 g/cm³; see below), and the specific mass loss (g/m²). Second, we thus need to estimate the density of the alteration layer. A measurement by X-ray reflectometry on a gel formed at 0.5 cm^{-1} and 50 °C in pure water gave an average density of 1.4 g/cm³ [41], but estimations of the density of gels formed under high alteration rates led to a gel density of about 1 g/cm³ [42]. The results of these calculations are summarised in Table 16.

From Table 16, it is seen that the estimated thickness of the alteration layer varies strongly with the assumptions on glass alteration mechanism (isovolumetric *versus* non-isovolumetric) and on density of the alteration layer. It is also seen that – especially for the samples of modules A (DBC) and B (BSG) – part of the alteration layer has dissolved or disappeared (compare with the measured thicknesses; Table 11). This is likely due to sorption of its constitutive elements on the clay and by secondary phase formation. Such reactions, which prolong the time necessary for the glass to reach the low final glass dissolution rate, have been reported in literature [58-60, 75]. The shape of the alteration layers in the SEM images of the cross sections corroborates this hypothesis. Although less clearly visible, it is likely that such loss of (some) elements occurred also to some (lower) extent in module C (BGF) (see detailed CEA report, annex 2 to the scientific and technical report).

The thickness of the alteration layer of the non-radioactive glass sample of tube 3 – module A (1.3 years, 90 °C, DBC) is relatively small in comparison with that of SON 68 glass altered in the CERBERUS test (5 years, 80-85 °C, gamma radiation), where the reaction layer was ~200 μm thick [25]. Several processes may account for this difference (differences in temperature, pH, swelling and/or total pressure exerted on the alteration layer), and we will have to wait for the results of test tube 4 (Table 1) for a detailed comparison.

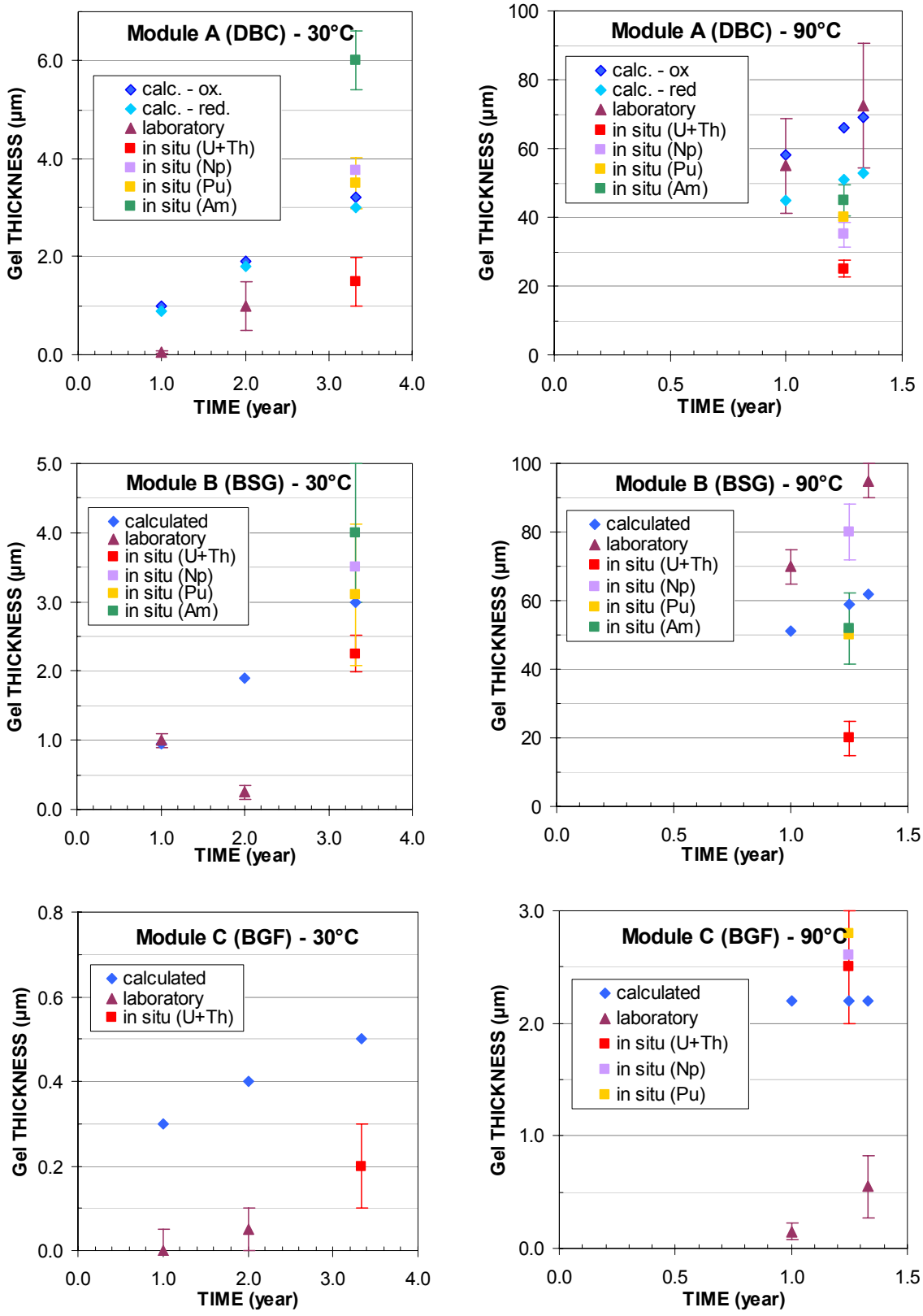

Figure 18 *Comparison between calculated and measured (surface laboratory and in situ experiments) gel thicknesses for module A (DBC; top), module B (BSG; centre), and module C (BGF; bottom) at 30 °C (left) and 90 °C (right). For DBC (top), separate calculations were made for reducing and oxidising conditions (referred to as calc. red. and calc. ox., respectively)*

Table 16 *Estimated alteration layer thicknesses (µm) from the sample mass losses, taking into account the density of the alteration layer.*

Test case (temperature, backfill)	Glass type	Specific daily mass loss ($g/m^2/day$)	Thickness of corroded glass * (µm)	Calculated thickness of alteration layer (µm)			
				Isovolumetric		Non-isovolumetric	
				d_{gel} = 1.0 g/cm^3	d_{gel} = 1.4 g/cm^3	d_{gel} = 1.4 g/cm^3	d_{gel} = 1.0 g/cm^3
30 °C, A (DBC)	**U+Th**	0.0093	4.05	6.4	8.3	8.0	11.1
30 °C, A (DBC)	**Np**	0.0008	0.36	0.6	0.7	0.7	1.0
30 °C, A (DBC)	**Am**	0.0143	6.20	9.7	12.6	12.2	17.1
30 °C, B (BSG)	**U+Th**	0.0075	3.30	5.2	6.7	6.4	9.0
30 °C, C (BGF)	**Np**	0.0013	0.6	0.9	1.2	1.1	1.6
90 °C, A (DBC)	**Am**	0.3000	48	75	98	94	132

* This is the thickness of glass, with density 2.75 g/cm^3, that is 'lost' due to the mass loss.

Inactive samples: comparison with modelling predictions [26]

The altered glass thicknesses were predicted with the LIXIVER 2 code for alteration durations up to 10 years, this is the maximum duration of the *in situ* tests (Table 1). The LIXIVER 2 code is based on the general hypotheses describing SON68 glass alteration with simplified allowance for the presence of environmental materials in contact with the glass [80]. The code includes four adjustable parameters to describe the glass alteration: one related to the glass (C^*: dissolved silicon concentration at saturation), another related to the gel (D_g: apparent diffusion coefficient of silicon in the interstitial water of the gel pores), and two others (D_p: silicon diffusion coefficient in the pores of the environmental material; K_d: silicon distribution coefficient in the environmental material) describing the silicon diffusion in and the adsorption capacity of the material in contact with the glass. In addition to these four parameters, the LIXIVER 2 code uses the values of three other parameters, *i.e.* the initial SON68 glass dissolution rate r_0, and the porosity ω and dry density ρ of the environmental material. The values of the last three parameters are measurable. As the code assumes that the glass alteration is an isovolumetric process, and as the glass alteration in the presence of boom clay is not isovolumetric (gel thickness different from altered glass thickness) because this clay consumes the gel when it forms, it was considered that only 20 % of the total gel thickness had a capacity of diffusion barrier. Furthermore, the LIXIVER 2 code describes glass alteration in a 1D Cartesian geometry, whereas the *in situ* tests were performed in a cylindrical geometry. A simplified calculation showed that the silicon adsorption capacity of the environmental materials is thus underestimated by about 25 %, but this is not expected to have an influence on the results.

Considering the uncertainty on some parameter values (D_g at 30 °C, K_d of boom clay), several calculations were performed to estimate the altered glass thickness during the *in situ* tests. All calculations were performed for an environmental material thickness of 34 mm (corresponding to a small test tube), since the differences in the altered glass thicknesses calculated for 34 and 53 mm of material yielded virtually the same results. The predicted gel thicknesses are graphically summarised in Figure 18, together with the experimentally determined thicknesses. For boom clay, separate calculations were performed for reducing and oxidising conditions.

From Figure 18, it is seen that the modelling predictions predict the same tendency as observed experimentally: a higher glass alteration at 90 °C and for the backfill materials without powdered glass frit. For all test cases except one (module C, BGF, of test tube 3, 90 °C, ^{60}Co sources), the predicted glass alteration increases linearly with time, indicating that the corrosion is still in the phase of the

[26] This part has been described in detail in the detailed report of CEA.

high initial glass alteration rate. For module C of test tube 3, the alteration layer thickness is almost constant with time because for this test case the long-term glass alteration rate conditions would have been reached within one year. If we take into account that for the *in situ* corroded glass samples part of the alteration layer was lost due to adsorption of leached glass constituents on the clay and/or removal of part of the alteration layer during manipulations, the modelling predictions agree reasonably well with the results of the *in situ* experiments. It is important to remark here that in fact the results of the modelling predictions have to be compared with the thicknesses for the inactive glass samples, for which the parameters used in the model were determined. The observation of thicker alteration layers for the radioactive samples is not accounted for in the LIXIVER 2 model. The agreement with the results of the surface laboratory glass corrosion tests is fairly good for modules A (DBC) and B (BSG), but less good for module C (BGF).

2.5.2.2.3 Retention of radionuclides in the alteration layer

In an integrated test such as CORALUS, the release of the actinides from the glass is influenced by many processes, and therefore difficult to comprehend. In the absence of clay, all the actinides are retained to some extent in the gel layer by sorption onto the gel [56, 60, 61, 64, 65, and references therein]. Np, and presumably also U, are released into solution to a greater extent than Pu and Am. Vernaz and Godon, for instance, conducted static and dynamic corrosion tests with borosilicate glass doped with Np, Pu, and Am under oxic and anoxic conditions and concluded that only about 10 % of Np, 3 % of Pu, and 0.3 % of Am were finally released into the solution [56]. Other processes that may account for the actinide retention are sorption onto and/or incorporation into secondary phases formed at the surface of the alteration layer (this depends obviously on the composition of the glass and the contacting solution, and on the temperature and pressure), and (co-)precipitation on the surface of the alteration layer or in the solution itself. The release rate of the actinides is influenced by the redox conditions (this is especially the case for Np and, presumably, U) and by the presence of ligands that may form stable RN complexes (carbonate, humic acid, etc.). Np is released as $Np(V)O_2^+$ which under reducing conditions is gradually reduced to Np(IV) [61,63]. The sorption of the single charged $Np(V)O_2^+$ species in the alteration layer is smaller than that of a multivalent positively charged actinide such as Th(IV), Pu(IV), and Am(III). The formation of (single) positively charged or (single or multiple) negatively charged (mixed) complexes may increase the actinide solution concentration.

In contact with clay, especially at high swelling pressure (resulting in a very intense contact between the clay and the glass, particularly the glass alteration layer), released actinides, as well as leached glass constituents, will strongly sorb onto these clay materials and onto secondary phases formed at the interface between the glass and the clay [56, 57, 59, 60, 61, 63, and references therein]. These processes act as a sink for the released actinides, thus increasing the actinides leaching from the glass, and possibly decreasing the actinides sorption on the alteration layer. Previous work on R7T7 glass has shown that in pure water typical radionuclide retention factors – defined as the ratio between the mass loss and the normalised actinide loss – are 5-10 for Np, 50-100 for Pu, and 500-1000 for Am, while actinide retention was lower in boom clay suspensions with retention factors of 3 for Np, 10 for Pu, and 40 for Am [57]. Lemmens *et al.,* for glass corrosion tests in contact with dense clay (Ca-bentonite with or without boom clay), report a retention factor for Np of about 1, meaning that there was (almost) no retention of Np in the alteration layer [64]. Formation of (mixed) complexes with carbonate, humic acids, *etc.* may increase the solution concentration of the actinide. Besides sorption onto 'immobile' solid phases, leached actinides may also strongly sorb onto colloids. Colloids may form from hydrolysis of dissolved metal ions in solution and polymerisation (real colloids), by adsorption of radionuclides onto existing natural groundwater (here: interstitial solution) colloids, or onto glass alteration products (pseudo colloids). Groundwater colloids are composed of inorganic and organic molecular constituents including mineral products (clay minerals, polysilicic acid, $CaCO_3$, FeOOH), hydrolysed precipitates of mixed metal ions, and macromolecular components of dissolved organic carbon (DOC).

The SIMS profiles for the actinides demonstrate that these elements followed a behaviour that mostly lies between that of La^{3+} and Nd (presumably present as Nd^{3+}) on the one hand and Zr^{4+} on the other hand.

Because for many samples the top surface of the alteration layer (with the 'precipitation layer') was lost, we cannot derive from the SIMS profiles if these elements were retained in the alteration layer, and if Np was less well retained than Pu and Am, as often reported in literature. In contrast, the results show that U was considerably less well retained than the other actinides. Am sometimes seems to be leached more in the alteration layer. This is possibly related to the high concentrations of carbonate and humic acids, resulting the formation of negatively charged complexes, and hence a smaller retention.

Since we cannot use the SIMS profiles to conclude on the retention of actinides in the alteration layer, we have to rely solely on the results from the radionuclide migration (Table 12) . These results indicate that the radionuclides are not very strongly retained in the alteration layer. Retention factors, defined as the ratio of the mass loss and the normalised radionuclide release, are between ~1 and ~3. This is in agreement with literature data for radionuclide release from active glass samples in contact with clay, as explained above.

2.5.3 Alteration of backfill material upon prolonged heating and irradiation

The study of the backfill material of module C (BGF) of test tube 3 (90 °C, ^{60}Co-sources) showed the high reactivity of a bentonite-based backfill material mixed with powdered glass frit, when heated and gamma irradiated. The observed precipitation of Si phases and the neo-formation of non-swelling phases in the clay in contact with the glass samples and glass powder makes clear that when the HLW glass will come in contact with pore water (designed > 500 years after disposal of the heat and gamma emitting waste), the mineralogy of and the geochemistry in a backfill material containing siliceous additives might be quite different from the initial conditions. This may have a large impact on the long-term performance of a disposal site. For instance, Si concentrations may increase, probably contributing in maintaining a very low glass alteration rate. Conversely, the formation of non-swelling phases at the expense of swelling phases might increase the diffusion rate of Si (and radionuclides), enlarging the thickness of the influence sphere [81] within which silica sorption on clay may enhance glass dissolution rates. More generally speaking, the continuously evolving geochemical conditions imposed by interaction between host formation, concrete liner, backfill, and corroding container materials need to be known, as well as the formation conditions for the neo-formed phases, to be able to determine the extent of their impact on the long-term performance of a disposal site. This issue is addressed in the EC co-funded project NF-PRO.

Given the high reactivity of the bentonite-powdered glass frit mixture and the possible negative consequences on radionuclide migration, it is probably better to include the powdered glass frit within the 'overpack' or any other barrier that is designed to last during the thermal period of the waste form. This way, the powdered glass frit should start to become functional only after the thermal period, this way probably avoiding or limiting the possible negative consequences. Indeed, the different experiments performed in the HADES Underground Research Facility, as well as in other research laboratories, do not demonstrate major changes in the mineralogy of the heated and gamma irradiated clay [25, and references therein]. For the experiments in the boom clay, the differences observed on the samples at the end of the experiments were more related to the heterogeneity of the boom clay than to the experimental conditions itself.

2.5.4 Leaching and migration of radionuclides

Concerning the migration of radionuclides and (stable) U, Cs, Th, Zr, and Pd, the results largely correspond to the expectations.

1. Highly compacted clay-based backfill materials with good radionuclide sorption properties are efficient in retarding radionuclide migration. Over a distance of ~5 mm, the specific activity of Np, Pu, Am, and U decreased by several orders of magnitude. The lower retention of Cs^+ is probably

due to the high concentration of Na^+, a competitive cation for the specific sorption sites, in combination with the relatively high chemical Cs^+ concentration and the relatively low number of specific sorption sites.

2. A contribution of colloidal transport of Am and Pu is observed in modules A (DBC) and B (BSG). It is likely that these are radionuclide – organic matter pseudo-colloids. We observed deeper in the clay ^{241}Am concentrations between 10 and 100 Bq per g oven dry clay, corresponding with ^{241}Am concentrations between $\sim 5\times10^{-10}$ and $\sim 5\times10^{-9}$ mol/l (assuming that all the ^{241}Am is present in colloids in the solution). However, based on the results of migration experiments with ^{241}Am and ^{14}C-labelled boom clay 'natural organic matter' (NOM) in undisturbed boom clay cores [66, 67], we can expect that if the layer of backfill and/or host formation clay is sufficiently thick, virtually all these colloids will dissociate, with consequent sorption of the radionuclide on the solid, when in contact with the surrounding material (backfill, host formation).

3. The type of backfill material has a very important effect on the general behaviour of the glass: glass alteration, radionuclide leaching, retention, and migration (*e.g.* addition of powdered glass frit, presence of mobile organic matter). Optimisation of the repository performance is thus possible. In this regard, it is probably better to include the powdered glass frit within the engineered barrier that should withstand the thermal period of the disposal phase.

4. Because we found not all potentially leached Np, Pu, and Am in the clay, we conclude that these radionuclides were to some extent retained in the alteration layer. The order is Am ≈ Pu > Np, except for DBC, where the order is Pu > Np ≈ Am. The rate of the glass matrix dissolution thus provides an upper limit for these elements. However, the retention factors for these elements were considerably lower than the values reported for R7T7 glass alteration in water or in (diluted) clay suspensions. The intense contact between the glass alteration layer and the dense clay with good radionuclide sorption properties results in a strong transfer of radionuclides to the clay.

5. Zr^{4+}, Th^{4+}, and Pd^{2+} did not migrate far, because they adsorb strongly onto clay minerals, and/or because they are poorly soluble.

6. U and Cs^+ migrated relatively fast. In the case of U, this is probably because it was present as negatively charged species such as $UO_2(CO_3)_2^{2-}$ (lower pH) or $UO_2(CO_3)_3^{4-}$ (higher pH), which are not well retained in clay-based backfill materials. The fast migration of Cs^+ is probably due to its weak sorption due to the high Na^+ concentration in the pore waters, in combination with a relatively high solution concentration.

3 Assessment of the results and conclusions

The CORALUS-2 project addresses the alteration of the French R7T7 HLW glass in contact with clay-based backfill materials in realistic disposal conditions. The main objectives were:

1 to provide realistic data on, and to gain more insights in the dissolution of SON 68 18 17 L1C2A2Z1 glass – a reference glass simulating the French R7T7 HLW glass – , and in the release and the migration of the radionuclides and some other incorporated elements into the high-density backfill materials. The data had to be compared with the results on glass dissolution from laboratory experiments, performed under the same or similar conditions, and with the derived modelling predictions. This would give an idea of the reliability of the present long-term predictions. The experimental setup allows estimating the influence of the type of backfill material, the presence of alpha radiation, and the combined effect of high temperature and gamma radiation
2 to estimate the extent of the thermal and radiolytic gas generation in the three backfill materials that are included in the CORALUS test tubes
3 to assess, for a Ca-bentonite-based backfill material, the mineralogical alteration upon prolonged heating and gamma irradiation.

The conclusions and assessment of the results are written with respect to the above objectives.

Realistic data

The data are expected to be realistic because the dissolution tests they are obtained from were performed under close-to-real disposal conditions. Both inactive and alpha-beta-gamma doped glass samples were studied, in contact with three different clay-based backfill materials exerting a high swelling pressure. The saturation of the backfill materials was followed through the evolution of the water pressure. The two test temperatures are internationally accepted reference temperatures, and the whole temperature measurement chain was calibrated. The gamma irradiation dose rate was chosen to be in agreement with the temperature of 90 °C, expected to occur about 100 years after production of the HLW glass canister. The use of glass samples with different specific alpha-beta-gamma activity enabled to study the effect of the increasing activity. The pH and E_h were governed by interaction of the surrounding host formation with the backfill materials, under the prevailing boundary conditions (temperature, gamma radiation field, presence of stainless steel).

It is important to note that this study relates to glass samples that were in direct contact with clay. The results can therefore not be directly transferred to a situation where the glass and the clay are separated by other materials, in particular container materials.

Glass dissolution and radionuclide release

The conclusions that can be drawn from the analysis of the altered glass samples correspond largely to the expectations.

The glass alteration was considerably higher at 90 °C. The specific daily mass losses were about 20 times higher than at 30° C. The thickness of the alteration layers was about 10 times higher at 90 °C. It is thus of high interest to avoid contact between HLW glass and water during the thermal phase.

The addition of powdered glass frit to a (bentonite-based) backfill material has a very beneficial effect: it diminishes the glass alteration with about two orders of magnitude or more. Optimisation of the repository performance is thus possible (see also under 'clay alteration').

From the analysis of the SIMS profiles, we conclude that the dissolution of the SON 68 samples is predominantly selective-substitutional leaching, as observed also in other SON 68 glass alteration tests. Yet, the loss of a distinct part ('layer') of the alteration layer, either because of the sorption of the glass constituents onto the clay (exerting a high swelling pressure) and/or secondary phase formation, or because of the treatment of the glass samples before analysis, can be interpreted as matrix dissolution.

Due to the loss of part of the alteration layer, especially for the radioactive samples, the results of the SIMS analyses do not allow to conclude on the retention of radionuclides in the alteration layer. Fortunately, the results of the radionuclide migration enable to calculate radionuclide retention factors. These retentions factors vary between 1 and 3, and are thus much smaller than the values normally reported for glass alteration in water in the absence of solids. This is due to the high affinity of the clay-based backfill material for the radionuclides, and this observation is in agreement with the results of 'integrated' surface laboratory tests studying glass alteration in contact with dense clay. The loss of part of the alteration layer also impeded the detection of secondary phases.

The results of the glass alteration revealed also two effects that were not expected.

First, and although the alpha-beta-gamma doped glasses behaved rather similarly as the inactive ones, the alteration layers were systematically thicker for the radioactive glass samples, with a tendency of increasing thickness with increasing specific alpha-beta-gamma activity. Also the surface of the radioactive glass samples corroded at 30 °C showed more alteration (for the samples corroded at 90 °C, any effect was masked by the high alteration degree). Because of the lack of sufficient data, we cannot conclude that also the mass loss increased. As this phenomenon was also observed for the samples of test tube 3 (90° C, ^{60}Co sources), for which the pH was already low and the gamma radiation dose rate high (> 100 Gy/h), we conclude that this effect is probably due to the increasing specific alpha activity. This conclusion differs from the conclusions from glass alteration tests in water or suspensions with samples doped exclusively with alpha emitters. The reason for our observation has probably to be looked for in the high water and/or swelling pressures prevailing during the glass alteration, in combination with the increasing alpha-beta-gamma activity of the samples. The results of the glass alteration of the samples loaded on test tube 4 (90 °C, ^{60}Co sources, 6 years) are awaited before making more stringent conclusions on any effect of the specific alpha activity.

Second, the mass losses (as far as available) for the tests with Dried boom clay at 90 °C in a gamma radiation field were similar to the results of integrated surface laboratory tests contacting SON 68 glass samples with boom clay at 90 °C without gamma radiation. If the effect of gamma radiation would be related to a decrease of the pH in the system, we conclude that if other processes make the pH to decrease, the contribution of gamma radiation in the overall pH decreasing process may become small. This may have been the case for our test, where the thermal decomposition of organic matter in the Dried boom clay backfill resulted in a high CO_2 production and a concomitant decrease of the pH (see under thermal and radiolytic gas production).

The mass losses of the CORALUS *in situ* tests (case dried boom clay) thus compare fairly well with the results of integrated surface laboratory tests. Due to the loss of part of the alteration layer, the thickness of the alteration layer of the *in situ* corroded glass samples was almost systematically smaller than for the 'CORALUS' surface laboratory tests. We attribute this to differences in swelling pressure and/or water pressure. If we take into account the loss of part of the alteration layer, the results compare fairly well with the modelling predictions. This confirms the high degree of understanding of the glass alteration phenomena. Yet, for more valid modelling hypotheses, we need a better understanding of the processes governing the Si solution concentration at the glass-clay interface and Si transport in the clay.

Radionuclide migration

Also concerning the migration of radionuclides and (stable) U, Cs, Th, Zr, and Pd, the results correspond to the expectations.

1. Highly compacted clay-based backfill materials with good radionuclide sorption properties are efficient in retarding radionuclide migration. Over a distance of ~5 mm, the specific activity of Np, Pu, and Am decreased by several orders of magnitude.

2. A contribution of colloidal transport of Am and Pu is observed in modules A (DBC) and B (BSG). It is likely that these are radionuclide – organic matter pseudo-colloids. Based on literature data, we expect that if the layer of backfill and/or host formation clay is sufficiently thick, virtually all these colloids will dissociate, with consequent sorption of the radionuclide on the solid, when migrating through the surrounding material (backfill, host formation).

3. The type of backfill material has a very important effect on the general behaviour of the glass: glass alteration, radionuclide leaching, retention, and migration (*e.g.* addition of powdered glass frit, presence of mobile organic matter). Optimisation of the repository performance is thus possible.

4. Zr^{4+}, Th^{4+}, and Pd^{2+} did not migrate far, because they adsorb strongly onto the glass alteration layer and clay minerals, and/or because they are poorly soluble. U and Cs^{+} migrated relatively fast. In the case of U, this is probably because it was present as negatively charged species, which is not well retained in clay-based backfill materials. The fast migration of Cs^{+} is probably due to its weak sorption due to the high concentration of the competing Na^{+} in the pore water.

Thermal and radiolytic gas production

Carbon dioxide was the most important dissolved gas. Especially at 90 °C, high CO_2 concentrations were produced by thermal and radiolytic decomposition of organic matter and, for module B, graphite (present at 5 weight% in the backfill material). Due to the high CO_2 contents, pH values in the test tubes at 90 °C (5.5-6.5) were by 1 unit or more lower than the corresponding values in the test tube at 30 °C (6.2-7.4). The concentrations of hydrogen and methane were very low. These gases will be dissolved in the interstitial water, and will thus not present a safety problem.

Clay alteration

The characterisation of the Ca-bentonite with powdered glass frit showed that after ~1.2 years of heating and gamma irradiation the interface between clay and glass was fully reactive. At the interface, Si had precipitated. Na^{+} leached from the glass frit had sorbed on the cationic exchange sites of the clay minerals. Kaolinite and interstratified kaolinite/smectite of the Ca-bentonite had started to become unstable, tending to form non-swelling 7Å minerals. As these reactions may have negative consequences (for instance, faster radionuclide migration through non-swelling clay minerals), it may be of interest to include the powdered glass frit within the water-tight engineered barrier ('overpack'), so that it starts to become effective after perforation of the overpack.

General conclusion

On the basis of all results and observations, we conclude that the CORALUS tests largely contribute to the validation of the laboratory tests and modelling predictions, and that they can be considered as a small-scale demonstration test of the good performance of SON 68 (R7T7) HLW glass in a repository with a high-density clay-based backfill material with high radionuclide sorption properties. The results and conclusions also demonstrate that integrated tests performed in realistic conditions provide complementary insights in the total system performance.

List of abbreviations

ALARA	as low as reasonably achievable
BGF	calcium-bentonite with powdered glass frit
BSG	calcium-bentonite with sand and graphite
CEA	Commissariat à l'énergie atomique (France)
CORALUS	*Corrosion of active glass in underground storage conditions*
DBC	dried boom clay
EC	European Commission/electric conductivity
EGBS	extension gallery bottom shaft
EPMA	electron probe microanalysis
FoCa clay	clay from *Fourges cahaines* (Paris Basin)
FTC	flow-through cell
GC-MS	gas chromatography – mass spectrometry
GRS	Gesellschaft für Anlagen- und Reaktorsicherheit (Germany)
HADES	high-activity disposal experimental site
HLW	high-level waste
HPGe	high-performance germanium
IC	ion chromatography
ICP-AES	inductively coupled plasma – atomic emission spectrometry
ICP-MS	inductively coupled plasma – mass spectrometry
NIRAS/ONDRAF	Nationale Instelling voor het Beheer van Radioactief Afval en Splijtbare Materialen/Organisme national pour la gestion des déchets radioactifs et des matières fissiles enrichies (Belgian Agency for Radioactive Waste and Enriched Fissile Materials)
OPHELIE	on-surface preliminary heating simulation experimenting later instruments and equipments
PSI	Paul Scherrer Institut (Switzerland)
SCK•CEN	Studiecentrum voor Kernenergie/Centre d'étude de l'énergie nucléaire
SEM	scanning electron microscopy
SEM-EDS	scanning electron microscopy – energy dispersive spectrometry
SIMS	secondary ion mass spectrometry
TC	total carbon
TEM	transmission electron microscopy
TOC/IC	total organic carbon/inorganic carbon
URF	underground research facility
URL	underground research laboratory
WP	work package
wt %	weight%
XRD	X-ray diffraction

References

[1] E. Valcke, P. Van Iseghem, S. Smets, S. Labat, N. Godon, N. Jockwer, K. Wieczoreck, 'An integrated *in situ* corrosion test on alpha-active HLW glass – Final report', EUR 19795, European Commission, Luxembourg, 2001.

[2] E. Valcke, P. Van Iseghem, N. Godon, and N. Jockwer, 'CORALUS: An integrated *in situ* corrosion test on alpha-active HLW glass', p. 427-430 in Proceedings of the Euradwaste '99 Conference, EUR 19143, European Commission, Luxembourg, 2000.

[3] W.J. Weber, PNNL, USA, personal communication, 2005.

[4] E. Vernaz, CEA-Valrhô, France, personal communication, 2001.

[5] S. Fillet, J.L. Nogues, E. Vernaz, and N. Jacquet-Francillon, 'Leaching of actinides from the French LWR reference glass', Sci. Basis for Nucl. Waste Man., Mat. Res. Soc. Symp. Proc. Vol. 50, p. 211-218, 1985.

[6] S. Fillet, 'Mécanismes de corrosion et comportement des actinides dans le verre nucleaire R7T7', Thèse Académie de Montpellier, Université des sciences et techniques du Languedoc, 1987.

[7] N. Godon and E. Vernaz, 'Radioactive SON 68 18 17 L1C2A2Z1glass interaction with environmental materials', RT DPR 90/002, CEA-Valrhô, 1990.

[8] J.L. Dussossoy, J.L. Chouchan, M. Bouchon, E. Vernaz, 'Characterisation of radioactive waste forms. A series of final reports (1985-1989)', EUR 13603, European Commission, Luxembourg, 1991.

[9] E. Vernaz and N. Godon, 'Leaching of actinides from nuclear waste glass: French experience', Sci. Basis for Nucl. Waste Man., Mat. Res. Soc. Symp. Proc. Vol. 257, p.37-48, 1992.

[10] K. Lemmens, M. Aertsens, P. De Cannière, and P. Van Iseghem, 'The corrosion of nuclear waste glasses in a clay environment: mechanisms and modelling', SCK•CEN document R-3092, Mol, Belgium, 1996.

[11] T. Advocat, P. Jollivet, Y. Minet, B. Luckscheiter, B. Grambow, R. Gens, K. Lemmens, P. Van Iseghem, M. Aertsens, V. Pirlet, and E. Curti, 'Experimental and modelling studies to formulate a nuclear waste glass source term in representative geological disposal conditions', EUR 19120, European Commission, Luxembourg, 1999.

[12] M. De Craen, D. Delleuze, G. Volckaert, A. Sneyers, and M. Put, 'The boom clay as natural analogue, Final report 1997-1999', SCK•CEN document R-3444, Mol, Belgium, 2000.

[13] G. Volckaert, B. Dereeper, M. Put, L. Ortiz, A. Gens, J. Vaunat, M. Villar, P.L. Martin, C. Imbert, T. Lassabatere, E. Mouche, and F. Cany, 'A large-scale *in situ* demonstration tests for repository sealing in an argillaceous host rock, RESEAL project - phase I', EUR 19612, European Commission, Luxembourg, 2000.

[14] G. Volckaert, personal communication, SCK•CEN, Mol, Belgium, 2002.

[15] J. Verstricht, personal communication, SCK•CEN, Mol Belgium, 2002.

[16] L. Noynaert, G. Volckaert, P. De Canniere, L. Meynendonckx, S. Labat, M. Put, M. Aertsens, A. Fonteyne, and F. Vandervoort, 'The CERBERUS Project: A Demonstration Test to Study the Near-field Effects of a HLW Canister in an Argillaceous Formation, Final report (July 1, 1990 to December 31, 1996)', EUR 18151, European Commission, Luxembourg, 1998.

[17] M. de Craen, L. Wang, M. Van Geet, and H. Moors, 'Geochemistry of boom clay pore water at the Mol site – status 2004', Scientific Report SCK•CEN-BLG-990, SCK•CEN, Mol, Belgium, 2004.

[18] I. Deniau, S. Derenne, C. Beaucaire, H. Pitsch, and C. Largeau, 'Simuation of thermal stress influence on the boom clay kerogen (Oligocene, Belgium) in relation to long-term storage of high activity nuclear waste. Part I: study of generated soluble compounds', Applied Geochemistry 20, 587-597, 2005.

[19] I. Deniau, F. Behar, C. Largeau, P. De Cannière, C. Beaucaire, and H. Pitsch, 'Determination of kinetic parameters and simulation of early CO_2 production from the boom clay kerogen under low thermal stress', Applied Geochemistry 20, 2097-2107, 2005.

[20] A. J. Swallow, 'Radiation Chemistry', ISBN 0 582 46286 X, Longman, London, 1973.

[21] W. Stumm and J.J. Morgan, p. 150 – 153 in 'Aquatic Chemistry', Third Edition, John Wiley & Sons, Inc., New York, Chichester, Brisbane, Toronto, Singapore, 1996.
[22] P. Wersin, P. De Cannière, F.J. Pearson, E. Gaucher, P. Höhener, L. Eichinger, S. Mettler, U. Mäder, A. Vinsot, H.-E. Gäbler, K. Hama, and P. Hernán, 'Results from an in situ porewater chemistry experiment in Opalinus Clay: evidence of microbially-mediated anaerobic redox processes', Communication at the 2nd International Meeting on 'Clays in Natural and Engineered Barriers for Radioactive Waste Confinement' organised by ANDRA (ANDRA 2005 International Meeting held in Tours, France, on 14-18 March 2005), http://www.andra.fr, follow option 'research', 2005.
[23] L. Ortiz, G. Volckaert, and D. Mallants, 'Gas generation and migration in boom clay, a potential host rock formation for nuclear waste storage', Engineering Geology 64, 287-296, 2002.
[24] B. Baeyens, A. Maes, A. Cremers, and P.N. Henrion, 'Aging Effects in boom clay', Radioactive Waste Management and the Nuclear Fuel Cycle, Volume 6 (3-4), p. 409-423, 1985.
[25] L. Noynaert (Ed.), 'Heat and Radiation Effects on the Near Field of a HLW or Spent Fuel Repository in a Clay Formation (CERBERUS Project), Final Report', EUR 19125, European Commission, Luxembourg, 2000.
[26] B. Kursten, B. Cornelis, S. Labat, and P. Van Iseghem, 'Completion of the Corrosion Programme in boom clay – In Situ Experiments (programme 1991-1994)', EUR 17105, European Commission, Luxembourg, 1997.
[27] J. Raynal et J.-C. Petronin, '*Projet PRACLAY – Expertise minéralogique de la maquette Ophélie: caractérisation d'un anneau représentatif',* Note Technique NT SAMRA 03-045 (report in French), CEA/DEN/CAD/DED, F-13 108 Saint Paul Lez Durance, France, 2003.
[28] K. Lemmens, personal communication, SCK•CEN, Mol, Belgium, 2006.
[29] F. Delage, D. Ghaleb, J-L. Dussossoy, O. Chevallier, E. Vernaz, 'A mechanistic model for understanding nuclear waste glass dissolution', J. Nucl. Mat. 190, p. 191-197, 1992.
[30] E. Vernaz, S. Gin, C. Jégou, and I. Ribet, 'Present understanding of R7T7 glass alteration kinetics and their impact on long-term behavior modeling', J. Nucl. Mat. 298, 1-2, p. 27-36, 2001.
[31] E. Rexer and L. Wuckel, 'Chemische Veränderungen von Stoffen durch energiereiche Strahlung', VEB Deutscher Verlag für Grundstoffindustrie, Leipzig, 268 p., 1965.
[32] L. Van Loon and Z. Kopajtic, 'Complexation of Cu^{2+}, Ni^{2+} and UO_2^{2+} by radiolytic degradation products of bitumen', Radiochimica Acta, 54, 193-199, 1991.
[33] B.F. Greenfield, M. Ito, M.W. Spindler, S.J. Williams, and M. Yui, 'The effects of the chemical and radiolytic degradation of asphalt on plutonium solubility', Mat. Res. Soc. Symp. Proc. Vol 465, 721-728, 1997.
[34] E. Valcke, A. Sneyers, and P. Van Iseghem, 'The effect of radiolytic degradation products of Eurobitum on the solubility and sorption of Pu and Am in boom clay', Mat. Res. Soc. Symp. Proc. Vol. 663, 141-149, 2001.
[35] Anonymus, 'Weltest 200 - Technical Description', Schlumberger-Geoquest, Logined BV, 1997.
[36] G. Volckaert, L. Ortiz, P. De Cannière, M. Put, S.T. Horseman, J.F. Harrington, V. Fioravante, M. Impey, 'MEGAS – Modelling and experiments on gas migration in repository host rocks', EUR 16235, European Commission, Luxembourg, 1995.
[37] G. Volckaert, F. Bernier, E. Alonso, A. Gens, J. Samper, M. Villar, P.L. Martin-Martin, J. Cuevas, R. Camppos, H. Thomas, C. Imbert, and V. Zingarelli, 'Thermal-hydraulic-mechanical and geochemical behaviour of the clay barrier in radioactive waste repositories (model development and validation)', Final Report, p. 166-167, EUR 16744, European Commission, Luxembourg, 1996.
[38] Anonymus, 'The PRACLAY project - Demonstration test on the Belgian Disposal Facility Concept for high activity vitrified waste', EUR 18047, European Commission, Luxembourg, 1998.
[39] H. Van Humbeeck, J. Verstricht, X. Li, P. De Cannière, and F. Bernier, 'The OPHELIE mockup: final report', ONDRAF/NIRAS document, Brussels, in preparation (expected June 2007).
[40] W. Bourcier, 'Overview of Chemical Modelling of Nuclear Waste Glass dissolution', Mat. Res. Soc. Symp. Proc. Vol. 212, p. 3-18, 1991.

[41] D. Rebiscoul, 'Etude de la pérennité des gels d'altération de verres nucléaires', PhD thesis, University of Montpellier II, France, 2004.
[42] S. Gin, 'Influence des matériaux argileux et des produits de corrosion du conteneur métalllique sur le comportement à long terme des verres nucléaires', in: proceedings of a workshop on Glass: Sci. research for high performance containment, August 31 – September 7, Méjannes-Le-Clap, CEA-Valrhô, France, 514-526, 1997.
[43] G. Wicks, 'US field testing programs and results', J. Nucl. Mat. 298, 1-2, p. 78-85, 2001.
[44] P. Van Iseghem, E. Valcke, and A. Lodding, 'In situ testing of the chemical durability of vitrified high-level waste in the boom clay formation in Belgium: discussion of recent data and concept of a new test', J. Nucl. Mat. 298, 1-2, p.86-94, 2001.
[45] S. Mitsui and R. Aoki, 'Effect of a siliceous additive on aqueous alteration of waste glass with engineered barrier materials', J. Nucl. Mat. 298, 1-2, p. 184-191, 2001.
[46] A. Lodding, P. Van Iseghem, 'In-depth distributions of elements in leached layers on two HLX waste glasses after burial in clay: step-scan by SIMS', J. Nucl. Mat. 298, 1-2, p. 197-202, 2001.
[47] D. Petit-Maire, 'Structure locale autour d'actinides et d'éléments nucléants dans des verres borosilicatés d'interêt nucléaire: Résultats de spectroscopie d'absorption de rayons X', PhD Univ. Paris VI, 1988.
[48] N. Ollier, 'Verres de confinement de déchets nucléaires de type SON68 et leurs produits d'altération: spectroscopie optique des terres rares et de l'uranium', PhD Univ. Lyon I, 2002.
[49] C. Lopez, 'Solubilité des actinides et de leurs simulants dans les verres nucléaires. Limites d'incorporation et compréhension des mécanismes', PhD. Univ. Paris XI, 2002.
[50] L. Wang, J. Marivoet, P. De Cannière, X. Sillen, H. Moors, M. Aertsens, M. Put, and A. Dierckx, 'Data collection form: the link between migration studies and performance assessment - Belgian Case', p. 181-190 in: 'The use of thermodynamic databases in Performance Assessment', Workshop Proceedings, Barcelona, Spain 29-30 May 2001, OECD/NEA, Paris, France, 2002.
[51] L. Wang, A. Dierckx, and P. De Cannière, 'Speciation and solubility of radionuclides in boom clay', SCK•CEN document R-3508, Mol, Belgium, 2000.
[52] J. van der Lee and L. Wang, 'Speciation and solubility calculations for uranium, plutonium, and selenium under boom clay conditions', topical report for WP1, in: N. Maes *et al.*, 'Migration case study: Transport of radionuclides in a reducing clay sediment (Trancom II)', EUR 21022, European Commission, Luxembourg, 2004; also published as Final Scientific and Technical Report of the TRANCOM-II EC project, SCK-CEN Report BLG-988, Mol, Belgium, 2004.
[53] A. Lajudie, J. Raynal, J.C. Petit, P. Toulhoat, 'Clay-based Materials for Engineered Barriers: a Review', in : Scientific Basis for Nuclear Waste Management XVIII (Ed. P. Murakami and R. Ewing), Mat.Res.Soc.Symp.Proc. 353, Part I, 221-230, 1995.
[54] C. Latrille, M. Julien, and C. Pozo, p. 291-294 in Vol. 1 of Proceedings of the WRI (Water Rock Interaction) Conference, Villasimius, Italy, R. Cidu (Ed.), 2001.
[55] M. Perronnet, PhD Thesis INPL (Geosciences), France, 2004.
[56] E. Vernaz and N. Godon, 'Leaching of actinides from nuclear waste glass: French experience', Mat. Res. Soc. Symp. Proc. Vol. 257, p. 37-48, 1992.
[57] E. Vernaz, B. Grambow, W. Lutze, K. Lemmens, and P. Van Iseghem, 'Assessment of the long-term durability of radioactive waste glass', p. 239 – 253 in: Proceedings of the Fourth European Conference on the Management and Disposal of Radioactive Waste, EUR 17543, European Commission, Luxembourg, 1997.
[58] S. Gin, P. Jollivet, J.P. Mestre, M. Jullien, and C. Pozo, 'French SON 68 nuclear glass alteration mechanisms on contact with clay media', Appl. Geochem. 16, 7-8, 861-881, 2001.
[59] K. Lemmens, 'The effect of clay on the dissolution of nuclear waste glass', J. Nucl. Mat. 298, 1-2, p. 11-18, 2001.
[60] E. Vernaz, S. Gin, C. Jégou, and I. Ribet, 'Present understanding of R7T7 glass alteration kinetics and their impact on long-term behavior modeling', J. Nucl. Mat. 298, 1-2, p. 27-36, 2001.
[61] V. Pirlet, 'Overview of actinides (Np, Pu, Am) and Tc release from waste glasses: influence of solution composition', J. Nucl. Mat. 298, 47-54, 2001.
[62] T. Advocat, P. Jollivet, J.L. Crovisier, and M. Del Nero, 'Long-term alteration mechanisms in water for SON 68 radioactive borosilicate glass', J. Nucl. Mat. 298, 1-2, p. 55-62, 2001.

[63] V. Pirlet, K. Lemmens, and P. Van Iseghem, 'Influence of the near-field conditions on the mobile concentrations of Np and Tc leached from vitrified HLW', Mat. Res. Soc. Symp. Proc. Vol. 824, p. 385 – 390, 2004.
[64] K. Lemmens, M. Aertsens, P. Lolivier, N. Malangreau, V. Pirlet, and P. De Cannière, 'Characterisation and compatibility with the disposal medium of Cogema and Eurochemic reprocessing waste forms, Tasks VM-6 and GV8 (vitrified waste), Final Report for the period 1996-2000', SCK•CEN document R-3644, SCK•CEN, Mol, Belgium, 2002.
[65] P. Jollivet and G. Parisot, 'Leach testing at 50 °C of α-doped SON68 glass alteration gels', J. Nucl. Mat. 345, 46-64, 2005.
[66] N. Maes, *et al.*, 'Migration case study: Transport of radionuclides in a reducing clay sediment (Trancom II)', EUR 21022, European Commission, Luxembourg, 2004; also published as Final Scientific and Technical Report of the TRANCOM-II EC project, SCK-CEN Report BLG-988, Mol, Belgium, 2004.
[67] N. Maes, L. Wang, T. Hicks, D. Bennett, P. Warwick, T. Hall, G. Walker, and A. Dierckx, 'The role of natural organic matter in the migration behaviour of americium in the boom clay – Part I: Migration Experiments', Physics and Chemistry of the Earth 31, p. 541-547, 2006.
[68] A. Cremers, A. Elsen, P. De Preter, and A. Maes, 'Quantitative analysis of radiocaesium retention in soils', Nature 335, 247-249, 1988.
[69] P. De Preter, L. Van Loon, A. Maes, and A. Cremers, 'Solid/liquid distribution of radiocaesium in boom clay. A quantitative interpretation.', Radiochim. Acta 52/53, 299-302, 1991.
[70] F. Degryse, E. Smolders, and A. Cremers, 'Enhanced sorption and fixation of radiocaesium in soils amended with K-bentonites, submitted to wetting-drying cycles', Eur. Journal of Soil Science, 55, 513-522, 2004.
[71] E. Valcke and A. Cremers, 'Sorption-desorption dynamics of radiocaesium in organic matter soils', Sci. Tot. Environ. 157, 275–283, 1994.
[72] E. Valcke, 'The behaviour dynamics of radiocesium and radiostrontium in soils rich in organic matter', PhD thesis 243 at the Faculty of Agronomy (Bioengineering) of the Catholic University of Leuven, Belgium, 1993.
[73] P.W. Atkins, 'Physical chemistry', 6th Edition, Oxford University Press, ISBN 0-19-850101-3, 2001.
[74] W.J. Moore and D.O. Hummel, 'Physikalische Chemie', 2e Auflage, Walter de Gruyter, 1976.
[75] K. Lemmens, M. Aertsens, V. Pirlet, N. Maes, H. Moors, and P. Van Iseghem, 'Measurement of glass corrosion in boom clay disposal conditions: first results of the experimental programme 2000-2003 of SCK•CEN', in: Proc. 9th Int. Conf. Env. Rem. and Rad. Waste Man. (ICEM '03), ASME, 2003.
[76] K. Lemmens, personal communication, SCK•CEN, Mol, Belgium, 2005.
[77] K. Lemmens and M. Aertsens, 'Validation of glass dissolution and Si diffusion parameters with a combined glass dissolution-diffusion experiment in boom clay', Mat. Res. Soc. Symp. Proc. Vol. 932, pp. 329-336, 2006.
[78] K. Lemmens and P. Van Iseghem, 'The effect of gamma radiation on the dissolution of high-level waste glass in boom clay', Mat. Res. Soc. Symp. Proc. Vol. 663, p. 227 – 235, 2001.
[79] M. Ojovan and W. Lee, 'Alkali ion exchange in gamma irradiated glass', J. Nucl. Mat. 335, 425-432, 2004.
[80] P. Jollivet, Y. Minet, M. Nicolas, and E. Vernaz, 'Simulated alteration tests on non-radioactive SON 68 nuclear glass in the presence of corrosion products and environmental materials', J. Nucl. Mat. 281 (2-3), p. 231-243, 2000.
[81] B. Grambow and E. Giffaut, 'Coupling of chemical processes in the near field', Mat. Res. Soc. Symp. Proc. Vol. 932, pp. 55-66, 2006.